



5-2008

## Regulation of *Atp10c*, a Novel Type 4 P-type ATPase, in 3T3-L1 Mouse Adipocytes

Amanda Lynn Peretich  
University of Tennessee - Knoxville

Follow this and additional works at: [https://trace.tennessee.edu/utk\\_gradthes](https://trace.tennessee.edu/utk_gradthes)



Part of the [Medicine and Health Sciences Commons](#)

### Recommended Citation

Peretich, Amanda Lynn, "Regulation of *Atp10c*, a Novel Type 4 P-type ATPase, in 3T3-L1 Mouse Adipocytes. " Master's Thesis, University of Tennessee, 2008.  
[https://trace.tennessee.edu/utk\\_gradthes/426](https://trace.tennessee.edu/utk_gradthes/426)

This Thesis is brought to you for free and open access by the Graduate School at TRACE: Tennessee Research and Creative Exchange. It has been accepted for inclusion in Masters Theses by an authorized administrator of TRACE: Tennessee Research and Creative Exchange. For more information, please contact [trace@utk.edu](mailto:trace@utk.edu).

To the Graduate Council:

I am submitting herewith a thesis written by Amanda Lynn Peretich entitled "Regulation of *Atp10c*, a Novel Type 4 P-type ATPase, in 3T3-L1 Mouse Adipocytes." I have examined the final electronic copy of this thesis for form and content and recommend that it be accepted in partial fulfillment of the requirements for the degree of Master of Science, with a major in Comparative and Experimental Medicine.

Madhu S. Dhar, Major Professor

We have read this thesis and recommend its acceptance:

Patricia K. Tithof, Roger C. Carroll

Accepted for the Council:

Carolyn R. Hodges

Vice Provost and Dean of the Graduate School

(Original signatures are on file with official student records.)

To the Graduate Council:

I am submitting herewith a dissertation written by Amanda Lynn Peretich entitled “Regulation of *Atp10c*, a Novel Type 4 P-type ATPase, in 3T3-L1 Mouse Adipocytes.” I have examined the final electronic copy of this dissertation for form and content and recommend that it be accepted in partial fulfillment of the requirements for the degree of Master of Science, with a major in Comparative and Experimental Medicine.

Madhu S. Dhar

Major Professor

We have read this dissertation  
and recommend its acceptance:

Patricia K. Tithof

Roger C. Carroll

Accepted for the Council:

Carolyn R. Hodges

Vice Provost and Dean of the  
Graduate School

(Original signatures are on file with official student records.)

# **Regulation of *Atp10c*, a novel type 4 P-type ATPase, in 3T3-L1 mouse adipocytes**

A Thesis  
Presented for the  
Master of Science Degree  
The University of Tennessee, Knoxville

Amanda Lynn Peretich  
May 2008

## DEDICATION

This thesis is dedicated

*to my husband*

the future Dr. Michael Peretich

*to my parents and “the in-laws”*

Mr. James “J.B.” Anderson II

Mrs. Jill Anderson

Mr. Edward Peretich

Mrs. Irene Peretich

*to my siblings*

James “Jamie” Anderson III

Brian Anderson

Mark Peretich

Melissa Peretich

*to my best friends*

James “Jamesway” the cat

Kylie “Chi-wee” the cat

## ACKNOWLEDGEMENTS

There are many people that deserve acknowledgement and thanks for their help (known or unknown) in the completion of this thesis. First and foremost, I'd like to thank my wonderful advisor, Dr. Madhu Dhar. During my time at the University of Tennessee (UT), I came to know and respect her as both my mentor and my friend. As one of the most dedicated, hard-working, balanced individuals I've ever had the privilege to work with, she provided exceptional guidance and taught me invaluable life lessons for which I will be eternally grateful. One of my professors during my undergraduate years at James Madison University once told me that choosing your graduate advisor is one of the most important decisions that you will ever make. I clearly made the best decision possible with Madhu.

I would also like to acknowledge the assistance and intellectual conversations from the other two members of my committee, Drs. Roger Carroll and Patricia Tithof. Their willingness and dedication to the betterment of my graduate research experience was greatly appreciated.

The Comparative and Experimental Medicine (CEM) graduate program at UT provided me with this exceptional opportunity for a graduate education. Dr. Robert "Buddy" Moore, Misty Bailey, Debbie Hampstead, and the rest of the staff in the CEM program were extremely supportive and helpful during my time at UT. In addition to support (educational and monetary) from the CEM program and the UTIA Center of Excellence, I would also like to recognize support from Dr. Robert Holland and the Large Animal Clinical Science department.

During my two years at UT, I learned the benefit of collaborative efforts in the advancement of research results. Ms. Nancy Neilsen provided extensive knowledge and guidance in the cell culture techniques used throughout my research project. Members of both Dr. Seung J. Baek and Dr. Howard Plummer's laboratories demonstrated compassion and cooperation, always willing to lend a reagent or some equipment. Both Dr. Baek and Dr. Maria Cekanova helped formulate the research investigating the effect of thiazolidinediones in this project. Dr. Guazhong Mao and Dr. Xuemin Xu provided assistance with the proteins, and Dr. Kania's laboratory allowed me to utilize and dominate their centrifuge for days at a time.

Last, but certainly not least, I'd like to acknowledge my family and friends for their love and support. It was extremely difficult to move away from everyone and everything I had grown up to know in Virginia, but the friends I have made here helped make that transition easier. As someone somewhere once said, "I get by with a little help from my friends," and I am extremely grateful for them. My family has also been tremendously supportive and loving, even with all of the losses we have all been through in the past few years. Always missing my angels in Heaven, I am able to carry on because I know they are watching over me. Sometimes I wonder if I would have finished this thesis without my wonderful husband, Michael. But with a love like ours, steadfast and true, my best friend has been by my side through good times and bad. He has been and will always be there for me, as will I for him.

## ABSTRACT

A recently identified phospholipid translocase, *Atp10c*, may be involved in the modulation of glucose and lipid metabolism in mouse adipocytes. Aminophospholipid translocases have previously been associated with cell signaling and intracellular protein trafficking. In this study, the role of *Atp10c* in the insulin signaling pathway and adipogenesis was investigated using the murine 3T3-L1 cell line.

*Atp10c* mRNA is highly expressed in undifferentiated cells and 2-fold down-regulated during adipogenesis. Interestingly, Western blotting showed a band for ATP10C protein at 70 kDa, a lower molecular weight than expected; ATP10C expression increased during differentiation. Possible reasons for these discrepancies will be discussed.

Since PPARgamma is considered to be the master regulator of adipogenesis and controls the expression of adipocyte genes, the effect of PPARgamma agonists on *Atp10c* expression was examined. The PPARgamma agonists and anti-diabetic drugs MCC555 and troglitazone both promoted adipogenesis and consequently reduced *Atp10c* expression by 5-fold and 3-fold, respectively. When used in combination with the PPARgamma antagonist GW9662, treatment rescued some of the decrease in *Atp10c* due to MCC555 or troglitazone alone. The pattern of *Atp10c* expression is shown to be opposite to that of *PPARgamma*.

Additionally, the correlation between effectors of glucose and lipid metabolism and *Atp10c* was investigated. Treatment of 3T3-L1 adipocytes with insulin and dexamethasone showed significantly increased expression of *Atp10c*; treatment with the  $\beta$ -adrenergic factor isoproterenol slightly decreased expression. This suggests



transcriptional control of *Atp10c* by hormonal factors, but not  $\beta$ -adrenergic factors, during differentiation.

To further explore the function of *Atp10c* in lipid metabolism, ATP10C silencing through transient transfection of 3T3-L1 cells was first optimized to ultimately allow the assessment of changes in proteins related to obesity and diabetes. An 84% and 77% knockdown of *Atp10c* gene expression in preadipocytes and adipocytes, respectively, was achieved. To elucidate a potential role for *Atp10c*/ATP10C in the insulin signaling pathway, glucose uptake was investigated. Following *Atp10c* silencing in 3T3-L1 adipocytes, glucose uptake was significantly increased at both 24 and 48 hours.

Based on the results presented herein, the *Atp10c* gene and ATP10C protein have an important role in the insulin signaling pathway and may be involved in adipogenesis.

## TABLE OF CONTENTS

CHAPTER 1. INTRODUCTION .....	1
CHAPTER 2. LITERATURE REVIEW .....	3
Obesity and Type 2 Diabetes Mellitus (T2DM).....	3
Animal models of obesity and T2DM .....	4
Atp10c .....	9
Insulin signaling pathway .....	14
Fatty acid uptake.....	16
Adipogenesis .....	19
PPARs and TZDs .....	21
RNA interference.....	24
Research project overview .....	27
CHAPTER 3. EXPERIMENTAL INVESTIGATIONS.....	29
Abstract .....	29
Introduction .....	30
Materials and methods.....	31
Results .....	41
Discussion .....	72
CHAPTER 4. CONCLUSIONS AND FUTURE DIRECTIONS.....	81
LIST OF REFERENCES .....	85
APPENDIX.....	100
VITA.....	120

## LIST OF FIGURES

Figure 1: Heterozygous mice inheriting a <i>p</i> deletion on MMU 7.....	8
Figure 2: An integrated physical and deletion map of MMU 7.....	10
Figure 3: Insulin action in target tissues. ....	15
Figure 4: A model for cellular fatty uptake. ....	18
Figure 5: A model for the development of adipocytes. ....	20
Figure 6: Possible modes of anti-diabetic TZD action. ....	25
Figure 7: RNAi pathway.....	26
Figure 8: <i>Atp10c</i> mRNA is expressed in 3T3-L1 cells. ....	42
Figure 9: <i>Atp10c</i> mRNA is expressed in primary preadipocytes and adipocytes.....	43
Figure 10: Different sample loading buffers can be used for Western blots. ....	45
Figure 11: Peptide neutralization shows an ATP10C protein band at 70kDa. ....	47
Figure 12: ATP10C protein expression increases throughout differentiation. ....	48
Figure 13: <i>Atp10c</i> mRNA expression is regulated by PPAR $\gamma$ agonists and antagonists..	50
Figure 14: <i>Atp10c</i> and PPAR $\gamma$ mRNAs are oppositely regulated in 3T3-L1 cells during adipogenesis.....	52
Figure 15: ORO staining shows morphological changes during adipogenesis in 3T3-L1 cells following treatment with PPAR $\gamma$ agonists and antagonists.....	53
Figure 16: ORO quantitation confirms adipogenesis in 3T3-L1 cells following treatment with PPAR $\gamma$ agonists and antagonists.....	54
Figure 17: <i>Atp10c</i> mRNA expression is regulated conversely to that of <i>resistin</i> mRNA in 3T3-L1 adipocytes following treatment with hormonal factors. ....	56
Figure 18: <i>Atp10c</i> mRNA expression is regulated in primary adipocytes following treatment with hormonal factors. ....	57
Figure 19: Standardization of <i>Atp10c</i> mRNA knockdown in 3T3-L1 preadipocytes using siRNA. ....	58

Figure 20: ATP10C protein is knocked down in 3T3-L1 preadipocytes using siRNA....	59
Figure 21: Standardization of <i>Atp10c</i> mRNA knockdown in 3T3-L1 adipocytes using siRNA. ....	61
Figure 22: ATP10C protein is knocked down in 3T3-L1 adipocytes using siRNA. ....	62
Figure 23: Expression of additional genes in 3T3-L1 adipocytes following <i>Atp10c</i> mRNA knockdown using siRNA. ....	63
Figure 24: <i>Atp10c</i> mRNA expression is knocked down throughout differentiation using siRNA. ....	64
Figure 25: Primary cultures treated with <i>Atp10c</i> siRNA show a knockdown in mRNA levels. ....	66
Figure 26: Standardization of glucose uptake in 3T3-L1 adipocytes. ....	67
Figure 27: Treatment of 3T3-L1 adipocytes with <i>Atp10c</i> siRNA increases glucose uptake. ....	68
Figure 28: Subcellular fractionation of 3T3-L1 preadipocytes and adipocytes.....	69
Figure 29: Subcellular fractionation of 3T3-L1 adipocytes treated with insulin.....	70
Figure 30: A second subcellular fractionation of 3T3-L1 adipocytes treated with insulin. ....	71

## LIST OF ABBREVIATIONS

Ad	Adipocyte
APLT	Aminophospholipid translocase
C/EBP	CCAAT/enhancer-binding protein
ER	Endoplasmic reticulum
ERAD	Endoplasmic reticulum-associated protein degradation
FATP	Fatty acid transport protein
HBSS	Hank's Balanced Salt Solution
IRS	Insulin receptor substrate
MMU 7	Mouse chromosome 7
ORO	Oil Red O
PA	Preadipocyte
PDK-1	Phosphate-dependent kinase-1
PE	Phosphatidylethanolamine
pi	Protease inhibitors
PI3K	Phosphoinositide 3-kinase
PPAR $\gamma$	Peroxisome proliferator-activated receptor $\gamma$
<i>pref-1</i>	Preadipocyte factor-1
PS	Phosphatidylserine
RISC	RNAi-induced silencing complex
RNAi	RNA interference
RT	Room temperature
RT-PCR	Reverse transcriptase-polymerase chain reaction

siRNA	Small interfering RNA
T2DM	Type 2 diabetes mellitus
TGZ	Troglitazone
TZD	Thiazolidinedione

## CHAPTER 1. INTRODUCTION

Obesity and diabetes are extremely prevalent in today's society, with the numbers continuing to rise each year [1-3]. With no recent research to indicate that these numbers are going to decline in the future, obesity and diabetes remain a major public health concern. New approaches must be undertaken to examine the correlation between the two in order to elucidate unknown players in metabolic pathways related to obesity and diabetes.

The novel type IV subfamily of P-type ATPases are putative aminophospholipid translocases that have been associated with human disorders of intramembranous transport [4, 5]. Studies in yeast have also shown that these flippases are important in protein trafficking in the exocytic and endocytic pathways [6, 7]. Using positional cloning and genomic sequencing strategies, the type IV P-type ATPase *Atp10c* has been cloned to mouse chromosome 7 [8]. Heterozygous mice inheriting a maternal deletion of the *Atp10c* gene exhibit typical hallmarks of insulin resistance syndrome including obesity, hyperinsulinemia, and insulin resistance [9] and represent a novel genetic model of diet-induced obesity and T2DM.

The precise biological role of these flippases in intracellular signaling and protein trafficking are poorly understood, although there is a consensus on the physiological function. The hypothesis of this project is that there is an association between type 4 ATPase mediated phospholipid translocase activities and cell signaling and intracellular protein trafficking. To investigate the biological role of *Atp10c*/ATP10C in the process of adipogenesis and the insulin signaling pathway, the Swiss murine 3T3-L1 cell line was used as an *in vitro* model [10]. RT-PCR and Western blotting experimental techniques

were employed to monitor gene and protein expression. Following a basic characterization of *Atp10c*/ATP10C, the effect of PPAR $\gamma$  agonists and effectors of glucose and lipid metabolism on *Atp10c* expression was examined. Lastly, glucose uptake was measured in adipocytes where *Atp10c*/ATP10C was knocked down with siRNA in order to elucidate the possibility that *Atp10c*/ATP10C is involved in the insulin signaling pathway.



## CHAPTER 2. LITERATURE REVIEW

### Obesity and Type 2 Diabetes Mellitus (T2DM)

Obesity is a major public health concern that continues to affect more individuals each year [1-3, 11-13]. Between 1980 and 2002, the prevalence of obesity doubled in adults and the prevalence of overweight children and adolescents tripled [3, 14, 15]. The most recent data from the 2003-2004 National Health and Nutrition Examination Survey (NHANES) demonstrate that the number of overweight children and adolescents and obese men has increased significantly from 1999 to 2004 in the United States [13]. Although there was no overall increase among women, the prevalence of obesity remained constant at 33.2%. Similar rising trends are being observed throughout the world [3, 16-19].

Obesity is a major risk factor for a number of common disorders, including non-insulin-dependent type 2 diabetes mellitus (T2DM) [20-22], atherosclerosis [23, 24], and non-alcoholic fatty liver disease [25, 26]. T2DM is characterized by insulin resistance in the muscle, fat, and liver, combined with a decreased ability of pancreatic  $\beta$  cells to properly respond to elevated glucose levels. Increases in both obesity and diabetes among adults in the United States continue in both sexes, all ages, all races, all educational levels, and all smoking levels [2]. The prevalence of diabetes is also on the rise throughout the world, with the projection that 366 million people will have diabetes by 2030 [27].

There has been no recent research to indicate that these numbers are declining, leaving the high levels of obesity and T2DM as a major public health concern. Based on these increasing statistics, there is a dire need for new approaches to examine the

correlation between obesity and T2DM, to understand what causes these diseases, and to elucidate unknown players in metabolic pathways related to obesity and T2DM. An important link between obesity and T2DM is insulin resistance, the etiology of which is complex in humans, with both genetic predisposition and environmental factors, including nutritional and/or hormonal factors, playing an important role [28-31]. However, research searching for genes related to obesity and T2DM in humans has two major pitfalls. First, the genetic influence on these diseases is based on multiple, polymorphic single genes that each interact with other genes and may be exposed to specific environmental factors. Second, if research focuses on the relation between a single gene and obesity or T2DM while failing to control for other involved genes and environmental exposures that have not been identified, then both experimental and observational studies become difficult to interpret. Because these factors are difficult to control in human subjects, polygenic diseases can be more easily studied in animal models and then translated into human homologs and phenotypes.

### **Animal models of obesity and T2DM**

Animal models have been used in research to investigate everything from drug testing [32] to Huntington's disease [33] to cancer [34] to obesity [35] to diabetes [36]. One of the common animal models used to study obesity and T2DM is the mouse model [28, 35, 37-42], which can include spontaneous or artificially generated single-gene loss-of-function mutation models [35].

### ***Spontaneous single-gene loss-of-function mutation mouse model***

Spontaneous mutational events in large breeding establishments can lead to genetic defects that have major loss-of-function effects in subsequent offspring. However, the time between discovery of the defect and subsequent genetic and physiological characterization may be delayed. For example, the *ob/ob* mouse was discovered in 1950 when a spontaneous mutation led to obese mice [43], but characterization of the gene did not reveal that the defect was a single base pair deletion resulting in a premature stop codon for the *leptin* gene, which is highly expressed in adipocytes, until 1994 [44].

Other spontaneous mutations have resulted in the discovery of  $A^y/A^y$  mice, which have a deletion of the *lethal yellow* ( $A^y$ ) gene and result in obese, diabetic mice with an all-yellow coat [45]. The *db/db* mouse represents a model for diabetic dyslipidemia, with a deletion of the *diabetes* (*db*) gene [46]. Additional spontaneous single-gene mutations in *fat* and *tubby* (*tub*) have also been identified, leading to obese mice that exhibit hyperglycemia, hyperinsulinemia, and elevated levels of total and HDL cholesterol [47, 48].

Although there are at least 10 single-gene loss-of-function mutations leading to obesity that have been discovered and genetically characterized, genetic screens in humans have indicated that very few individuals actually have a loss-of-function mutation in any of these genes [49, 50]. The importance of these genes lies in further understanding how the energy regulation system works and identifying other key players of adipogenesis and the insulin signaling pathway [35].

### *Artificially generated single-gene loss-of-function mutation mouse model*

After witnessing spontaneous single-gene loss-of-function mutations, scientists began to accelerate the process by increasing the mutation rate artificially through exposure to mutagenic chemicals or radiation [8, 51]. These models can be used to look at energy regulation as well as other aspects of animal function [35]. But this approach can be costly in order to phenotype the mice, considering the mouse genome consists of close to 40,000 genes. In addition, the effect of the gene deletion still must be visible in the progeny. On the other hand, after these models are generated, they can be maintained and used for further research purposes. One such mouse model is described in a later section.

### *Transgenic mouse model*

Single-gene mutations can also be artificially generated as a transgenic model, where the mouse is genetically engineered to contain a transgene to cause overexpression of, mutation in, or silencing of a target gene [42]. The first transgenic mouse was created by Brinster *et al* in 1982 where the promoter region of the mouse metallothionein-I gene fused to the herpesvirus thymidine kinase gene was injected into fertilized mouse eggs, which were then transferred to a surrogate [52].

Transgenic mice can be generated not only to overexpress a certain gene [53-55], but also to completely silence a gene. These “knockout” mice are created by complete ablation of the target gene in all tissues to yield an associated phenotype [35]. For example, silencing estrogen receptor- $\alpha$  in male and female mice leads to increased white adipose tissue [56] whereas silencing the cannabinoid receptor CB1 leads to leanness and resistance to diet-induced obesity [57].

These models can also sometimes lead to unexpected phenotypes, such as the *axl* model that was originally generated to investigate the role of the tyrosine kinase receptor *axl* in leukemia. Augustine *et al* found that constitutively expressing the *axl* gene actually resulted in mice with T2DM [58].

Although expensive to generate, transgenic mouse models can be extremely useful in scientific research to provide clues concerning the normal function of a specific gene and how it may cause or contribute to a certain disease.

#### *A novel polygenic mouse model*

Mice containing radiation-induced chromosomal deletions on mouse chromosome 7 (MMU 7) located at the *pink-eyed dilution (p)* locus were generated and maintained at Oak Ridge National Laboratory [59, 60]. The *p*-locus-associated obesity-1 (*plo 1*) region of MMU 7 is associated with T2DM and maps to a region of quantitative trait loci affecting body fat [8]. Using genetic mapping and phenotypic analyses, two distally extending heterozygous deletions,  $p^{23DFiOD}$  and  $p^{30PUb}$ , were identified that encompass the *p* locus on MMU 7 and cause diet-induced obesity and T2DM [59-61]. Heterozygous mice inheriting either of the two *p* deletions maternally that were fed a high-fat diet showed a significantly higher body weight, adiposity index, and plasma insulin, leptin, and triglyceride concentrations compared to heterozygotes inheriting the deletion paternally (Figure 1) [8].

Intraperitoneal glucose and insulin tolerance tests showed altered glucose tolerance and insulin resistance after consumption of a high-fat diet for 4, 8, and 12 weeks. A 30% decrease in insulin-stimulated glucose uptake in white adipose tissue was also seen after eating a high-fat diet for both 4 and 12 weeks, while a 35% decrease in the



**Figure 1: Heterozygous mice inheriting a  $p$  deletion on MMU 7.**

Mice inheriting the *pl* locus maternally (right mouse) are significantly fatter than those inheriting the same deletion paternally (left mouse). These mice are age- and sex-matched. *Photo courtesy of E. Michaud, ORNL.*

soleus muscle was achieved only after 12 weeks [9]. Based on the above data, these *p* deletion mutants represent a novel polygenic mouse model associated with obesity and T2DM.

### **Atp10c**

After the novel polygenic mouse model of obesity and T2DM described above was generated, this phenotype was deletion-mapped to the *plo 1* region, which encompasses the 1 cM region between  $\gamma$ -aminobutyric acid A receptor  $\beta$ -3 (*Gabrb3*) and ubiquitin protein ligase E3A (*Ube3a*) of MMU 7. *Gabrb3* has been linked to cleft palate formation in humans, while mutations in *Ube3a* cause the human neurological disorder Angelman Syndrome [8]. This region is syntenic to the human chromosomal region HSA 15q11-q13 [62-65]. DNA sequencing showed that the only gene within this interval was a P-type ATPase [8], which was later identified as *Atp10c*, or *pfatp* (Figure 2) [62, 66].

*Atp10c* is a novel type IV P-type ATPase and putative aminophospholipid transporter (APLT) containing 21 exons. In  $p^{23DFiOD}$  heterozygotes, the complete *Ube3a* and the first two exons including the 5' promoter region of *Atp10c* are deleted whereas the complete *Atp10c* and *Ube3a* genes along with the 5' and 3' flanking regions are deleted in  $p^{30PUb}$  mice [66]. Since *Ube3a* transgenic mice are not obese [67, 68], it is reasonable to expect that it is not the candidate for the altered glucose and lipid metabolism disorders associated with the *p* locus deletions.

The sequence of the human ortholog, *ATP10C*, has been mapped to 15q12, which is part of the critical region for Angelman Syndrome [62-64, 69]. Another deletion

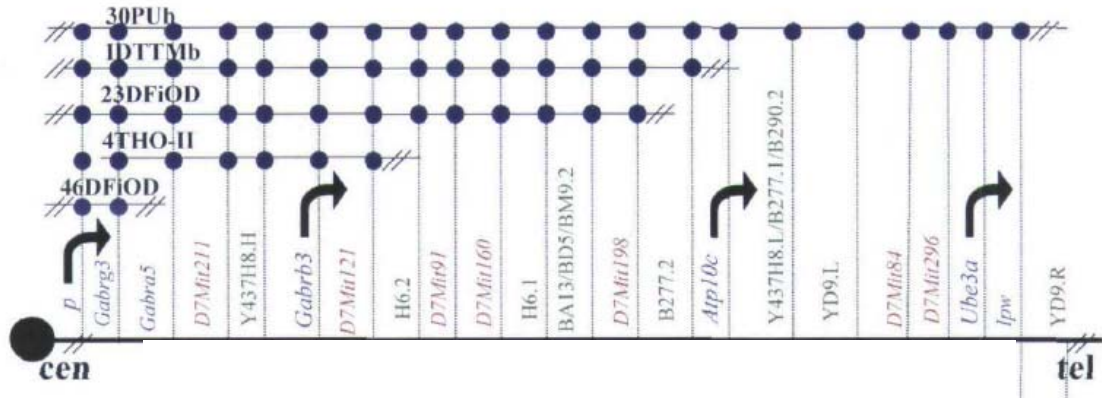


**Figure 2: An integrated physical and deletion map of MMU 7.**

This deletion map shows that *Atp10c* is the only transcript located in the region between *Gabrb3* and *Ube3a* on MMU 7. The solid black line in the middle is MMU 7 extending from the centromeric (cen) to telomeric (tel) end. The arrows above the genes denote the direction of transcription and the solid lines above the chromosome show the *p* deletions generated. Modified from Dhar et al [66].



mouse model has been reported that encompasses the same region as that of *Atp10c*, which carries a transgene insertion that created a 4Mb deletion and represents a model of Angelman Syndrome when maternally inherited [70]. The Angelman Syndrome mice are viable and fertile but become obese at 4-6 months of age [70]. Cattanaach *et al* also reported a mouse model of Angelman Syndrome with late-onset obesity reported [71]. All of these models implicate *Atp10c* to be a strong candidate for the obesity phenotype. Human geneticists have also identified a class of AS patients with the additional phenotype of increased body mass index [72], suggesting that *Atp10c/ATP10C* may play an important role in obesity of multiple etiologies, in mice and humans, respectively.

### ***P-type ATPases***

P-type adenosine triphosphatases (P-type ATPases) are the best known and most extensively studied membrane transporters. Many of these integral membrane proteins mediate the ATP-dependent transport of small cations across biological membranes by the addition or removal of a high energy inorganic phosphate to or from an aspartate residue in the conserved DKTGTLT amino acid sequence [73, 74].

Using phylogenetic analysis, P-type ATPases have been divided into five major subfamilies [5]. The type I subfamily of P-type ATPases includes heavy metal ion transporters, while the type II subfamily catalyzes transport of non-heavy metal ions, such as the  $\text{Na}^+\text{K}^+$ -ATPase [73, 74]. The type III subfamily includes ATPases expressed in plants and fungi that transport magnesium and hydrogen ions, while the type IV subfamily members are found to transport phospholipids in eukaryotic cells. Although only one member has been identified in the type V subfamily, this yeast ATPase has been implicated in cellular calcium homeostasis and endoplasmic reticulum (ER) function [5].

Type IV P-type ATPases can be further subdivided into six different classes based on sequence similarities [75]. *Atp10c* is part of class 1, which includes the aminophospholipid translocases that are responsible for the asymmetric distribution of membrane phospholipids [76]. Numerous type IV P-type ATPases have already been associated with human disorders of intramembranous transport [4, 5], providing additional evidence to look at the role of the novel type IV P-type ATPase *Atp10c* in metabolic pathways.

### ***Aminophospholipid transporters***

The asymmetric phospholipid bilayer of a cell includes the choline-containing phosphatidylcholine (PC) and sphingomyelin (SM) along with the aminophospholipids phosphatidylserine (PS) and phosphatidylethanolamine (PE). PC and SM are localized in the outer leaflet, while PS and PE are concentrated in the inner leaflet [6, 77-79]. This asymmetry is essential to the mechanisms involved in normal cellular homeostasis and is maintained by an energy-dependent translocation of aminophospholipids from the outer to the inner leaflet catalyzed by aminophospholipid transporters (APLTs). Randomization of phospholipids, which tend to equilibrate between the two leaflets, can affect the structure and activity of channels, transporters, and signal transducing proteins. In order to actively maintain the asymmetric phospholipid distribution, proteins that translocate the phospholipids are necessary.

These lipid flippases, or lipid translocases, are a class of proteins involved in regulation of phospholipid distribution in membrane bilayers [7]. Studies in yeast have also shown that these flippases are important in protein trafficking in the exocytic and endocytic pathways [6, 7]. Members of the type IV P-type ATPase subfamily are thought

to catalyze the transbilayer transport of amphipathic molecules, such as the aminophospholipids PS and PE [79-81]. The founding member of this subfamily is the yeast *drs2* gene, which is an ortholog of mouse *Atp10c* that has been linked to ribosomal assembly, formation of Golgi-coated vesicles, and maintenance of bilayer asymmetry [82-84]. The murine *Atp8a1* gene has also been recently investigated as a potential aminophospholipid flippase; it was found to have properties similar to, but distinct from, the properties of these flippases [85]. A deficiency of the human type IV P-type ATPase *ATP8B1* caused a loss of membrane asymmetry and reduced resistance to hydrophobic bile salts. This loss of phospholipid asymmetry due to lack of a lipid flippase may subsequently impair bile salt transport and cause cholestasis [86].

Translocase activity has been detected in a variety of membranes, including the plasma membranes of erythrocytes, fibroblasts, spermatozoa, and the Golgi apparatus. Changes in the physical properties of the lipid bilayers are suggested to alter several functions such as cell-cell interaction, signal transduction pathways, and clotting disorders by modulating the activity of lipid-dependent proteins. A loss of erythrocyte PS asymmetry is seen in patients with diabetes or strokes [87-89], which emphasizes the need to maintain the asymmetry of the lipid bilayer for normal cellular functions. Changes in the composition of the lipid bilayer along with alterations in the asymmetry of the adipocyte membranes result in obesity-related phenotypes. Studies have suggested that SM, which accumulates in cell membranes in diseases with peroxisomal disorders, may be involved with peroxisome proliferator-activated receptors (PPARs) and may also contribute to insulin resistance [88, 89]. APLTs have a role(s) in insulin signaling,

illustrating the importance of type IV P-type ATPases in cell biology and human health and disease.

### **Insulin signaling pathway**

Insulin is an important anabolic hormone that regulates a number of cell processes with a strong, direct impact on cellular homeostasis. It increases the storage of triglycerides in adipocytes via stimulation of lipogenesis (fat synthesis), inhibition of lipolysis (fat breakdown), and differentiation of preadipocytes to adipocytes. The resulting increase in adiposity causes secretion of various adipokines that can also lead to secondary effects in liver and skeletal muscle. An abnormality in any of these processes will result in insulin resistance, producing high levels of glucose and lipids in the blood. Insulin resistance in skeletal muscle and adipose tissue can be caused by alterations in insulin binding and signaling that effect glucose and lipid metabolism. In both tissues, insulin sensitivity improves when insulin binds to its receptor, resulting in downstream effects that lead to the uptake of glucose from the blood [90, 91].

A key rate-limiting step involved in an impaired insulin response is a defect in glucose transport. Insulin stimulates glucose transport via translocation of an adipose tissue- and muscle-specific glucose transporter protein, GLUT4, from the intracellular space to the cell surface. Stimulation occurs when insulin binds to its heterotetrameric integral membrane receptor, leading to activation of the tyrosine kinase domain of the receptor. This triggers a signaling cascade that results in the translocation and fusion of intracellular vesicles containing GLUT4 to the plasma membrane, which accounts for the majority of glucose disposal in both muscle and adipose tissue (Figure 3) [92-95].

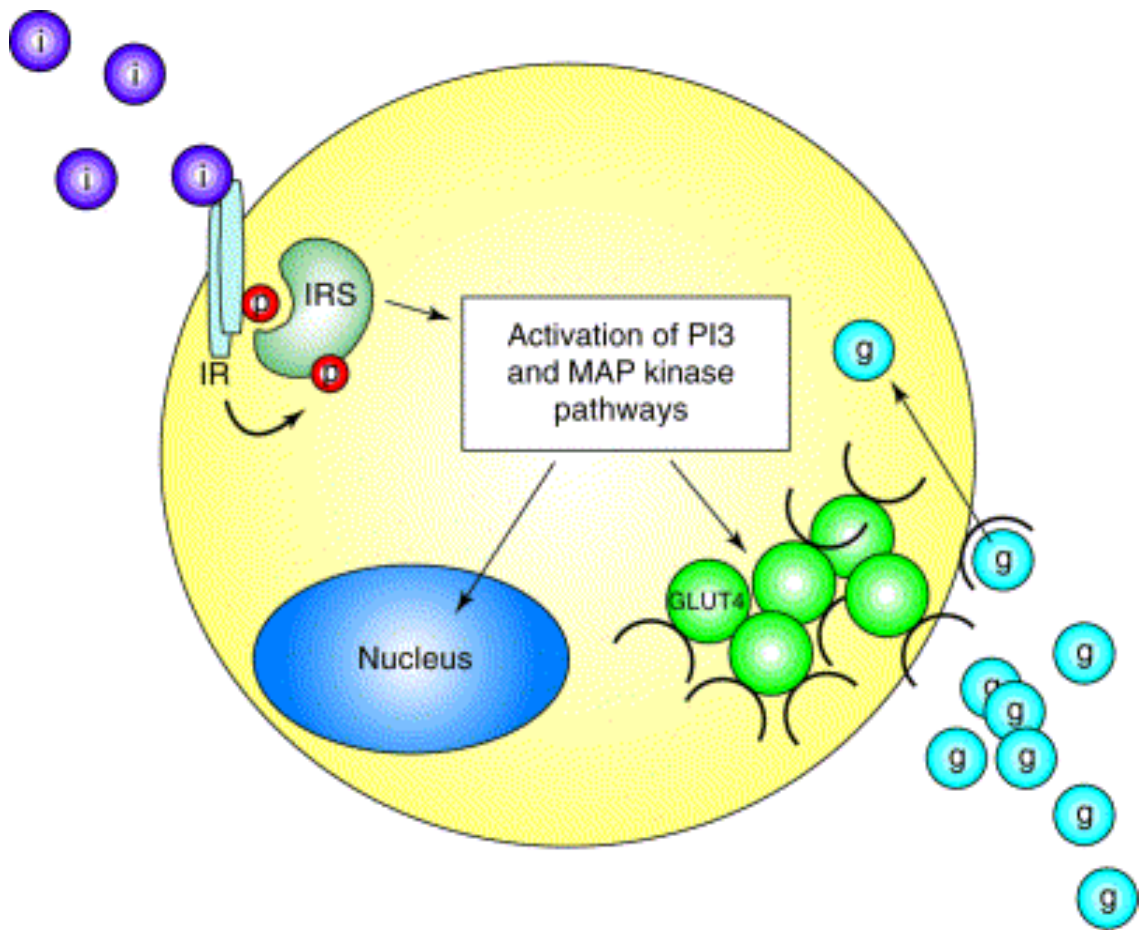


**Figure 3: Insulin action in target tissues.**

Insulin (i) binds to hetero-oligomeric insulin receptor (IR), stimulating autophosphorylation of the receptor. This, in turn, leads to phosphorylation of the docking proteins IRS1 and IRS2. IRS1 and IRS2 are coupled to the mitogen-activated protein (MAP) kinase and phosphoinositide 3 (PI3) kinase signaling cascades. This leads to translocation of vesicles containing the GLUT4 glucose transporter to the plasma membrane, facilitating glucose (g) uptake by target tissues. Insulin signaling also ultimately leads to changes in gene expression. *Modified from Gannon [38].*

A major cause of insulin resistance in adipose tissue appears to be a depletion of GLUT4. Conversely, GLUT4 levels are normal in the skeletal muscle. Thus, insulin resistance seems to be caused by a defect in GLUT4 translocation. Abnormalities in glucose uptake leading to insulin resistance can also arise from defects in insulin signal transduction involving effector molecules in the pathway such as the insulin receptors IRS-1, IRS-2, and IRS-3, and phosphoinositide 3-kinase (PI3K). Defects in any part of the insulin signaling pathway have been shown to be important in the pathogenesis of insulin resistance [92, 96, 97]. The question of how impaired glucose uptake and defective insulin signaling in adipose tissue and skeletal muscle contributes to whole body insulin resistance remains unanswered, but targeting insulin resistance has still become an important therapeutic goal in the treatment of T2DM.

### **Fatty acid uptake**

In addition to abnormalities in the insulin signaling pathway, a second aspect of insulin resistance is its strong linkage with the regional distribution of adipose tissue. Abdominal adipose tissue is more metabolically active than peripheral adipose tissue, resulting in the release of more free fatty acids into the blood that are absorbed by the liver and ultimately elevate glucose levels. In the peripheral tissues, elevated levels of free fatty acids impair insulin secretion by the pancreas and result in increased insulin resistance [98].

Fatty acids containing aliphatic tails with 16 or more carbons are known as long-chain fatty acids and act as fuels to generate energy in the form of ATP. These fatty acids are imported into adipocytes and transformed into triglycerides when bound to

glycerol. The first step in the utilization of fatty acids is uptake across the plasma membrane, which can occur either through diffusion or by protein mediation. Similar to the uptake of glucose in the insulin signaling pathway, fatty acid uptake is also controlled by insulin. A highly regulated process, fatty acid uptake mainly requires fatty acid transport proteins (FATPs), which are also known as solute carrier family 27 (SLC27) [99, 100]. Insulin induces an increase in fatty acid uptake by translocation of FATPs from an intracellular compartment to the plasma membrane in adipocytes. There have been six FATP genes identified in human and mouse genomes that each have special physiological functions and specific tissue distribution [99-101]. Analyses of FATP1-knockout mice have shown that insulin causes translocation of FATP1, which is expressed in adipose tissue, skeletal muscle, and heart, and leads to enhanced fatty acid uptake. However, the closely related FATP4 and CD36 proteins did not show a similar localization, suggesting that FATP1 activity has an important role in cellular homeostasis. FATP1 translocation has been suggested to involve a flip-flop or translocase mechanism [102-104]. Stahl proposed a similar model for cellular fatty uptake (Figure 4) in which long-chain fatty acids may be transported across the plasma membrane directly by FATP complexes or first bind to CD36 proteins, which then transfer the fatty acids on to FATPs [99]. Compared to research on GLUT4 trafficking and the insulin signaling pathway, mechanisms underlying FATP1 trafficking in the uptake of fatty acids are not clearly understood. However, there is some overlap between these two pathways.

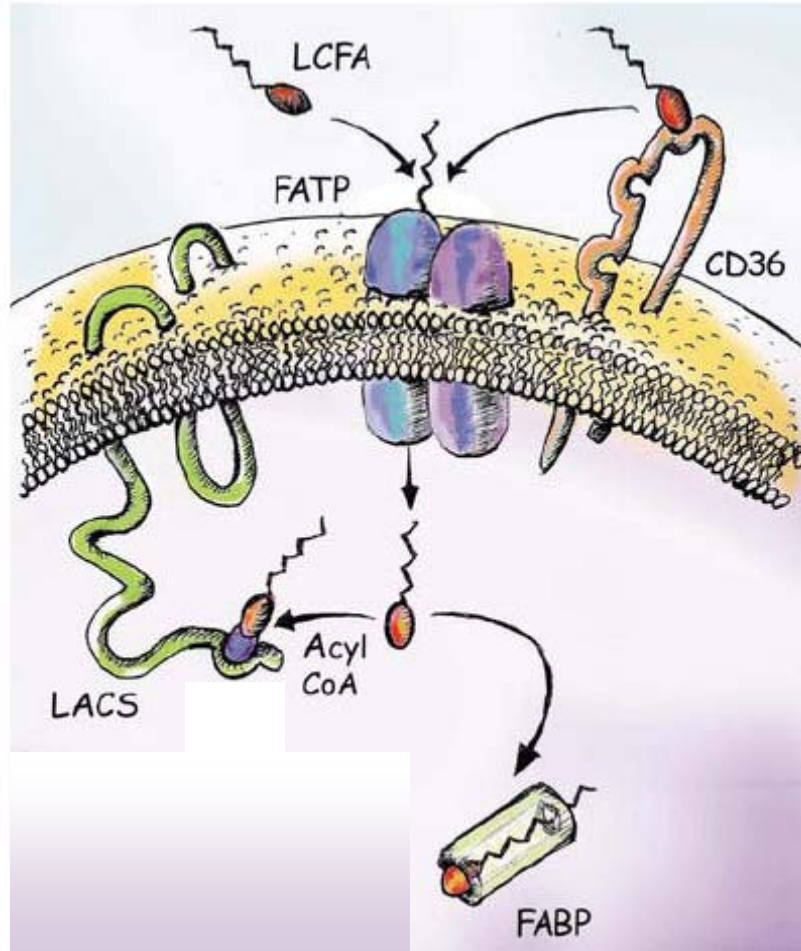


**Figure 4: A model for cellular fatty uptake.**

Extracellular long-chain fatty acids (LCFA) may bind directly to fatty acid transport protein (FATP) complexes to be transported into cells or they could bind to CD36 that will then transfer the LCFA to a FATP dimer. In order to prevent their efflux out of the cell, intracellular LCFAs are coupled to coenzyme A (CoA) by long-chain fatty acyl-CoA synthetase (LACS). Fatty acid binding proteins (FABPs) act as a cytoplasmic buffer.

*Modified from Stahl [99].*



## Adipogenesis

As described above, free fatty acids are imported into adipocytes and transformed into lipid molecules. An increase in the number and/or size of these adipocytes leads to obesity. The development of adipocytes, or adipogenesis, is an important process leading to the deposition of fat that involves biochemical, physical, and molecular changes in the conversion of undifferentiated to differentiated cells. This process is also largely regulated by insulin, which exerts transcriptional and translational controls on adipogenic factors.

The transition from an egg to the determination and conversion of preadipocytes into mature adipocytes occurs in a series of stages *in vivo* (Figure 5). Adipogenesis is the conversion of undifferentiated, fibroblast-like preadipocytes to mature, rounded adipocytes following a phase of clonal expansion and subsequent growth arrest. Since fat cell differentiation *in vitro* recapitulates most of the key features of adipogenesis *in vivo*, cell culture techniques are extensively used to investigate this process [105].

Research aimed at identifying regulatory factors involved in adipocyte differentiation has begun to provide important clues about adipocyte biology and its role in the development of obesity and T2DM. Efforts to identify key inhibitors or activators of adipogenesis assume that the potential to control or reverse this process might ultimately lead to a way to inhibit the development of obesity and its associated pathologies. Studies have shown that lipoprotein lipase is expressed early in the process, followed by expression of C/EBP $\beta$  and C/EBP $\delta$ . Subsequently, the master regulators of differentiation, C/EBP $\alpha$  and PPAR $\gamma$ , are expressed. Triglycerides also accumulate in the

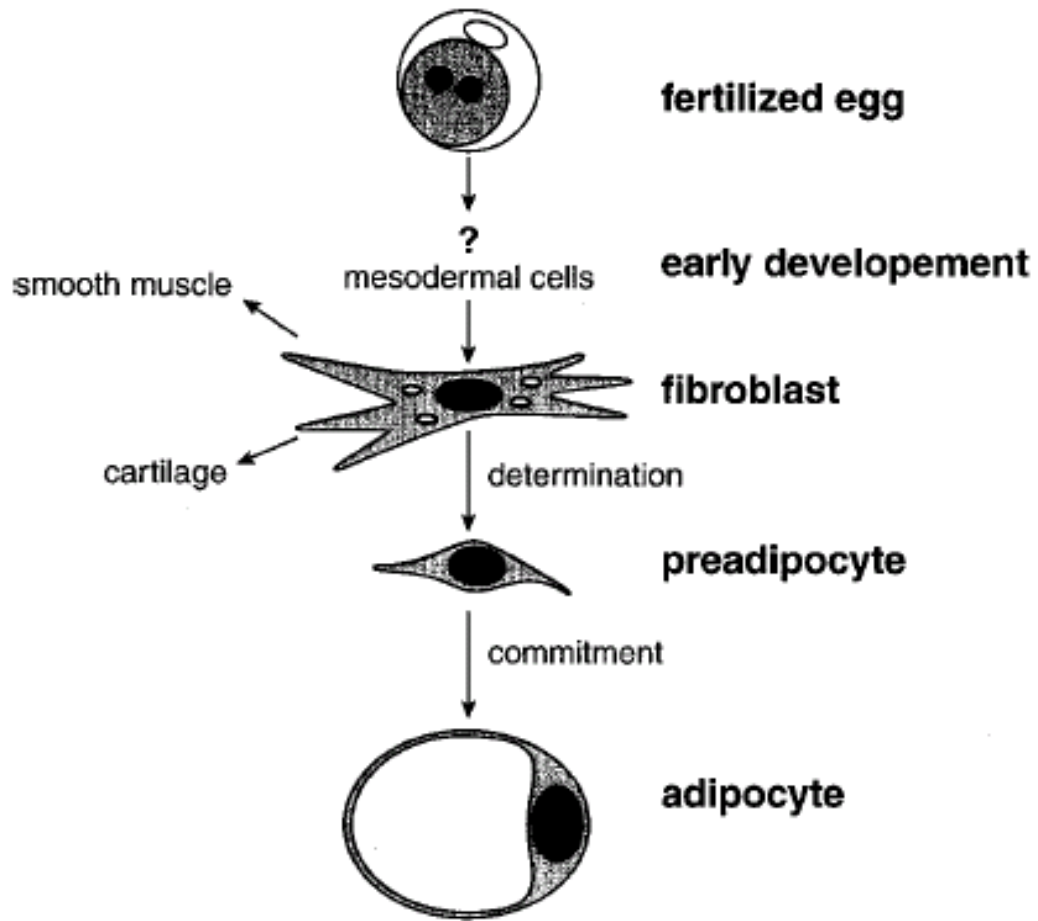


**Figure 5: A model for the development of adipocytes.**

Beginning with a fertilized egg, this shows a potential model for the development of adipocytes based on the developmental stages of determination and commitment.

Darkened shapes represent nuclei or pronuclei. *Modified from Ntambi and Kim [105].*

adipocytes and expression of fatty acid synthase, GLUT4, adipocyte binding protein 2, and resistin increases [105-107].

## **PPARs and TZDs**

### *Peroxisome proliferator-activated receptors (PPARs)*

The nuclear receptor subfamily peroxisome proliferator-activated receptors (PPARs) are transcription factors that bind to specific peroxisome proliferator response elements (PPREs) in an enhancer site of a target gene upon binding of a ligand to the PPAR [108, 109]. When an agonist binds to a PPAR, the conformation of PPAR is altered and stabilized to allow recruitment of transcriptional coactivators and result in increased gene transcription. Conversely, binding of an antagonist to PPAR will alter the conformation to ultimately result in decreased gene transcription.

There are three isoforms that are each encoded by separate genes: PPAR $\gamma$ , PPAR $\alpha$ , and PPAR $\delta$ . All of the PPARs are the primary targets of synthetic compounds used to treat diabetes and dyslipidemia, while many of them also have putative roles in other metabolic disorders [108, 109]. One of the more widely studied isoforms is PPAR $\gamma$ , which is involved in both adipogenesis and the insulin signaling pathway.

#### *PPAR $\gamma$ and adipogenesis*

PPAR $\gamma$  is considered to be the master regulator of adipogenesis, controlling many known and currently undiscovered aspects of the process. Differentiation is partly regulated by a cascade of transcriptional events that lead to activation of CCAT/enhancer binding proteins (C/EBPs) and PPAR $\gamma$  by insulin, dexamethasone, and isobutylmethylxanthine that constitute the induction cocktail [110, 111]. Additional

regulation of PPAR $\gamma$  activity during this process is a widely studied area with recent studies showing a role for mitogen-activated protein kinase/extracellular regulated kinase (MEK/ERK) signaling along with activation of C/EBP $\beta$  in the regulation of PPAR $\gamma$  activity [110, 112]. Although intimately involved with fat cell differentiation, there is still so much missing information concerning the role of PPAR $\gamma$  in this process that constitutes the focus of many current research projects.

#### *PPAR $\gamma$ and the insulin signaling pathway*

In addition to its role in adipogenesis, PPAR $\gamma$  is involved in the insulin signaling pathway. Liao *et al* recently demonstrated that suppression of PPAR $\gamma$  decreased insulin-stimulated glucose uptake [113]. They also showed that PPAR $\gamma$  is essential for the process of adipogenesis, but is not as necessary for the maintenance of an adipocyte state. Although a PPAR $\gamma$  ligand with a high affinity, the novel modulator LG100641 does not actually activate PPAR $\gamma$ ; it blocks thiazolidinedione-induced PPAR $\gamma$  activation and subsequent adipocyte differentiation [114]. Similar to other PPAR $\gamma$  ligands that do activate PPAR $\gamma$ , LG100641 surprisingly increases glucose uptake in 3T3-L1 adipocytes. The discovery of such PPAR $\gamma$  modulators that increase insulin sensitivity but do not increase adipogenesis is important in the future of improved therapy for metabolic diseases.

#### ***Thiazolidinediones (TZDs)***

Thiazolidinediones (TZDs) are anti-diabetic drugs that enhance insulin sensitivity and improve glucose uptake through the activation of PPAR $\gamma$ . Typically used in the management of T2DM [115], TZDs have also been shown to exert anti-inflammatory

effects on vascular cells [116]. Activation of PPAR $\gamma$  leads to increased adipogenesis, thus treatment with TZDs should increase adiposity. Interestingly, TZDs actually inhibit *leptin (ob)* gene expression, which is predominantly expressed in adipose cells, following treatment of 3T3-L1 adipocytes [117]. These results suggest that the negative regulation of *leptin* by TZDs may indicate that these compounds induce a state of adipocyte differentiation that is subtly different from that induced by the differentiation cocktail. There are numerous types of TZDs, although troglitazone (TGZ) and MCC555 will be discussed here within.

#### *Troglitazone (TGZ)*

Troglitazone (TGZ), originally named CS-045 [118, 119], was the first member of the TZD class of medications to be approved for clinical use [120, 121]. Previous research indicated direct improvement of insulin action in liver, skeletal muscle, and adipose tissue [118-120], along with the reduction of elevated plasma glucose in animal models T2DM [119]. The marketed form of TGZ (Rezulin) was withdrawn in 2000 due to increased hepatotoxicity compared to the TZDs rosiglitazone (Avandia) and pioglitazone (Actos) [122]. However, TGZ is still used in laboratory research today as a representative TZD to investigate effects on PPAR $\gamma$ , adipogenesis, and/or the insulin signaling pathway [123-125].

#### *MCC555*

MCC555, also known as RWJ-241947 [126], is a novel TZD that has been found to have unique characteristics compared to the other TZDs [116, 127, 128]. Its effect on the transcriptional activity of PPAR $\gamma$  depends on the cell type or DNA binding site; it can act as a full agonist, partial agonist, or antagonist [129]. It is also the only TZD thus far

that can activate PPAR $\gamma$ , PPAR $\alpha$ , and PPAR $\delta$  [116]. MCC555 not only exhibits anti-diabetic effects, but also anti-proliferative activity against prostate cancer cells [126] and anti-tumorigenic and/or pro-apoptotic activity in human colorectal cancer cells [130].

### ***Mode of TZD action***

It has been demonstrated that TZDs reduce insulin resistance in adipose tissue, muscle, and the liver through a mechanism that involves activation of PPAR $\gamma$  [131]. However, PPAR $\gamma$  is predominantly expressed only in adipose tissue, not muscle or the liver. This has led to investigations into a more exact mechanism of the action of TZDs.

Although the exact mode of the anti-diabetic action of TZDs drugs is still unknown, there are two main hypotheses [131]. TZDs may cause PPAR $\gamma$ -mediated actions on adipose tissue that indirectly trigger improved glucose homeostasis of skeletal muscle and liver or they may improve insulin sensitivity by direct interaction with muscle and liver *in vivo* (Figure 6). Further research is needed to elucidate an exact mechanism.

### **RNA interference**

RNA interference (RNAi) is a post-transcriptional gene silencing that was first coined in 1998 to describe the observation that double-stranded RNA could be used to block gene expression [132]. It is initiated by a 21-23 nucleotide short interfering RNA (siRNA) that is either generated *in vitro* by cleavage of double-stranded RNA using the enzyme Dicer [133] or generated synthetically and introduced into the cell experimentally (Figure 7). After the siRNA associates with the RNAi-induced silencing complex (RISC), complementary mRNA transcripts are targeted for degradation. This leads to silencing of the gene and, consequently, no new protein is translated.

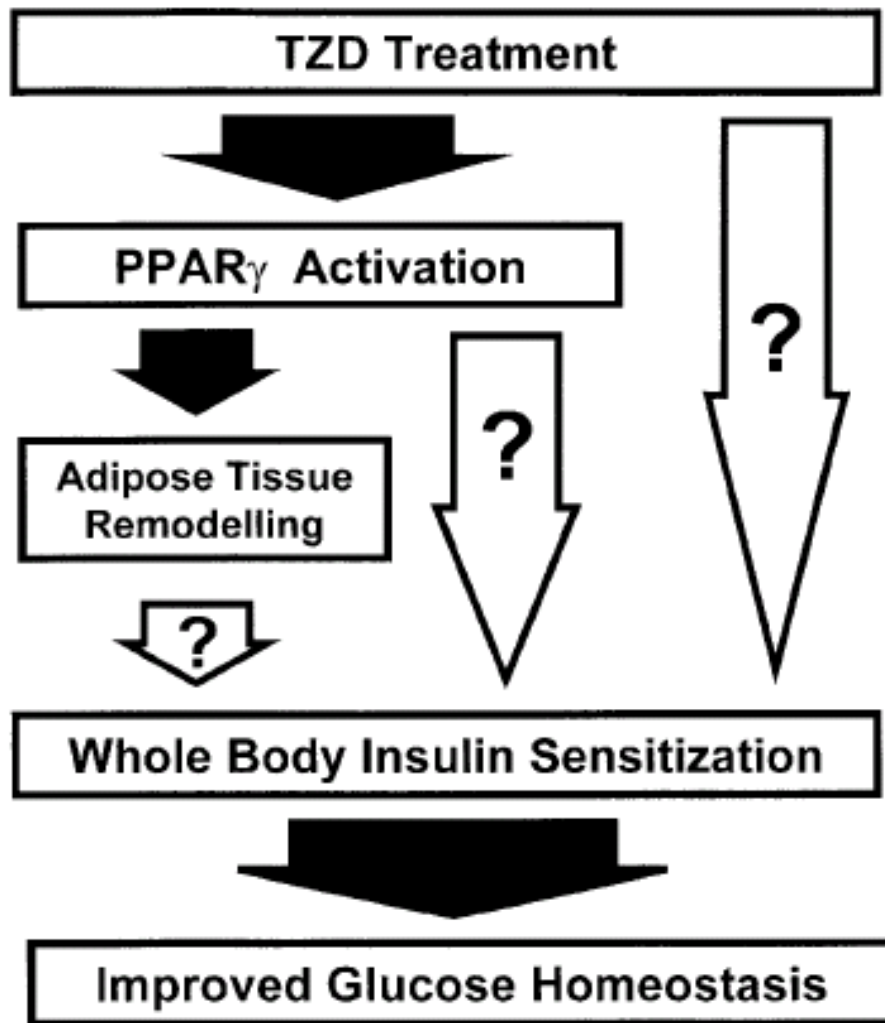


**Figure 6: Possible modes of anti-diabetic TZD action.**

It is known that TZD treatment activates PPAR $\gamma$  and leads to adipose tissue remodelling along with the fact that insulin sensitization leads to improved glucose homeostasis. However, the chain of events leading from TZD treatment to improved glucose homeostasis is unknown. PPAR $\gamma$  activation and/or direct effects on adipose tissue may be the sole cause of improved glucose homeostasis, or TZD treatment may directly improve glucose homeostasis by direct interaction. *Modified from Fursinn et al [131].*

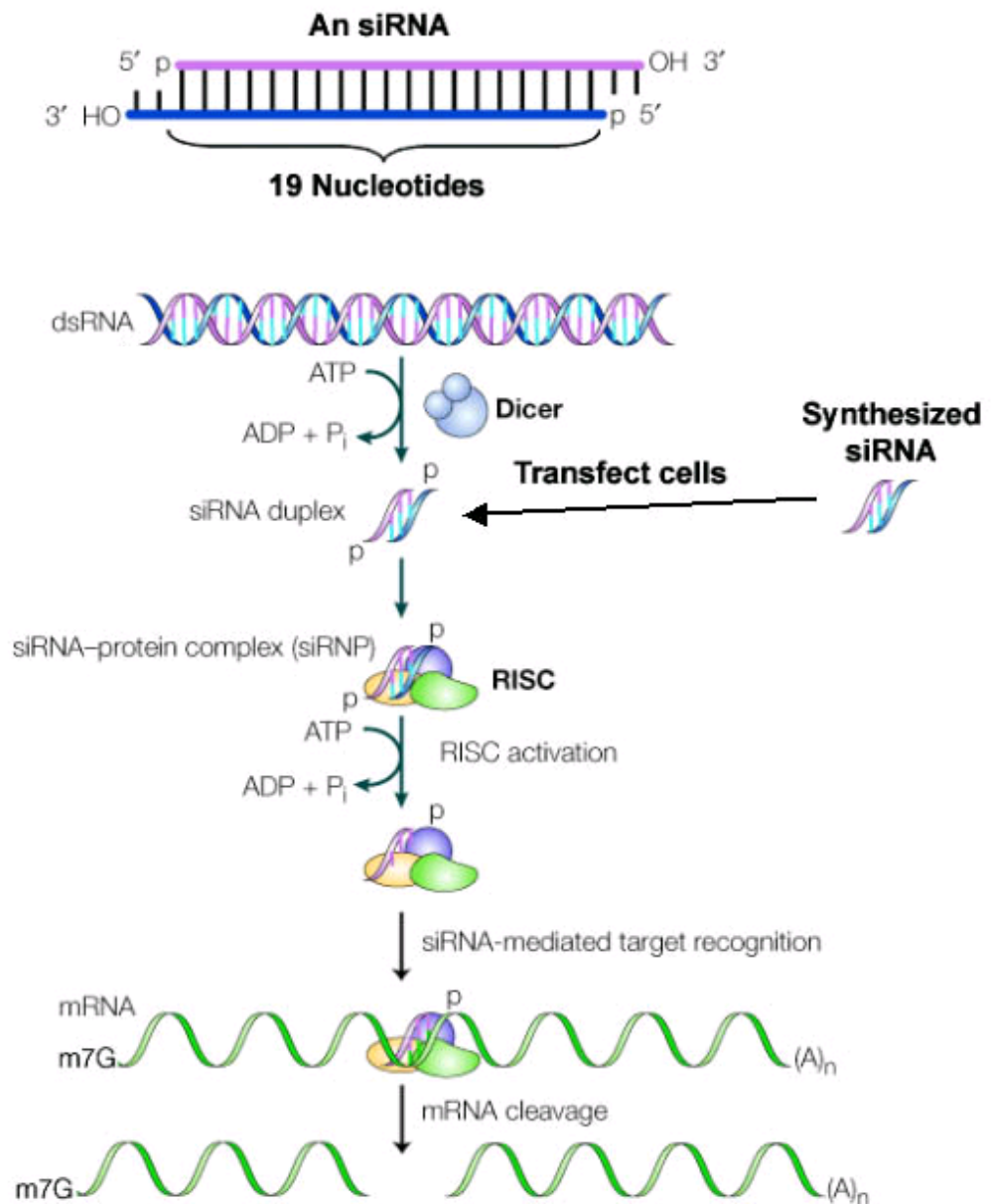


**Figure 7: RNAi pathway.**

In order to form siRNA, long double-stranded RNA (dsRNA) is cleaved *in vitro* by the Dicer enzyme in an ATP-dependent reaction or experimentally synthesized siRNA is generated and transfected into the cells. The siRNA then forms a complex with the RNAi-induced silencing complex (RISC). After the siRNA duplex is unwound with the required ATP, the single-stranded antisense strand guides RISC to the messenger RNA (mRNA). The complex binds to the strand at the complementary sequence, resulting in cleavage of the target mRNA. *Modified from Dykxhoorn et al [134].*



With the recent advent of synthetic siRNA technology, RNAi-based gene silencing in cultured 3T3-L1 adipocytes has been extremely valuable in dissecting elements crucial for the insulin signaling pathway and adipocyte differentiation [135-137]. Gene silencing in cultured mammalian cells is being used as an effective way to quickly screen if a specific gene is required for a biological function. It is also being used in high throughput screens to determine if there are any genes within a large set of genes required for a particular function [138]. The use of RNAi is definitely an important experiment to do before more expensive experiments to generate transgenic mice are undertaken.

RNAi has been used to examine the role of various genes and proteins in the insulin signaling pathway. For example, knockdown of Golgin-160, a peripheral Golgi protein known to be a caspase inhibitor during programmed cell death, actually led to increased translocation of GLUT4 to the plasma membrane and the subsequent increase in glucose uptake [139]. This suggests that Golgin-160 is required for the proper sorting of GLUT4 to the insulin-responsive compartment for the uptake of glucose. On the other hand, knockdown of the GTPase TC10 $\alpha$  indicated that it is specifically required for insulin-stimulated glucose uptake in adipocytes due to the inhibition of glucose uptake and GLUT4 translocation upon silencing [140]. RNAi will be used in a similar fashion for this project to study the role of *Atp10c*/ATP10C in the insulin signaling pathway.

### **Research project overview**

Although there is a consensus on the physiological function of flippases in intracellular signaling and protein trafficking, their precise biological roles are poorly

understood. The hypothesis of this project is that there is an association between type 4 ATPase mediated phospholipid translocase activities and cell signaling and intracellular protein trafficking. The Swiss murine 3T3-L1 cell line [10] was used to investigate the biological role of *Atp10c*/ATP10C in the process of adipogenesis and the insulin signaling pathway. Specific experiments and the corresponding results will be discussed.

## CHAPTER 3. EXPERIMENTAL INVESTIGATIONS

### Abstract

Previous research has shown that heterozygous mice inheriting a maternal deletion of the *Atp10c* gene become obese and exhibit hyperinsulinemia, hyperlipidemia, and hyperglycemia traditionally associated with T2DM [8, 66, 141]. Given the complexity in the phenotype of these *Atp10c* heterozygous mice, it is difficult to distinguish between primary and secondary effects in the whole animal model. Therefore, the Swiss murine 3T3-L1 cell line [10] was used as an *in vitro* model and primary preadipocytes isolated from mouse adipose tissue, plated, and differentiated in culture were used as an *ex vivo* model to study the transcriptional and translational regulation of *Atp10c*/ATP10C.

The aim of the present study was to investigate the biological role of *Atp10c*/ATP10C in the process of adipogenesis and the insulin signaling pathway in the *in vitro* model. Using RT-PCR to monitor gene expression and Western blotting to monitor protein expression, *Atp10c* mRNA was 2-fold down-regulated while ATP10C protein was up-regulated during adipogenesis. Treatment of adipocytes with a PPAR $\gamma$  agonist further down-regulated *Atp10c* while increasing adipogenesis, suggesting a potential role for *Atp10c* in the differentiation process and as a PPAR $\gamma$  modulator. Glucose uptake in adipocytes was increased when *Atp10c*/ATP10C was knocked down using siRNA, elucidating the possibility that *Atp10c*/ATP10C is involved in the insulin signaling pathway. Based on these results, *Atp10c*/ATP10C has a role in the insulin signaling pathway and may have a role in adipogenesis; further research is necessary to confirm the exact function.

## Introduction

The prevalence of obesity and diabetes in society today continues to rise each year [1-3]. In the United States, obesity increased from 19.8% to 20.9% while the prevalence of diabetes increased from 7.3% to 7.9% from 2000 to 2001, respectively [2]. Similar rising trends are being observed throughout the world, with the projection that 366 million people will have diabetes by 2030 [27]. There has been no recent research to indicate that these numbers are declining, leaving the high levels of obesity and T2DM as a major public health concern. Based on these increasing statistics, there is a dire need for new approaches to examine the correlation between obesity and T2DM, to understand what causes these diseases, and to elucidate unknown players in metabolic pathways related to obesity and T2DM.

The novel type IV subfamily of P-type ATPases are putative aminophospholipid translocases that have been associated with human disorders of intramembranous transport [4, 5]. Studies in yeast have also shown that these flippases are important in protein trafficking in the exocytic and endocytic pathways [6, 7]. Using positional cloning and genomic sequencing strategies, the novel type IV P-type ATPase *Atp10c* has been cloned to mouse chromosome 7 [8]. Heterozygous mice inheriting a maternal deletion of the *Atp10c* gene exhibit typical hallmarks of insulin resistance syndrome including obesity, hyperinsulinemia, and insulin resistance [9]. These mice represent a novel genetic model of diet-induced obesity and T2DM.

Although there is a consensus on the physiological function of these flippases in intracellular signaling and protein trafficking, their precise biological roles are poorly understood. The hypothesis of this project is that there is an association between type 4

ATPase mediated phospholipid translocase activities and cell signaling and intracellular protein trafficking. To investigate the biological role of *Atp10c*/ATP10C in the process of adipogenesis and the insulin signaling pathway using the Swiss murine 3T3-L1 cell line [10], reverse transcriptase-polymerase chain reaction (RT-PCR) and Western blotting were used to monitor gene and protein expression. A basic characterization of *Atp10c*/ATP10C was performed, followed by examination of the effect of PPAR $\gamma$  agonists and effectors of glucose and lipid metabolism on *Atp10c* expression. Lastly, glucose uptake was measured in adipocytes where *Atp10c*/ATP10C was knocked down with siRNA in order to elucidate the possibility that *Atp10c*/ATP10C is involved in the insulin signaling pathway.

## **Materials and methods**

More detailed, step-by-step instructions for many of the following methods are located in the Appendix.

### ***Materials***

Cell culture reagents and oligonucleotides were obtained from Fisher Scientific (Fairlawn, NJ). Insulin, isobutylmethylxanthine, isoproterenol, dexamethasone, and fetal bovine serum were purchased from Sigma (St. Louis, MO). Thiazolidinediones MCC555 and troglitazone (TGZ) and the PPAR $\gamma$  inhibitor GW9662 were obtained from Cayman (Ann Arbor, MI). *Atp10c* siRNA and HiPerfect transfection reagent was obtained from Qiagen (Valencia, CA). DeliverX transfection reagent was purchased from Panomics, Inc. (Fremont, CA).

## ***Animals***

Mice containing the radiation-induced chromosomal deletion  $p^{23\text{FiOD}}$  located at the *pink-eyed dilution* ( $p$ ) locus on MMU 7 were previously generated at Oak Ridge National Laboratory [59, 60]. A homozygous deletion at the  $p$  locus is lethal, while heterozygous mice will survive. The  $p^{23\text{FiOD}}$  strain contains a deletion of the first two of the 21 exons of *Atp10c*, including the 5' promoter region [9]. These mice are currently housed and maintained at the University of Tennessee as previously described [61]. The wild-type males are heavier than their age-matched female counterparts, thus only female mice are currently being used for experimentation.

Previous research has shown that heterozygous mice fed a high-fat diet (45% fat) maternally inheriting the *Atp10c* deletion exhibit a significantly higher body weight, adiposity index, and plasma insulin, leptin, and triglyceride concentrations compared to heterozygous mice that inherit the deletion paternally [9]. Therefore the mutant mice inherit the deletion maternally, while the control mice inherit it paternally.

For the following methods, mice were fed a regular chow diet (Laboratory Rodent Diet, Checkers PMI Nutritional International, Brentwood, MO) and killed by CO<sub>2</sub> asphyxiation. Only control mice were used for this study. All procedures were approved by and in accordance with the University of Tennessee Institutional Animal Care and Use Committee (protocol #1309-1206).

### ***Isolation and differentiation of primary preadipocytes and adipocytes***

Preadipocytes and adipocytes were isolated from adipose tissue of 4–6 month old adult female control mice [61] using the procedure of Rodbell with modifications [142]. Approximately 2 g of tissue was collected, minced into small pieces and digested with

collagenase (2 g/L) (type I, Worthington Biochemical Corp., Lakewood, NJ) at 37°C for 25 min in modified Krebs-Ringer bicarbonate albumin buffer pH 7.4, containing 1 g/L BSA and 4.4 mM glucose. Digested fat tissue was filtered through a 100 µm nylon mesh and adipocytes were isolated by a low speed centrifugation at 800 rpm for 10 min. These floating adipocytes were washed once with Hank's balanced salt solution (HBSS) and collected. The stromal vascular fraction rich in primary preadipocytes was then pelleted by a high speed centrifugation at 1500 rpm for 15 min. Resulting stromal vascular fraction cell pellets were treated with red blood cell lysis buffer (eBioscience, San Diego, CA) for 5 min at room temperature, rinsed with phosphate buffered saline supplemented with 1% BSA, and centrifuged at 800 rpm for 10 min. Stromal vascular fraction cells were either collected or seeded in 6-well cell culture plates at a density of  $5 \times 10^5$  cells/well.

At 70–80% confluency, primary preadipocytes in the stromal vascular fraction cells were induced to differentiate in growth medium supplemented with 10 µg/ml insulin (high insulin medium). Differentiation was complete in 8–10 days as assessed by Oil Red O (ORO) staining and RT-PCR. These cells are the primary adipocytes obtained from primary preadipocytes differentiated in culture.

### ***3T3-L1 cell culture***

3T3-L1 preadipocytes obtained from ATCC (Manassas, VA) were grown at 37°C in 5% CO<sub>2</sub> in Dulbecco's modified Eagle's medium containing 10% fetal bovine serum and 1% penicillin/streptomycin (growth medium). At 70–80% confluency, adipocyte differentiation was induced by incubating the cells in growth medium supplemented with 0.5 mM isobutylmethylxanthine, 1 µM dexamethasone, 1 µg/ml insulin, and 10 µM

troglitazone (differentiation medium) for two days. After 2 days, cells were maintained in growth medium supplemented with 1 µg/ml insulin and 10 µM troglitazone (maintenance medium) and grown for 7–10 days; the medium was changed every two to three days. Cells were fully differentiated (>80%) by day 8–10 as assessed by ORO staining and RT-PCR; these are 3T3-L1 adipocytes. Day 0 represents the day on which the differentiation media is added.

Confluent 3T3-L1 preadipocytes or adipocytes were incubated for 24 hours in serum-free medium before various effectors were added as described in the results. PPAR $\gamma$  agonists and antagonists were replenished every time the media was changed.

### ***Oil Red O staining***

Differentiation was assessed using a modified procedure of ORO staining [143]. Cells were washed with HBSS and fixed with 1% paraformaldehyde for 5 min. Cells were then rinsed with deionized water followed by the addition of two aliquots of 85% propylene glycol for 5 min each. ORO stain was added (0.7% w/v in 85% propylene glycol) and cells were gently swirled for 20 min at room temperature. Following a final wash with 85% propylene glycol, cells were counterstained with hematoxylin. They were visualized and photographed using a Zeiss Invertoskop 40C microscope and Canon Powershot A620 digital camera.

ORO quantitation was performed using the procedure from the McNeil lab [144]. Briefly, cells were stained with ORO similar to above without the addition of hematoxylin counterstain. After drying at RT for 10 min, ORO was eluted with the addition of 100% isopropanol for 15 min, followed by OD measurement at 540 nm.



### ***Small interfering RNA (siRNA)***

Two different *Atp10c* siRNAs were obtained (Qiagen, Valencia, CA); one was generated from the sequence at the 3' end of the *Atp10c* gene (sense: r(CCU GGG UAU UGA AAC CAA A)dTdT and antisense: r(UUU GGU UUC AAU ACC CAG G) dTdG) and the second was generated from the sequence at the 5' end (sense: r(CGU CUU UGC UGC AAU GAA A)dTdT and antisense: r(UUU CAU UGC AGC AAA GAC G)dGdA).

HiPerfect transfection reagent (Qiagen, Valencia, CA) was used to transfect preadipocytes with 200 nM *Atp10c* siRNA while the lipid-based DeliverX transfection reagent (Panomics, Fremont, CA) was used to transfect adipocytes with 30 nM *Atp10c* siRNA. Preadipocytes or adipocytes were transfected with siRNA and either collected or used for glucose uptake at 24 h, 48 h, or 72 h post-transfection. For experiments looking at different days during adipogenesis, siRNA was added each time the media was changed throughout differentiation. Beginning at day 6, siRNA was transfected using both HiPerfect and DeliverX transfection reagents.

To transfect preadipocytes, equal volumes of 20  $\mu$ M *Atp10c* siRNA and HiPerfect transfection reagent were combined, flicked to mix, and left at room temperature for 10 min. Following incubation, 40  $\mu$ l of the transfection complex was added to the medium in each 60 mm cell culture dish.

Adipocytes were transfected as described [145]. Briefly, cells were washed once with PBS and 300  $\mu$ l of the 30 nM working siRNA transfection complex was added per dish. Cells were incubated at room temperature for 3-5 min, followed by the addition of 300  $\mu$ l serum-free media per dish and incubation under normal cell culture conditions for

2-4 h. Finally, 1000 µl complete growth media was added per dish and incubated under normal cell conditions for 24-72 h.

### ***Semiquantitative RT-PCR***

These procedures are as previously described, with modifications [141]. Total RNA was extracted from 3T3-L1 preadipocytes and adipocytes, primary preadipocytes and adipocytes fractionated from adipose tissue, and primary preadipocytes and adipocytes plated and differentiated in culture using RNeasy Mini RNA kit (Qiagen, Valencia, CA) according to the manufacturer's instructions. About  $1 \times 10^6$  cells yield 30–50 µg of total RNA. Double-stranded cDNA was synthesized using the iScript cDNA synthesis kit (Bio-Rad, Hercules, CA). Semi-quantitative RT-PCR was performed for *Atp10c* (F-5'CCTGTGCTCTTCATTCTGGC3', R-5'CACTGCAGCTGTGAATCTGT3'), *resistin* (F-5'ACTGAGTTGTGTCCTGCTAAG3', R-5'CCACGCTCACTTCCCCGACATC3'), and *PPAR $\gamma$*  (F-5'GGTGAAACTCTGGGAGATTC3', R-5'CAACCATTGGGTCAGCTCTT3') mRNAs using GoTaq<sup>®</sup> Green Master Mix (Promega Inc., Madison, WI) with  *$\beta$ -actin* (F-5'ATGGGTCAGAAGGACTCCTA3', R-5'CAACATAGCACAGCTTCTCT3') as an internal control. RT-PCR was performed under the following conditions: 5 min at 94°C followed by 30 cycles of denaturation at 94°C for 30 s, annealing at 54°C for 30 s, and extension at 72°C for 30 s, and finishing with 5 min at 72°C. RT-PCR products were analyzed on 1% agarose gels containing 1 µg/µl ethidium bromide and viewed under ultraviolet light. Data are expressed as the ratio of the target gene expression to that of an internal control.

## ***Protein preparations***

### *Total membrane proteins*

Total membrane proteins were isolated as described with modifications [146]. Briefly, cells were harvested and homogenized in homogenization buffer (20 mM HEPES, pH 7.5 and 10 mM KCl), containing 1 mM protease inhibitors (pi), with a PowerGen 700 polytron for 10 sec followed by passage through a 20-gauge needle 30 times. Following centrifugation, membrane pellets were resuspended in PARP buffer (50 mM tris, pH 6.8; 8 M urea; 2% SDS) with 1 mM DTT and 1 mM pi.

### *Whole cell lysates or total cellular extracts*

Total proteins were isolated using two different methods: by SDS lysis buffer [147] or by the standard radioimmunoprecipitation (RIPA) buffer.

Briefly, cells were washed twice with PBS at room temperature followed by the addition of 1 ml lysis buffer at p 7.4 (4% SDS, 50 mM HEPES, 150 mM NaCl, 10 mM DTT, 1:1000 pi). Cells were harvested with a cell scraper, transferred to a small eppendorf tube, heated to 100°C for 5 min, and immediately stored at -80°C.

Total cell lysates were isolated using RIPA buffer according to the manufacturer's instructions (Boston Bioproducts, Inc., Worcester, MA). Briefly, cells were washed twice with PBS on ice followed by the addition of 100 µl RIPA buffer supplemented with pi (sodium orthovanadate, sodium fluoride, PMSF, aprotinin, leupeptin). Cells were scraped, transferred to a small eppendorf tube, and stored at -80°C.

### *Subcellular proteins*

Subcellular fractions of 3T3-L1 cells were isolated as follows [147]. Cells were serum starved overnight at 37°C in DMEM supplemented with 1 mg/ml BSA. Then

DMEM with or without 1  $\mu$ M insulin was added and cells were incubated at 37°C for 30 min. Cells were washed once with HES buffer (250 mM sucrose, 20 mM HEPES, 1 mM EDTA, pH 7.4) at room temperature. To each flask or dish, 3 ml HES supplemented with 1:1000 pi was added. Cells were scraped, collected in 50 ml Falcon tubes, and homogenized for 10 sec with a PowerGen 700 Polytron followed by passage through a 20-gauge needle 30 times. The homogenate was transferred to a centrifuge tube; 300  $\mu$ l was collected as the whole cell lysate (WCL) fraction. Following centrifugation at 12000 rpm for 15 min at 4°C, the infranant, which is comprised of the high density microsomal (HDM), low density microsomal (LDM), and cytosolic fractions, was collected in another centrifuge tube as the HLC fraction. The pellet was resuspended in HES and homogenized with a 20-gauge needle 5 times followed by another centrifugation at 12000 rpm for 20 min at 4°C. The supernatant was discarded and the pellet was resuspended in HES again, followed by homogenization with a 20-gauge needle 5 times. This homogenate was overlaid on a 1.12 M sucrose cushion (29.78 g sucrose in 100 ml HES) and centrifuged at 25000 rpm for 60 min at 4°C. The cloudy interface was collected, resuspended in HES, and centrifuged at 18000 rpm for 30 min at 4°C. During centrifugation, the mitochondrial nuclear pellet from the previous run was resuspended in 2 ml HES/pi and stored. After centrifugation, the plasma membrane pellet was resuspended in 150  $\mu$ l HES/pi and stored. The HLC fraction from earlier was centrifuged at 20000 rpm for 30 min at 4°C. The supernatant was transferred to another centrifuge tube and spun at 45000 rpm for 1.5 hr for 4°C. During centrifugation, the HDM pellet was resuspended in 300  $\mu$ l HES/pi and stored. Following centrifugation, the

cytosolic supernatant was discarded and the LDM pellet was resuspended in 200  $\mu$ l HES/pi and stored.

Protein concentrations were determined using bicinchoninic acid (BCA) Protein Assay Reagent (Pierce Biotech Inc., Rockford, IL).

### ***Antibodies***

Anti-mouse GLUT1 (Alpha Diagnostic International, San Antonio, TX), anti-rabbit GLUT 4 (Biogenesis, Mill Creek, WA, and Abcam, Cambridge, MA), anti-mouse Na<sup>+</sup>/K<sup>+</sup> ATPase (Novus Biologicals, Littleton, CO), anti-rabbit  $\beta$ -TUBULIN (Sigma Genosys, St. Louis, MO), and anti-rabbit ATP10C (Sigma Genosys, St. Louis, MO) antibodies were used for Western blot analysis. Anti-rabbit ATP10C was prepared and affinity purified commercially against a 15 amino acid peptide (Sigma Genosys, St. Louis, MO) followed by characterization using ELISA and peptide binding.

### ***Western blot analysis***

Western blotting was carried out according to standard procedures and as previously described [148]. 20–100  $\mu$ g of proteins were resolved on 10% SDS-PAGE, using 2X sample buffer containing  $\beta$ -mercaptoethanol as a reducing agent. Proteins were transferred to nitrocellulose membranes and blocked for 1 h in blocking solution (1% nonfat milk and 1% BSA in TBST buffer). Membranes were incubated with specific primary antibodies overnight at 4°C. Primary antibodies were detected with horseradish peroxidase-coupled secondary antibody and antibody-protein complexes were detected by Enhanced Chemiluminescence Western Blotting Detection Kit (Pierce Biotech Inc., Rockford, IL). Data from two independent experiments is reported. Results are expressed as the ratio of target protein expression to that of an internal loading control.

### ***Glucose uptake***

Glucose uptake in differentiated adipocytes was measured as previously described [149]. Briefly, adipocytes were plated in 6-well cell culture plates at a density of  $3 \times 10^5$  cells/well. Cells were washed with DMEM twice and serum starved in DMEM only for 3–5 hrs. Each 6-well plate was set-up such that wells 1, 2, and 3 did not contain insulin and wells 4, 5, and 6 did contain insulin. Cells were stimulated with 100  $\mu$ M insulin in DMEM for 30 min at 37°C. The insulin induction was stopped by washing the cells twice with 1 ml Krebs-Ringer HEPES (KRH) (121 mM NaCl, 4.9 mM KCl, 1.2 mM  $MgSO_4$ , 0.33 mM  $CaCl_2$ , 12 mM HEPES) minus glucose at room temperature. Cytochalasin B (5  $\mu$ l of 1 mM stock/1 ml cocktail) was used to normalize for non-specific glucose uptake. Glucose uptake was determined after the addition of  $^3H$ -2-deoxyglucose (1  $\mu$ l of 10 Ci/mmol stock/1 ml cocktail) in KRH buffer at 37°C for 5 min. Incorporation was terminated by washing the cells twice with 1ml ice cold KRH plus glucose (25 mM glucose). Cells were lysed at room temperature for 5 min with 2.2 ml digitonin release buffer (0.25 M mannitol, 17 mM MOPS, 2.5 mM EDTA, 0.25 M digitonin). Following incubation, 2 ml of the cell lysates were mixed with 10 ml scintillation fluid and counted. 200  $\mu$ l of the lysate was stored at -80°C for protein quantitation.

### ***Statistical analysis***

Semiquantitative RT-PCR products on the agarose gels and protein bands on the Western blots were quantitated using Scion Imaging Software (<http://www.scioncorp.com>). Results are shown as means  $\pm$  SD. Mean comparisons

were tested by two-tailed unpaired Student's *t*-test with *P* values <0.01 considered highly significant and <0.05 considered significant.

## Results

### *Atp10c mRNA is expressed in 3T3-L1 cells*

In order to use 3T3-L1 cells as an *in vitro* system to study the regulation of the novel gene *Atp10c*, its presence was first demonstrated in these cells. Using RT-PCR, an 886 bp product was detected in both the undifferentiated and differentiated 3T3-L1 cells (Figure 8). This product has been demonstrated and confirmed to be a part of *Atp10c* cDNA (Dhar 2004). Quantitative analysis showed that *Atp10c* is 2-fold down-regulated in 3T3-L1 adipocytes after differentiation using  $\beta$ -actin as the control. As expected, *PPAR $\gamma$*  and *resistin* were up-regulated, serving as internal positive controls.

### *Atp10c mRNA is expressed in primary preadipocytes and adipocytes*

To investigate whether the pattern of expression of *Atp10c* mRNA *in vitro* is comparable to that *ex vivo* and determine if a significant decrease in *Atp10c* expression is indeed related to the adipogenesis process, *Atp10c* mRNA was next quantitated in purified primary preadipocytes and adipocytes from mouse adipose tissue and in primary preadipocytes differentiated in culture. *Atp10c* was expressed in all of these types of cells (Figure 9). Compared to primary preadipocytes from mouse adipose tissue, *Atp10c* mRNA was significantly down-regulated in primary adipocytes from mouse adipose tissue, again confirming the regulation of *Atp10c* expression during adipogenesis (Figure 9A).

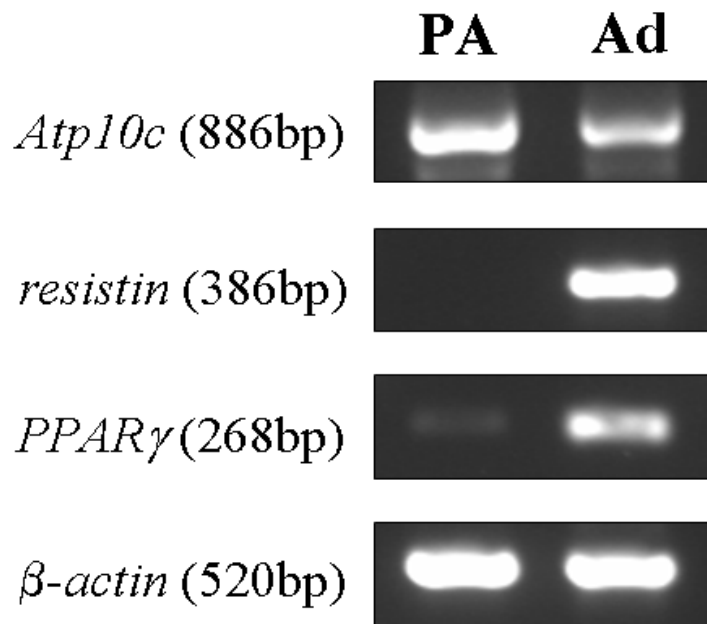


**Figure 8: *Atp10c* mRNA is expressed in 3T3-L1 cells.**

*Atp10c*, *resistin*, and *PPARγ* expression was examined by RT-PCR in 3T3-L1 preadipocytes (PA) and adipocytes (Ad);  $\beta$ -*actin* served as an internal control. Numbers in parentheses denote PCR product size in base pairs (bp).



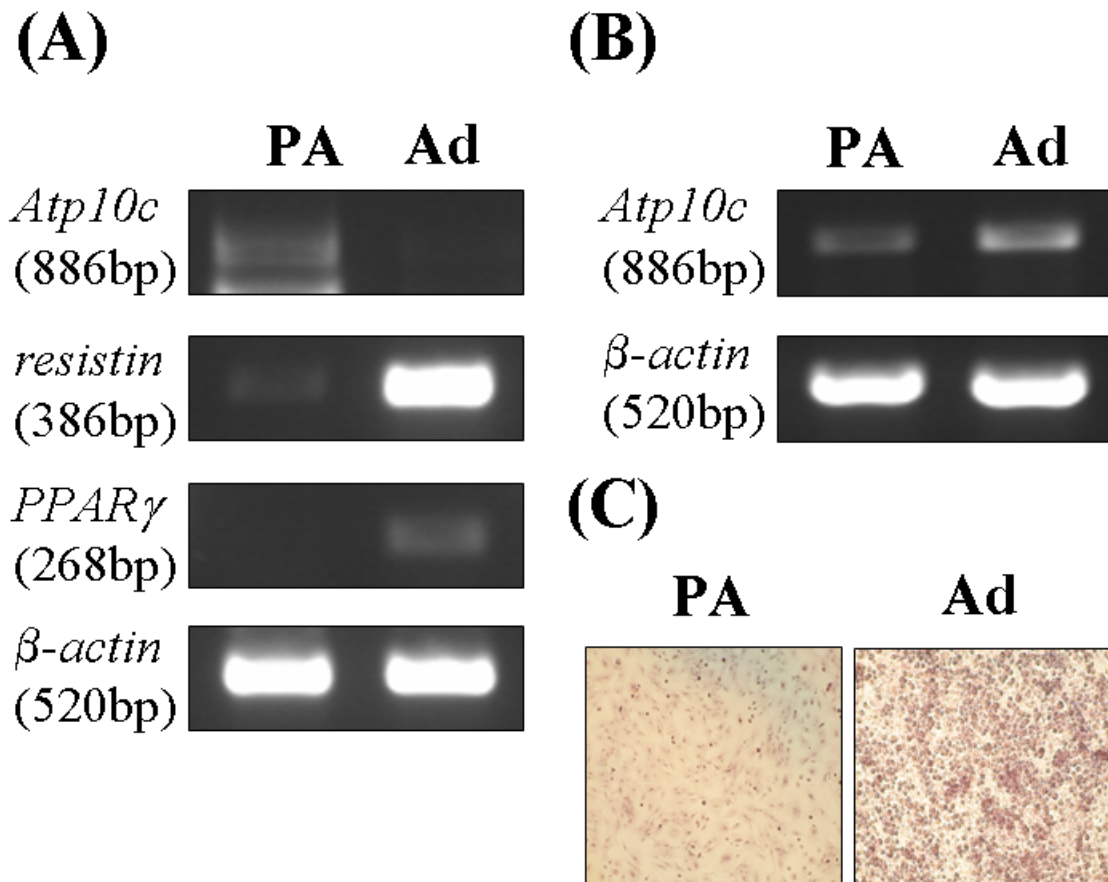


**Figure 9: *Atp10c* mRNA is expressed in primary preadipocytes and adipocytes.** RT-PCR analysis was used to determine *Atp10c*, *resistin*, and *PPARγ* expression in primary preadipocytes (PA) and adipocytes (Ad); *β-actin* served as an internal control. Expression is shown in primary preadipocytes and primary adipocytes purified from mouse adipose tissue (A) or harvested from culture (B). ORO staining (C) was used to monitor and confirm differentiation of primary preadipocytes in culture. Numbers in parentheses denote PCR product size in base pairs (bp).

Adipose tissue is comprised of several types of cells such as fibroblasts, non-differentiated mesenchymal cells, preadipocytes, and adipocytes. Adipocytes develop from fibroblast-like preadipocytes within the stromal vascular fraction [150, 151]. To ensure that stromal vascular fraction cells in the preparations were comprised mainly of preadipocytes and that *Atp10c* expression was specific to the preadipocyte fraction, stromal vascular fraction cells were plated in cell culture dishes and differentiated to adipocytes. *Atp10c* expression was then measured and, interestingly, was 2-fold up-regulated when primary preadipocytes were differentiated to adipocytes in culture (Figure 9B). ORO staining was used to monitor differentiation in culture and to confirm that the harvested cells showed >80% differentiation (Figure 9C). This increase in *Atp10c* expression may be due to high insulin present in the differentiation and maintenance media used for primary cultures.

Due to the fact that *Atp10c* is similarly regulated both *in vitro* and *ex vivo*, and 3T3-L1 cells are widely used as models of adipogenesis, most experiments were carried out mainly in 3T3-L1 cells.

#### ***ATP10C protein is expressed in 3T3-L1 cells***

After demonstrating the expression of *Atp10c* at the mRNA level, the next step was to investigate the expression of ATP10C protein. Based on the amino acid sequence of ATP10C, the expected molecular weight of the protein is 169 kDa. At first, there were no bands present in that range on the protein blots. This led to an experiment looking at different sample loading buffers with or without the addition of a reducing agent (Figure 10). The original sample loading buffer used from New England BioLabs (NEB) without DTT did not have any bands present in the 169 kDa range and very faint bands in the 70

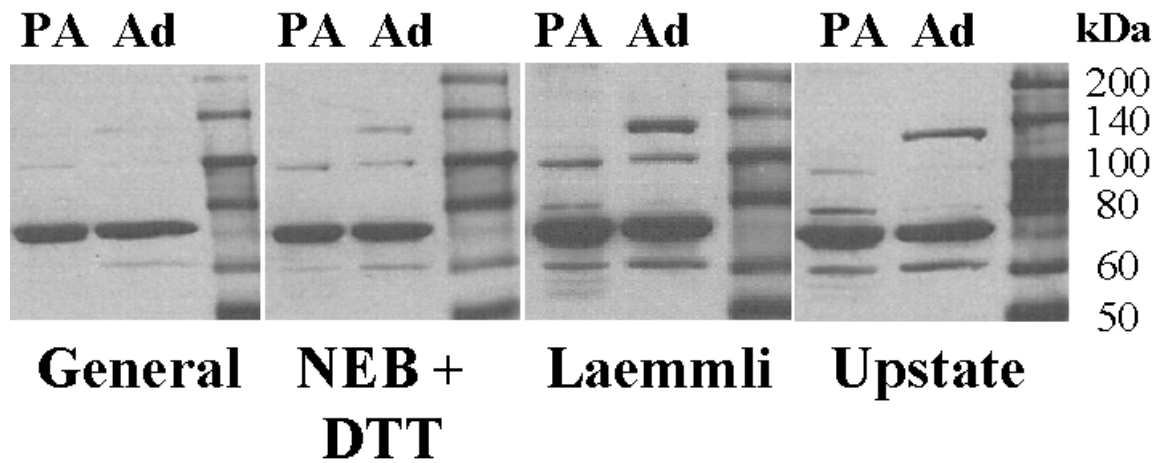


**Figure 10: Different sample loading buffers can be used for Western blots.** Equal amounts of preadipocyte (PA) and adipocyte (Ad) whole cell lysate proteins were loaded on a Western gel using four sample loading buffers: general, NEB + DTT, Laemmli, and Upstate (which contained  $\beta$ -mercaptoethanol). The membranes were probed with ATP10C antibody.

kDa range. The other sample loading buffers tested included a general buffer [152], NEB with DTT [153], Laemmli [154], and Upstate [155]. After switching to Upstate sample loading buffer, distinct bands were apparent in an upper range close to 140 kDa and a lower range at 70 kDa.

To confirm that the upper band was indeed ATP10C, a peptide neutralization experiment was performed. In this experiment, a neutralizing (or blocking) peptide consisting of the 15 amino acids used to generate the ATP10C antibody was added in 10-fold excess to the ATP10C antibody. This neutralizing peptide competed with the ATP10C antibody to block binding of the antibody to the antigen. After developing the Western blot, the addition of the neutralizing peptide will compete out the ATP10C protein band. Surprisingly, this experiment showed that the ATP10C protein band that was competed out is 70 kDa (Figure 11). Therefore, this lower molecular weight ATP10C band was the focus for future experiments.

Since *Atp10c* mRNA showed a 2-fold decrease during adipogenesis, expression of ATP10C protein was monitored to see if a similar pattern existed. Interestingly, ATP10C protein actually increased throughout differentiation of preadipocytes to adipocytes, with  $\beta$ -TUBULIN serving as the control (Figure 12).

#### ***Atp10c* mRNA expression is regulated by PPAR $\gamma$ agonists and antagonists**

Since PPAR $\gamma$  is considered to be the master regulator of adipogenesis [110] and controls the expression of adipocyte genes, the effect of PPAR $\gamma$  agonists on *Atp10c* expression was investigated to assess whether *Atp10c* expression is also under PPAR $\gamma$  control. Two anti-diabetic drugs that activate PPAR $\gamma$  and thus promote adipogenesis,

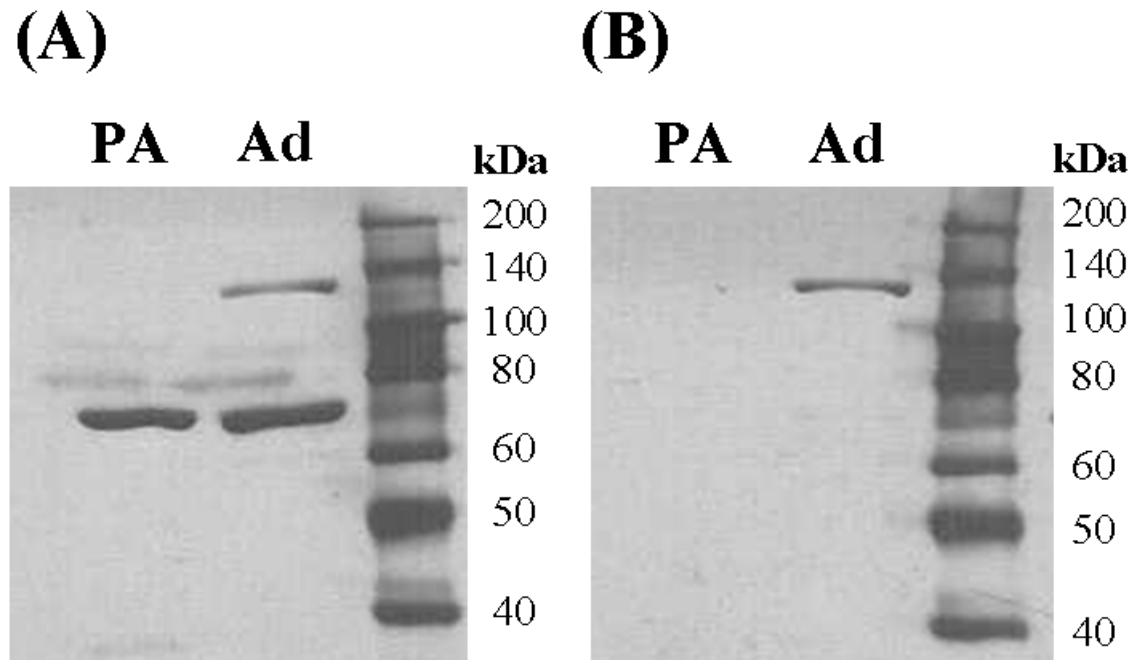


**Figure 11: Peptide neutralization shows an ATP10C protein band at 70kDa.**

Equal amounts of preadipocyte (PA) and adipocyte (Ad) whole cell lysate proteins were loaded on a Western gel and probed in the absence (A) or presence (B) of 10-fold excess neutralizing peptide with ATP10C antibody.

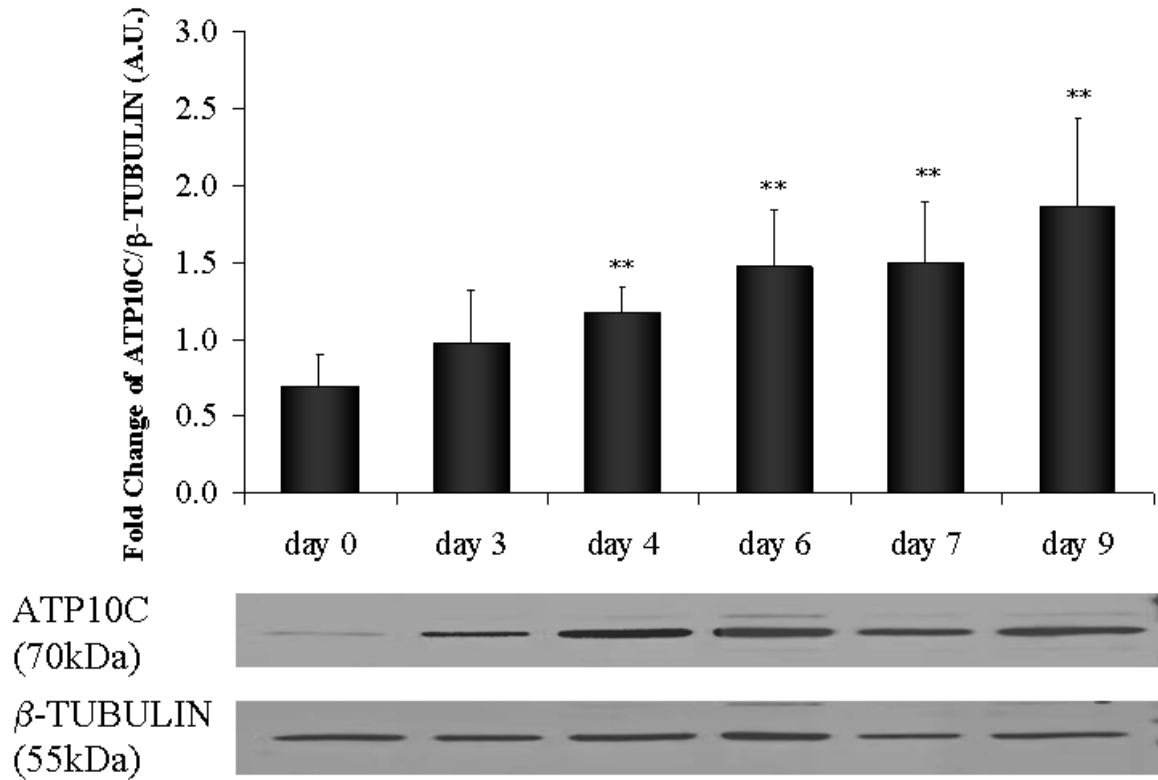


**Figure 12: ATP10C protein expression increases throughout differentiation.** ATP10C expression was examined by Western blotting using 3T3-L1 total proteins collected in SDS lysis buffer at days 0, 3, 4, 6, 7, and 9 post-induction; β-TUBULIN served as an internal control. The expression of ATP10C is denoted as arbitrary units (A.U.) and represented as the fold change normalized to β-TUBULIN. \*\* $P < 0.01$ .

MCC555 and troglitazone (TGZ), were used [109, 130]. Confluent preadipocytes were maintained in serum-free media supplemented with 10  $\mu$ M TGZ or 10  $\mu$ M MCC555 and harvested after 24 h. 3T3-L1 adipocytes were also treated with the same reagents throughout differentiation and harvested. *Atp10c* mRNA expression was quantitated in both cell types. As demonstrated by RT-PCR and ORO staining, both MCC555 and TGZ promoted adipogenesis and consequently reduced *Atp10c* expression by 5-fold and 3-fold respectively (Figure 13). This significant decrease in adipocytes confirmed not only that *Atp10c* expression was reduced in differentiated cells, but also that these PPAR $\gamma$  agonists further down-regulate its expression.

To clarify and confirm that the decrease in *Atp10c* was indeed due to the process of adipogenesis controlled by PPAR $\gamma$ , *Atp10c* expression was also assessed in cells treated with a PPAR $\gamma$  antagonist, GW9662 [156]. *Atp10c* expression in adipocytes treated with GW9662 alone did not decrease and was similar to that in control cells treated with the vehicle DMSO (Figure 13). However, when GW9662 was added to the cells along with MCC555 or TGZ, there was only a 2-fold or a 4-fold decrease in *Atp10c* expression, respectively. This suggests that GW9662 inhibited adipogenesis and rescued some of the decrease in *Atp10c* expression due to MCC555 or TGZ alone.

***Atp10c and PPAR $\gamma$ mRNAs are oppositely regulated in 3T3-L1 cells during adipogenesis***

Both MCC555 and TGZ are PPAR $\gamma$  agonists that decrease *Atp10c* expression along with anti-diabetic drugs that are members of the thiazolidinedione class. Due to the fact that TGZ was withdrawn from the market because of adverse side effects while

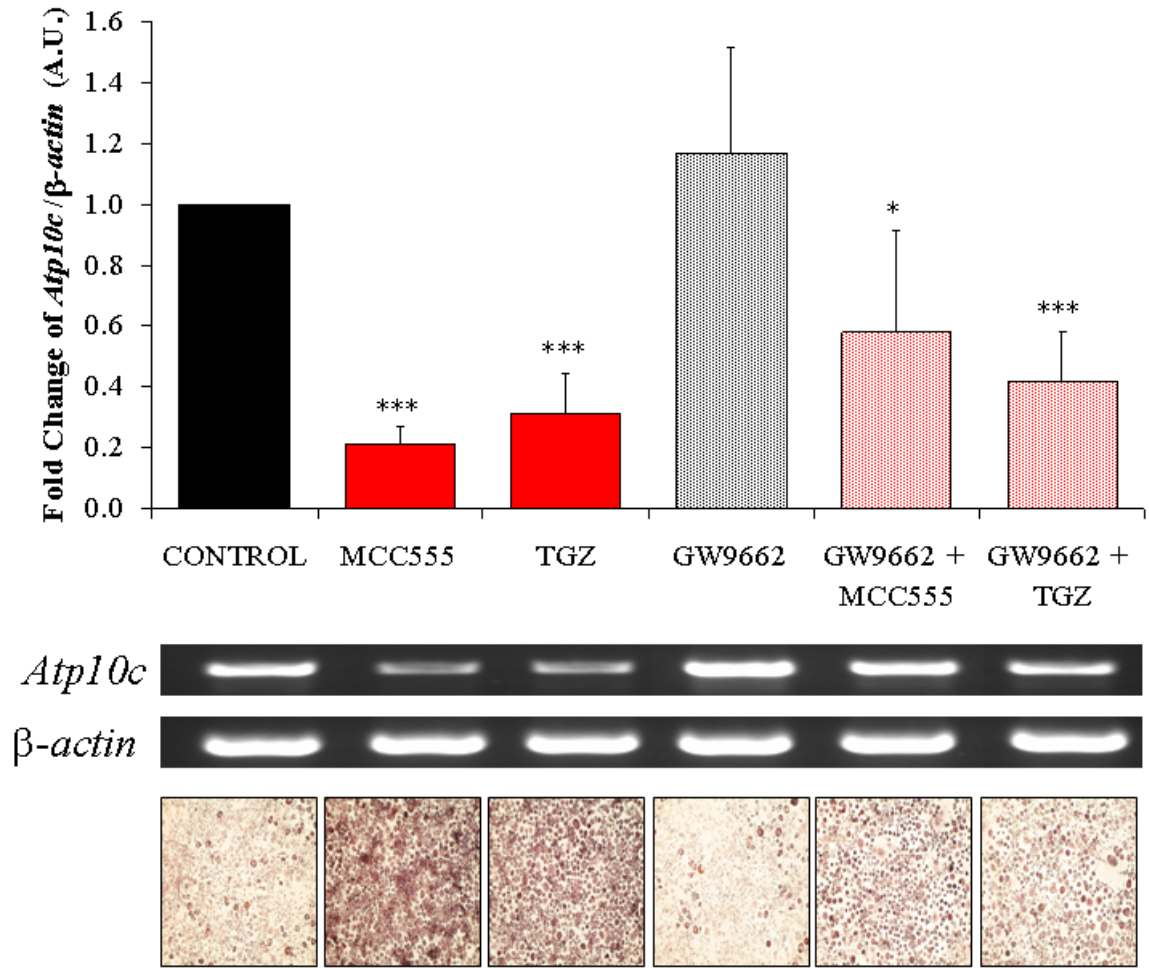


**Figure 13: *Atp10c* mRNA expression is regulated by PPAR $\gamma$  agonists and antagonists.**

RT-PCR analysis shows *Atp10c* expression in 3T3-L1 adipocytes harvested between days 8–10 of differentiation. MCC555, troglitazone (TGZ), and GW9662 were added to the media throughout the differentiation process and replenished whenever the media was changed. Expression of *Atp10c* mRNA in adipocytes treated with DMSO (CONTROL), MCC555, TGZ, and/or GW9662 is shown, with  $\beta$ -actin serving as an internal control. The expression of *Atp10c* is denoted as arbitrary units (A.U.) and represented as the fold change normalized to  $\beta$ -actin. ORO staining was used to monitor morphological changes in adipocytes in the presence of PPAR $\gamma$  agonists and antagonists. \* $P$ <0.05, \*\*\* $P$ <0.001.



MCC555 is a newer experimental drug, the following experiments examined the effect of MCC555 only.

*Atp10c* expression was compared to that of *PPAR $\gamma$*  in cells treated with MCC555, GW9662, a combination of MCC555 and GW9662. Cells were harvested at days 3, 4, 5, and 9 post-induction to gain further insight into the transcriptional control of *Atp10c* during adipogenesis (Figure 14). In the control cells, high levels of *Atp10c* were expressed at day 3 that gradually decreased through days 4–9 (Figure 14A). When >80% of preadipocytes were differentiated into adipocytes at day 9, *Atp10c* expression was 2-fold down-regulated, supporting the earlier results. Cells treated with the *PPAR $\gamma$*  agonist and/or antagonist showed a similar pattern of decreased *Atp10c* expression. However, treatment with MCC555 showed even lower *Atp10c* levels throughout differentiation compared to control cells; some of this decrease was rescued by the combination of GW9662 with MCC555, confirming the earlier results. As expected, *PPAR $\gamma$*  expression increased significantly through days 3–9 (Figure 14B). ORO staining was carried out to monitor the differentiation process (Figure 15); quantitation confirms increased adipogenesis of cells treated with MCC555 compared to control cells treated with DMSO (Figure 16).

#### ***Atp10c mRNA is regulated by hormonal inducers***

Since *Atp10c* was expressed and levels were modulated during the differentiation of 3T3-L1 preadipocytes to adipocytes, the regulation of *Atp10c* mRNA expression by effector molecules of glucose and fat metabolism in undifferentiated and differentiated cells was investigated. This was examined by incubating cells with 100 nM insulin, 100

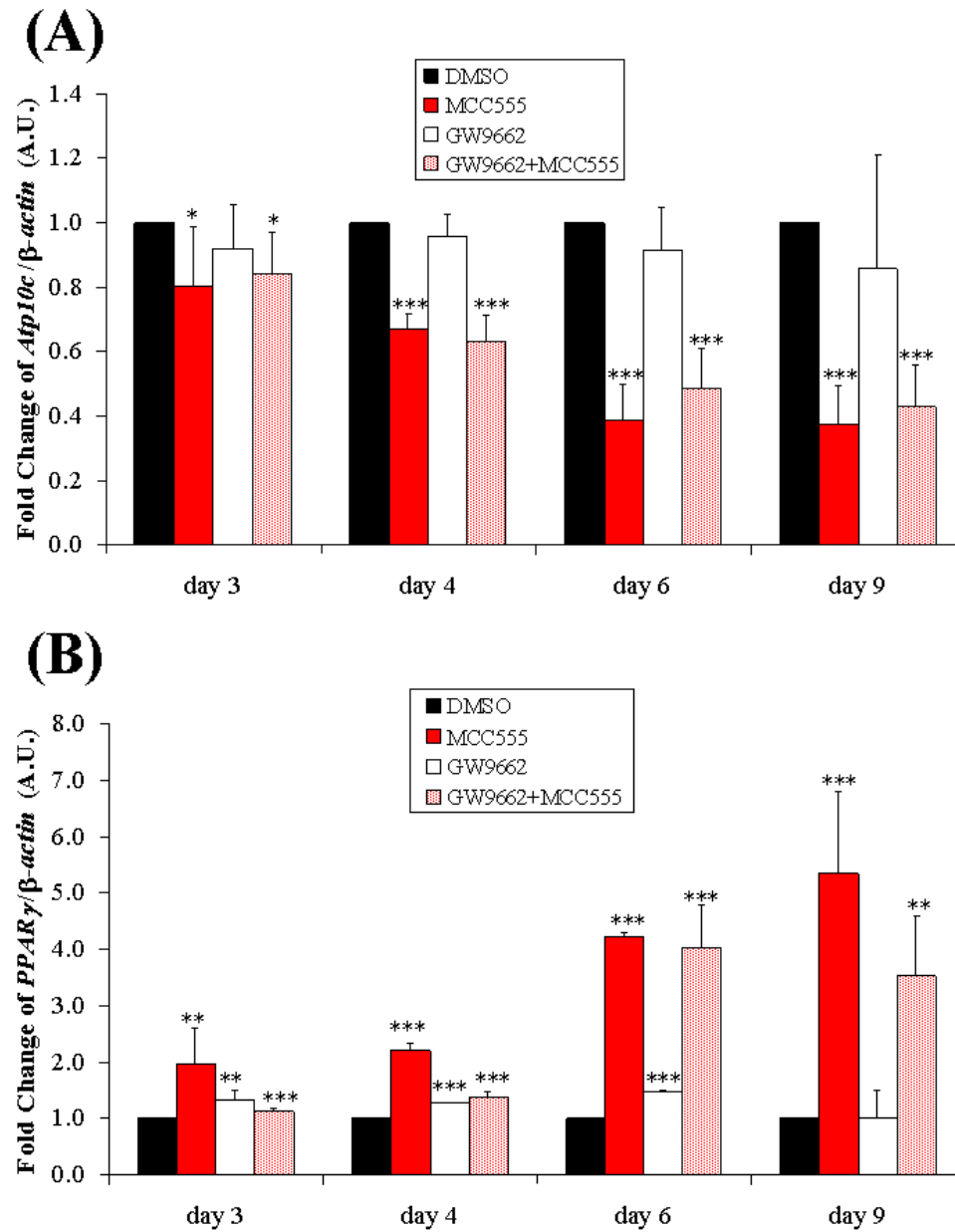


**Figure 14: *Atp10c* and *PPARγ* mRNAs are oppositely regulated in 3T3-L1 cells during adipogenesis.**

RT-PCR analysis was used to determine *Atp10c* (A) and *PPARγ* (B) mRNA expression in 3T3-L1 cells at days 3, 4, 6, and 9 post-induction;  $\beta$ -actin served as an internal control. Cells were treated throughout differentiation with the vehicle DMSO, MCC555, and/or GW9662. Expression of *Atp10c* and *PPARγ* mRNA is denoted as arbitrary units (A.U.) and represented as the fold change normalized to  $\beta$ -actin. \* $P$ <0.05, \*\* $P$ <0.01, \*\*\* $P$ <0.001.

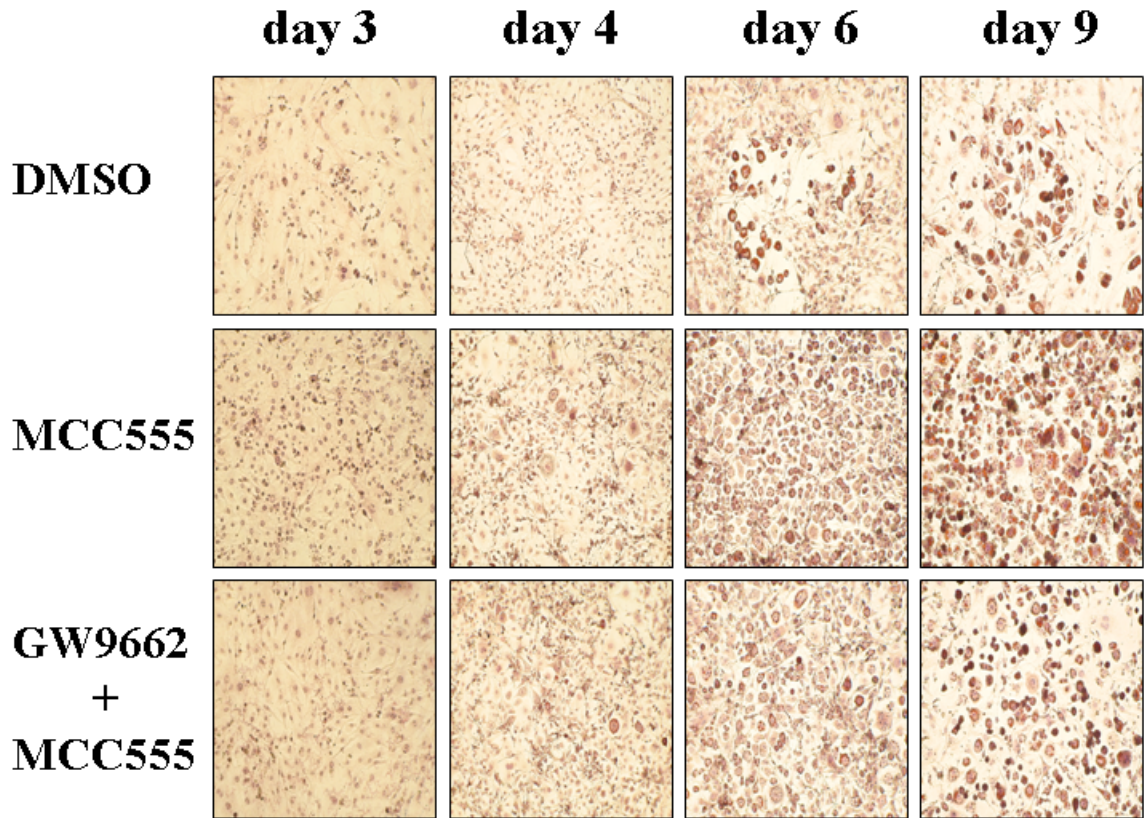


**Figure 15: ORO staining shows morphological changes during adipogenesis in 3T3-L1 cells following treatment with PPAR $\gamma$  agonists and antagonists.**

ORO staining was used to assess the morphological changes in 3T3-L1 cells at days 3, 4, 6, and 9 post-induction. Cells were treated throughout differentiation with the vehicle DMSO, MCC555, or a combination of MCC555 and GW9662.

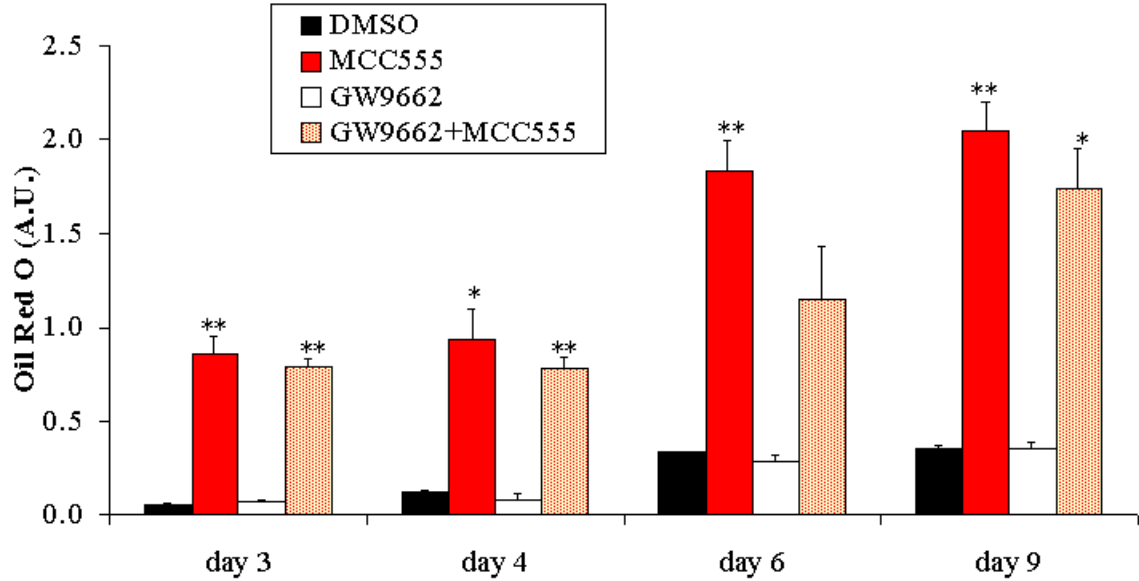


**Figure 16: ORO quantitation confirms adipogenesis in 3T3-L1 cells following treatment with PPAR $\gamma$  agonists and antagonists.**

ORO quantitation was used to determine the extent of adipose conversion in 3T3-L1 cells at days 3, 4, 6, and 9 post-induction. Cells were treated throughout differentiation with the vehicle DMSO, MCC555, and/or GW9662. On the specified days, cells were treated with ORO, which stains only the fat cells. The total ORO stain taken up by the cells was eluted with 100% isopropanol and the OD measured at 540 nm. Expression of ORO is denoted as arbitrary units (A.U.) and represented as the fold change of the PPAR $\gamma$  agonist or antagonist normalized to DMSO. \* $P < 0.05$ , \*\* $P < 0.01$ .

nM dexamethasone, or 100 nM isoproterenol for 24 h. *Atp10c* mRNA increased 4-fold or 6-fold, respectively, when insulin or dexamethasone was added to 3T3-L1 adipocytes (Figure 17A); there was no significant change in preadipocytes. As expected, *resistin* mRNA decreased following treatment with insulin or dexamethasone (Figure 17B).

*Atp10c* mRNA expression slightly decreased after incubating the cells with 100 nM isoproterenol, but this was not statistically significant (data not shown). The regulation of *Atp10c* mRNA expression by 100 nM insulin or 100 nM dexamethasone was also investigated in primary preadipocytes differentiated in culture. *Atp10c* mRNA slightly increased 1.5-fold or 1.4-fold, respectively, when insulin or dexamethasone was added to differentiated primary adipocytes (Figure 18). Based on these results, the up-regulation of *Atp10c* observed in primary adipocytes differentiated in culture (Figure 9B) was most likely due to the high insulin that is used in the differentiation media, which is 10-fold higher than this treatment with insulin.

#### ***Atp10c* mRNA and protein are knocked down in 3T3-L1 preadipocytes using siRNA**

Small interfering RNA (siRNA) can be used to knockdown the expression of a specific target gene and protein for further studies. Using two synthetic siRNAs, the knockdown of *Atp10c* mRNA was standardized in 3T3-L1 preadipocytes at different time points (Figure 19). Transient transfection with 200 nM of 5' *Atp10c* siRNA using HiPerfect transfection reagent showed the most consistent decrease in *Atp10c* expression, with 87%, 80%, and 93% knockdown at 24, 48, and 72 h, respectively. Transfection of 3T3-L1 preadipocytes also showed knockdown at the protein level, with 25% and 28% decrease in *Atp10c* expression at 48 and 72 h, respectively (Figure 20).

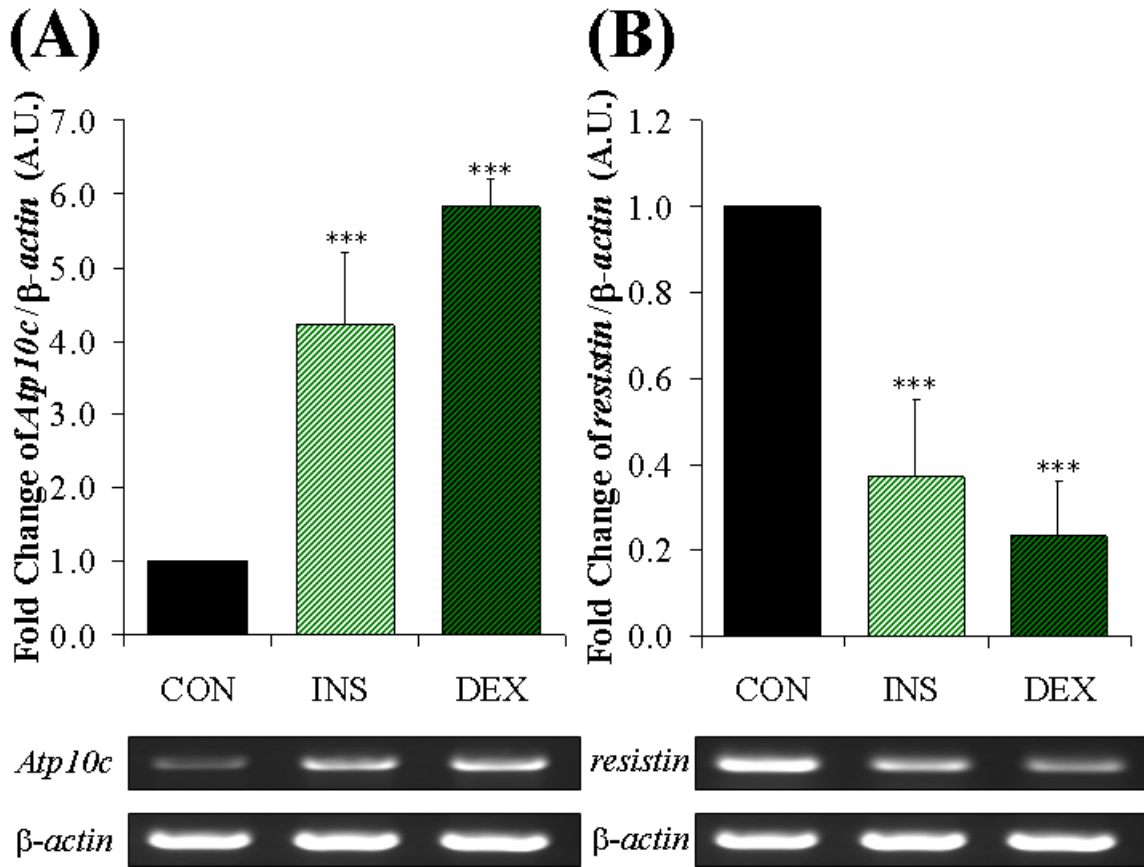


**Figure 17: *Atp10c* mRNA expression is regulated conversely to that of *resistin* mRNA in 3T3-L1 adipocytes following treatment with hormonal factors.**

RT-PCR analysis was used to determine *Atp10c* (A) and *resistin* (B) mRNA expression in untreated 3T3-L1 adipocytes (CON), and following treatment with 100 nM insulin (INS) or 100 nM dexamethasone (DEX) for 24 h.  $\beta$ -actin is used as an internal control. Expression of *Atp10c* and *resistin* mRNA is denoted as arbitrary units (A.U.) and represented as the fold change normalized to  $\beta$ -actin. \*\*\* $P$ <0.001.

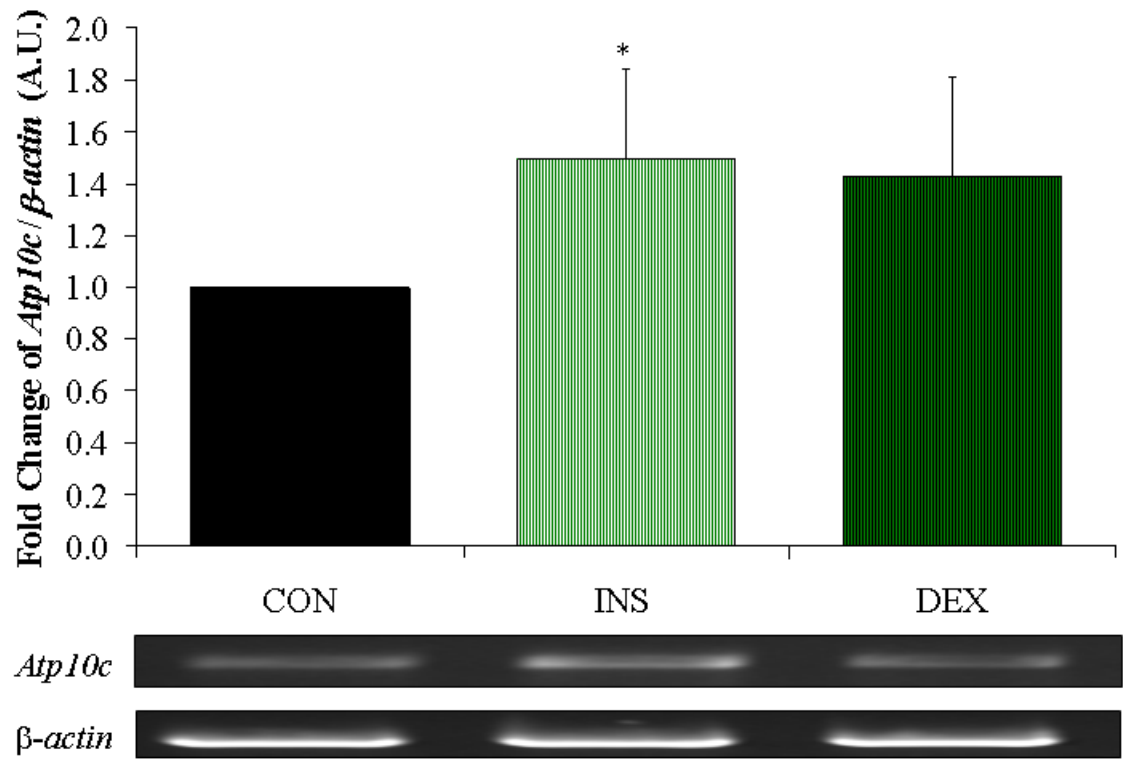


**Figure 18: *Atp10c* mRNA expression is regulated in primary adipocytes following treatment with hormonal factors.**

RT-PCR analysis was used to determine *Atp10c* mRNA expression in primary adipocytes differentiated in culture from control mice. Primary adipocytes were untreated (CON), or treated with 100 nM insulin (INS) or 100 nM dexamethasone (DEX) for 24 hours. *β-actin* is used as an internal control. Expression of *Atp10c* mRNA is denoted as arbitrary units (A.U.) and represented as the fold change normalized to *β-actin*. \* $P < 0.05$ .

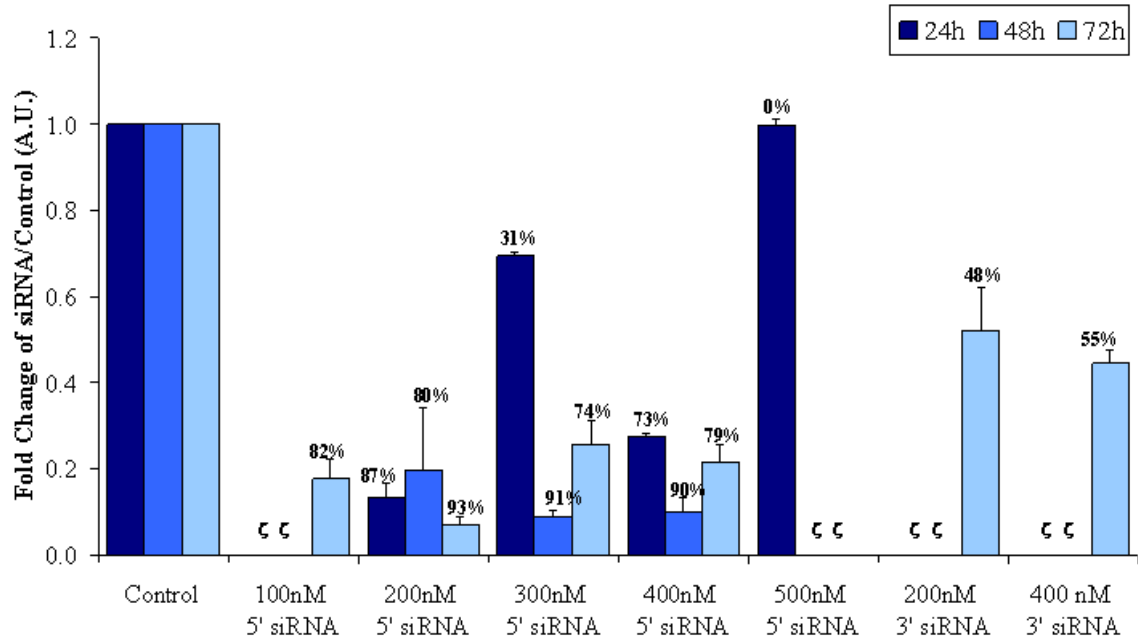


**Figure 19: Standardization of *Atp10c* mRNA knockdown in 3T3-L1 preadipocytes using siRNA.**

RT-PCR analysis was used to determine *Atp10c* mRNA expression in 3T3-L1 preadipocytes treated with 100 nM, 200 nM, 300 nM, 400 nM, or 500 nM of 5' or 3' *Atp10c* siRNA for 24, 48, or 72 h.  $\beta$ -actin is used as an internal control. Not all concentrations or times were tested (indicated by  $\zeta$ ). Expression of *Atp10c* mRNA is denoted as arbitrary units (A.U.) and represented as the fold change normalized to  $\beta$ -actin.



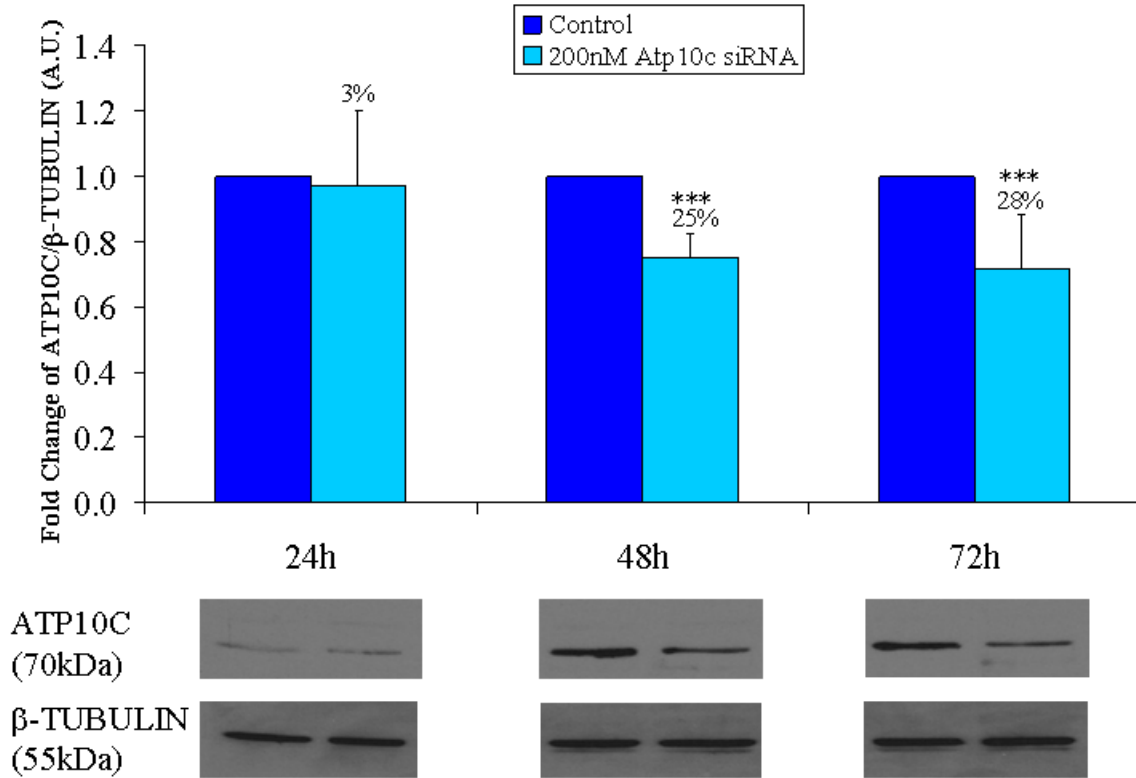


**Figure 20: ATP10C protein is knocked down in 3T3-L1 preadipocytes using siRNA.** Western blotting was used to determine ATP10C protein expression in 3T3-L1 preadipocytes treated with 200 nM of 5' ATP10C siRNA for 24, 48, or 72 h;  $\beta$ -TUBULIN is used as an internal control. Expression of ATP10C is denoted as arbitrary units (A.U.) and represented as the fold change normalized to  $\beta$ -TUBULIN. \*\*\* $P < 0.001$ .

### ***Atp10c mRNA and protein are knocked down in 3T3-L1 adipocytes using siRNA***

After determining that siRNA could be used to knockdown *Atp10c*/ATP10C expression in 3T3-L1 preadipocytes, the effect of siRNA in adipocytes was investigated. Adipocytes are generally more difficult to transfect than preadipocytes, however the novel “MPG” delivery technology (Panomics) uses virus-derived amphipathic MPG peptides that surround the siRNA, diffuse through the lipid bilayer membrane, and release the contents inside the cell. Knockdown of *Atp10c* mRNA in adipocytes was investigated using two concentrations and three time points (Figure 21). Transient transfection with 30 nM of 5' *Atp10c* siRNA using DeliverX transfection reagent yielded 88%, 64%, and 65% knockdown of *Atp10c* mRNA at 24, 48, and 72 h, respectively. At the protein level, a 38% knockdown of ATP10C was seen at 48 h (Figure 22).

The use of siRNA can sometimes lead to off-target effects, where the siRNA binds to and decreases expression of a different gene. In order to determine if the 5' *Atp10c* siRNA would lead to off-target effects, the expression of additional genes was analyzed in 3T3-L1 adipocytes following knockdown of *Atp10c* (Figure 23). Decreased *Atp10c* mRNA expression lead to decreased expression in genes involved in adipogenesis and/or glucose uptake: CCAAT-enhancer-binding protein  $\alpha$  (C/EBP $\alpha$ ), glucose transporter 4 (GLUT4), and PPAR $\gamma$ . These results support a role for *Atp10c* in the process of adipogenesis and/or glucose uptake.

*Atp10c* siRNA can be used to transiently knockdown *Atp10c*/ATP10C expression in 3T3-L1 preadipocytes or adipocytes as well as to transiently knockdown *Atp10c*/ATP10C expression in 3T3-L1 cells throughout adipogenesis (Figure 24).

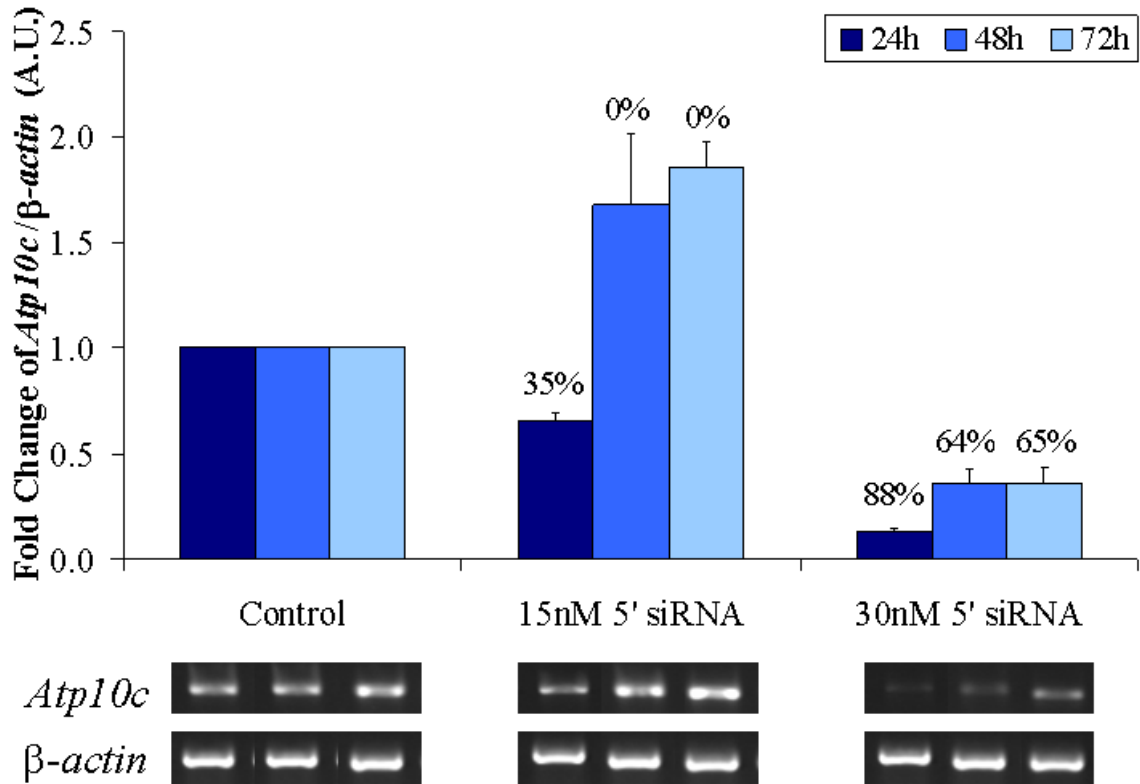


**Figure 21: Standardization of *Atp10c* mRNA knockdown in 3T3-L1 adipocytes using siRNA.**

RT-PCR analysis was used to determine *Atp10c* mRNA expression in 3T3-L1 adipocytes treated with 15 nM or 30 nM of 5' *Atp10c* siRNA for 24, 48, or 72 h.  $\beta$ -actin is used as an internal control. Expression of *Atp10c* mRNA is denoted as arbitrary units (A.U.) and represented as the fold change normalized to  $\beta$ -actin.

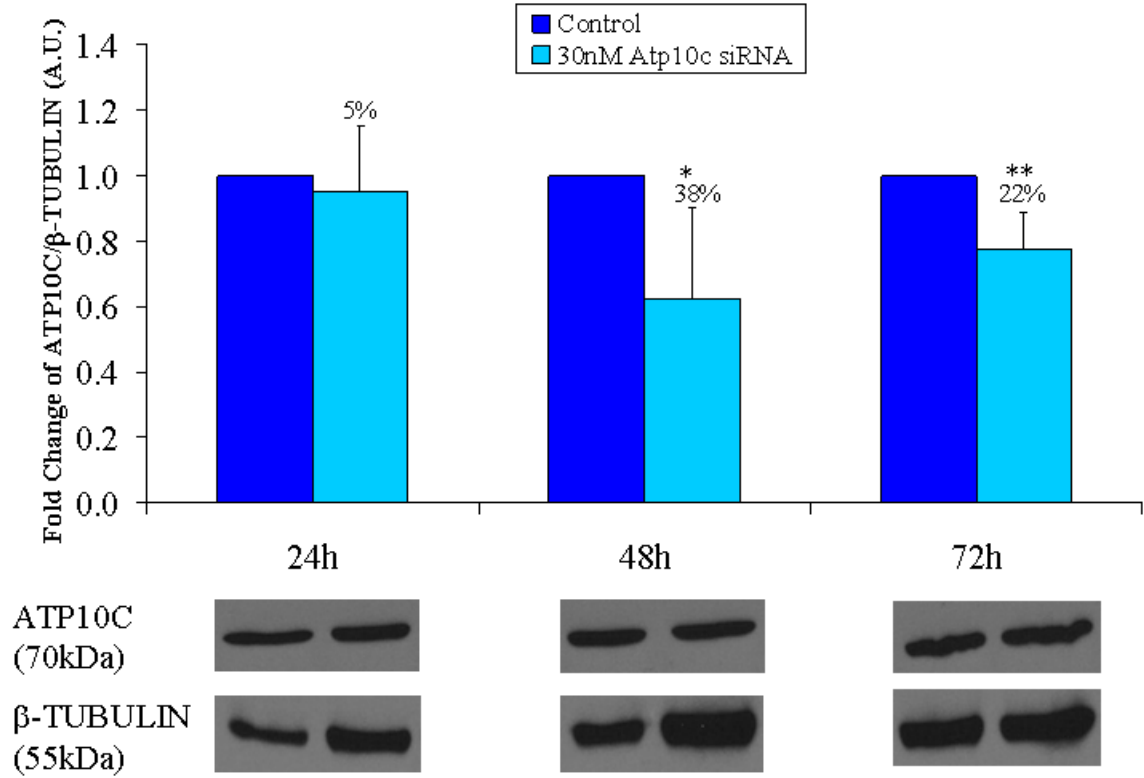


**Figure 22: ATP10C protein is knocked down in 3T3-L1 adipocytes using siRNA.**

Western blotting was used to determine ATP10C protein expression in 3T3-L1 adipocytes treated with 30 nM of 5' ATP10C siRNA for 24, 48, or 72 h;  $\beta$ -TUBULIN is used as an internal control. Expression of ATP10C is denoted as arbitrary units (A.U.) and represented as the fold change normalized to  $\beta$ -TUBULIN. \* $P$ <0.05, \*\* $P$ <0.01.

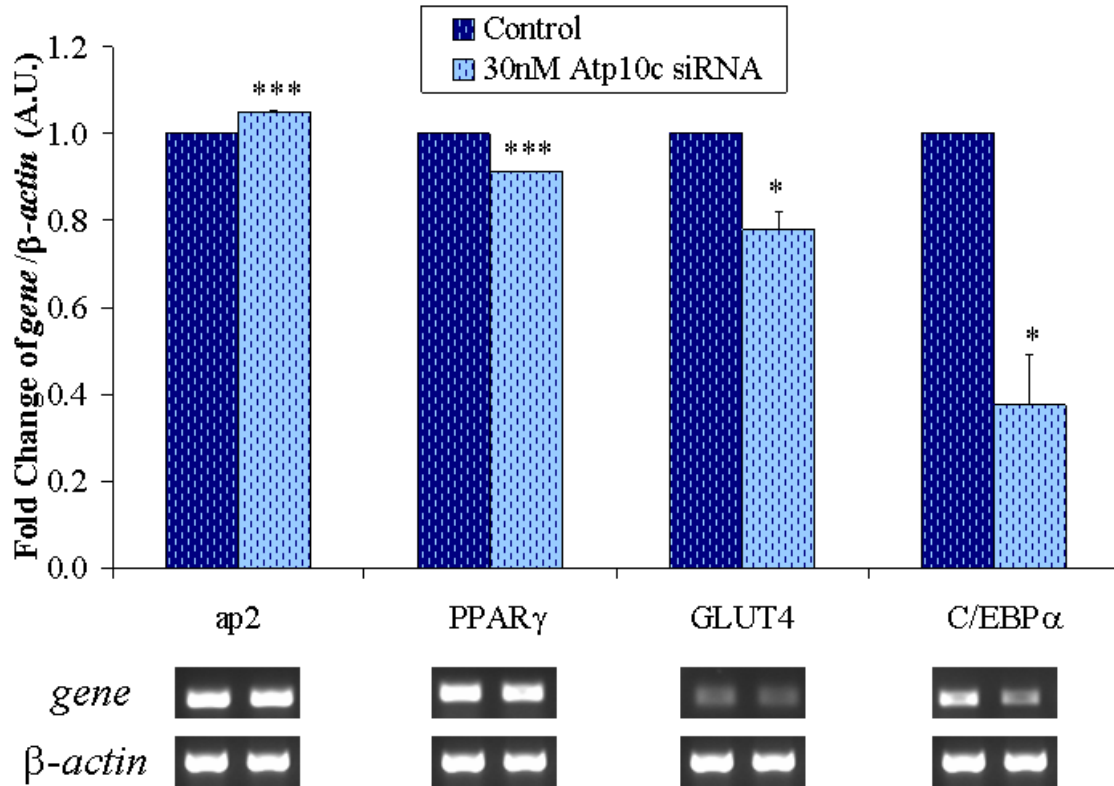


**Figure 23: Expression of additional genes in 3T3-L1 adipocytes following *Atp10c* mRNA knockdown using siRNA.**

RT-PCR analysis was used to determine mRNA expression of *ap2*, *PPARγ*, *GLUT4*, and *C/EBPα* in 3T3-L1 adipocytes treated with 30 nM of 5' *Atp10c* siRNA for 24 h. *β-actin* is used as an internal control. Expression of each gene is denoted as arbitrary units (A.U.) and represented as the fold change normalized to *β-actin*. \* $P < 0.01$ , \*\*\* $P < 0.001$ .

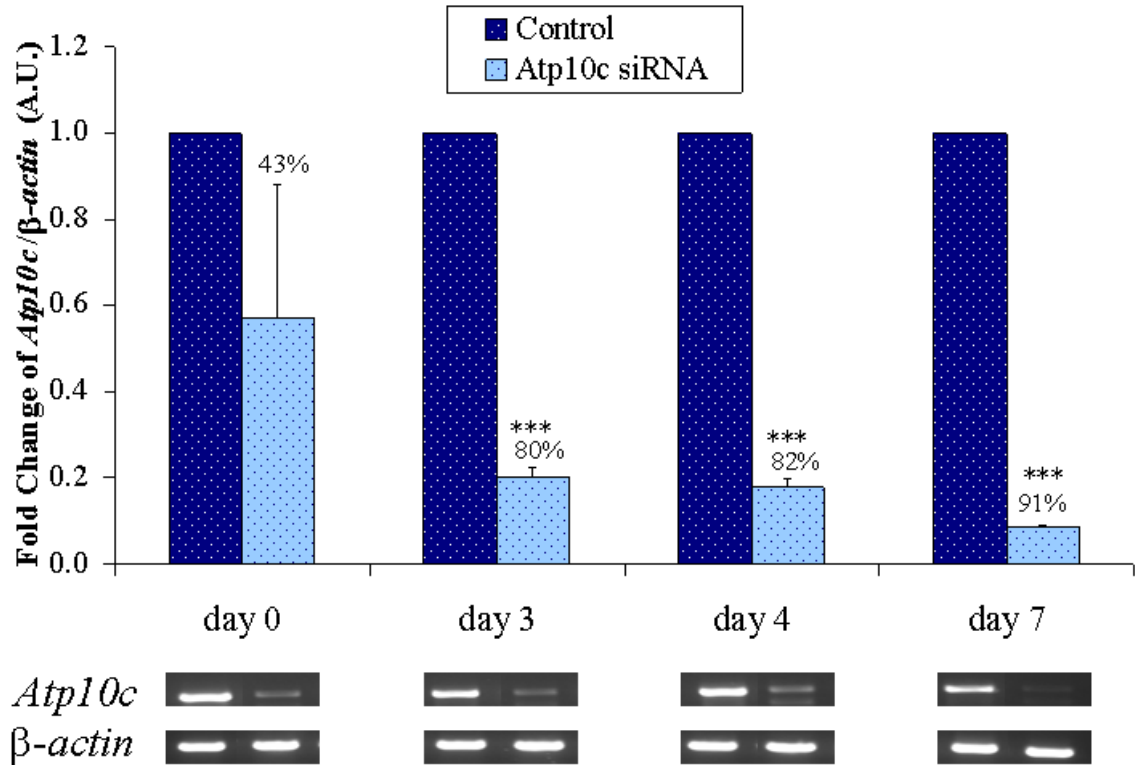


**Figure 24: *Atp10c* mRNA expression is knocked down throughout differentiation using siRNA.**

RT-PCR analysis was used to determine *Atp10c* mRNA expression in 3T3-L1 cells collected at days 0, 3, 4, and 7 post-induction treated with 5' *Atp10c* siRNA, which was added every time the media was changed.  $\beta$ -actin is used as an internal control. Expression of *Atp10c* is denoted as arbitrary units (A.U.) and represented as the fold change normalized to  $\beta$ -actin. \*\*\* $P < 0.001$ .

### ***Atp10c siRNA can be used to knockdown gene expression in primary cultures***

After confirming that siRNA could be used to transiently knockdown *Atp10c* in 3T3-L1 cells, the effect of siRNA in primary preadipocytes differentiated in culture was monitored (Figure 25). In primary preadipocytes, 200 nM of 5' *Atp10c* siRNA showed a 94% and 91% knockdown after 24 and 48 h, respectively. In primary adipocytes, 30 nM of 5' *Atp10c* siRNA showed a 51% knockdown after 24 h.

### ***Glucose uptake is increased following knockdown of Atp10c/ATP10C with siRNA***

The last part of the insulin signaling pathway after insulin binds to the insulin receptor is the uptake of glucose into the cell mediated by GLUT4. In order to study the effect of decreased *Atp10c/ATP10C* on glucose uptake in 3T3-L1 cells, the process was first standardized (Figure 26). Treatment of cells with 100 nM insulin for 30 min showed a 3-fold increase in glucose uptake compared to untreated cells. Glucose uptake was next measured in 3T3-L1 adipocytes following knockdown of *Atp10c/ATP10C* with siRNA. There was a 4-fold or 10-fold increase in glucose uptake of transfected adipocytes compared to control adipocytes after 24 or 48 h, respectively (Figure 27).

### ***Subcellular fractionation of 3T3-L1 cells can be used to localize ATP10C protein***

Following treatment with insulin, the movement of ATP10C between cellular fractions can be investigated to elucidate a potential role of ATP10C in the insulin signaling pathway. Subcellular fractionation of 3T3-L1 preadipocytes and adipocytes was performed (Figure 28). Following standardization of the fractionation procedure, cells were treated with or without insulin to localize the ATP10C protein (Figures 29, 30). The concentration of  $\text{Na}^+\text{K}^+$ -ATPase, which remains the same in the plasma

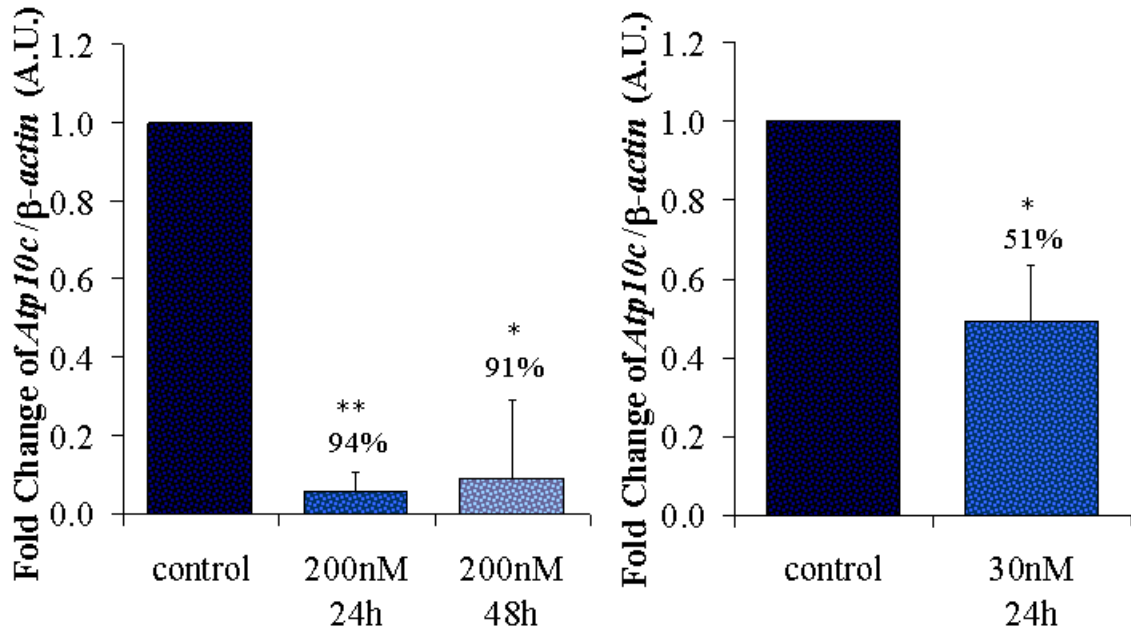


**Figure 25: Primary cultures treated with *Atp10c* siRNA show a knockdown in mRNA levels.**

RT-PCR analysis was used to determine *Atp10c* mRNA expression in primary preadipocytes (A) and adipocytes (B) collected from mouse tissue, plated, and differentiated in culture. Cells were treated with 5' *Atp10c* siRNA for 24 h.  $\beta$ -actin is used as an internal control. Expression of *Atp10c* is denoted as arbitrary units (A.U.) and represented as the fold change normalized to  $\beta$ -actin. \* $P$ <0.01, \*\* $P$ <0.05.



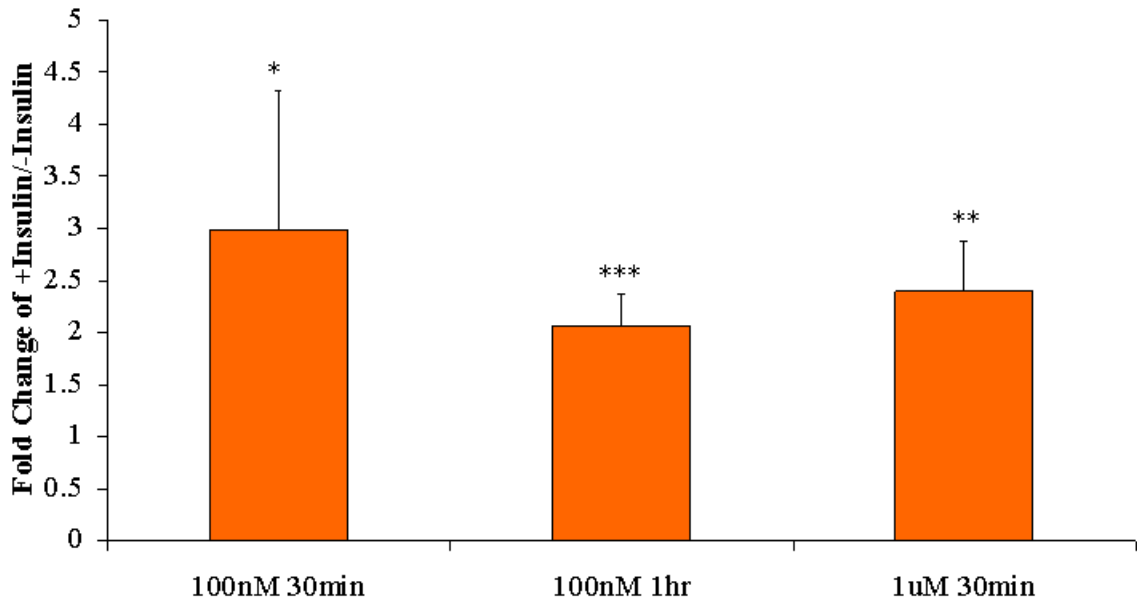


**Figure 26: Standardization of glucose uptake in 3T3-L1 adipocytes.**

Glucose uptake was used to determine the amount of 2-deoxyglucose incorporated into 3T3-L1 adipocytes. Standardization of concentration and time for insulin stimulation was performed. Glucose uptake is denoted as the fold change of glucose uptake with insulin stimulation normalized to basal glucose uptake (without the addition of insulin). \* $P < 0.01$ , \*\* $P < 0.05$ , \*\*\* $P < 0.001$ .

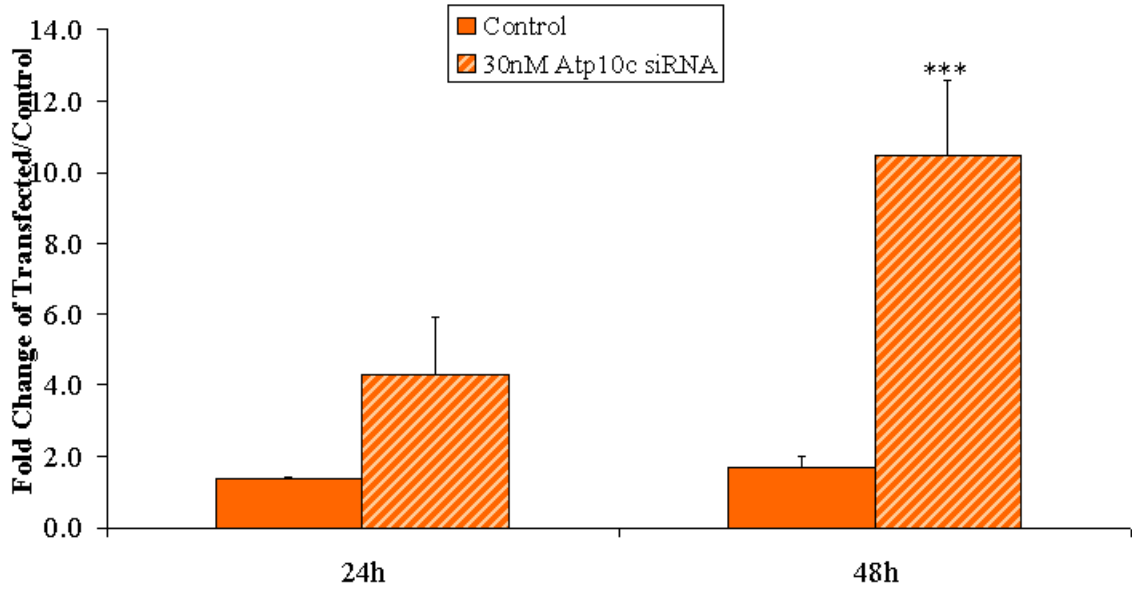


**Figure 27: Treatment of 3T3-L1 adipocytes with *Atp10c* siRNA increases glucose uptake.**

3T3-L1 adipocytes were treated with 30 nM of 5' *Atp10c* siRNA for 24 h or 48 h; glucose uptake was used to determine the amount of 2-deoxyglucose incorporated into the adipocytes. Glucose uptake in transfected cells is denoted as the fold change of glucose uptake normalized to glucose uptake in control cells. \*\*\* $P < 0.001$ .

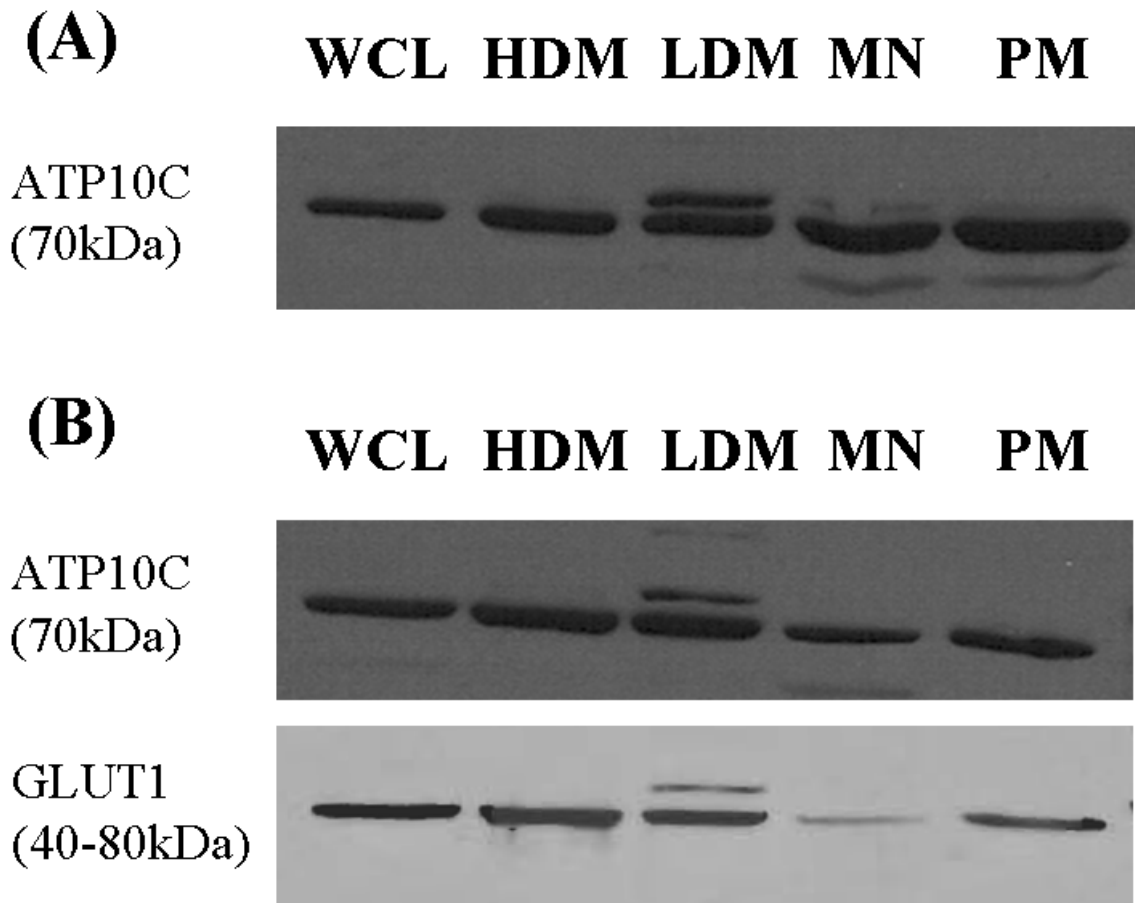


**Figure 28: Subcellular fractionation of 3T3-L1 preadipocytes and adipocytes.** Western blotting was used to determine ATP10C and GLUT1 protein expression in 3T3-L1 preadipocytes (A) and adipocytes (B) fractionated into whole cell lysate (WCL), high density microsomal (HDM), low density microsomal (LDM), mitochondrial nuclear (MN), and plasma membrane (PM) fractions.

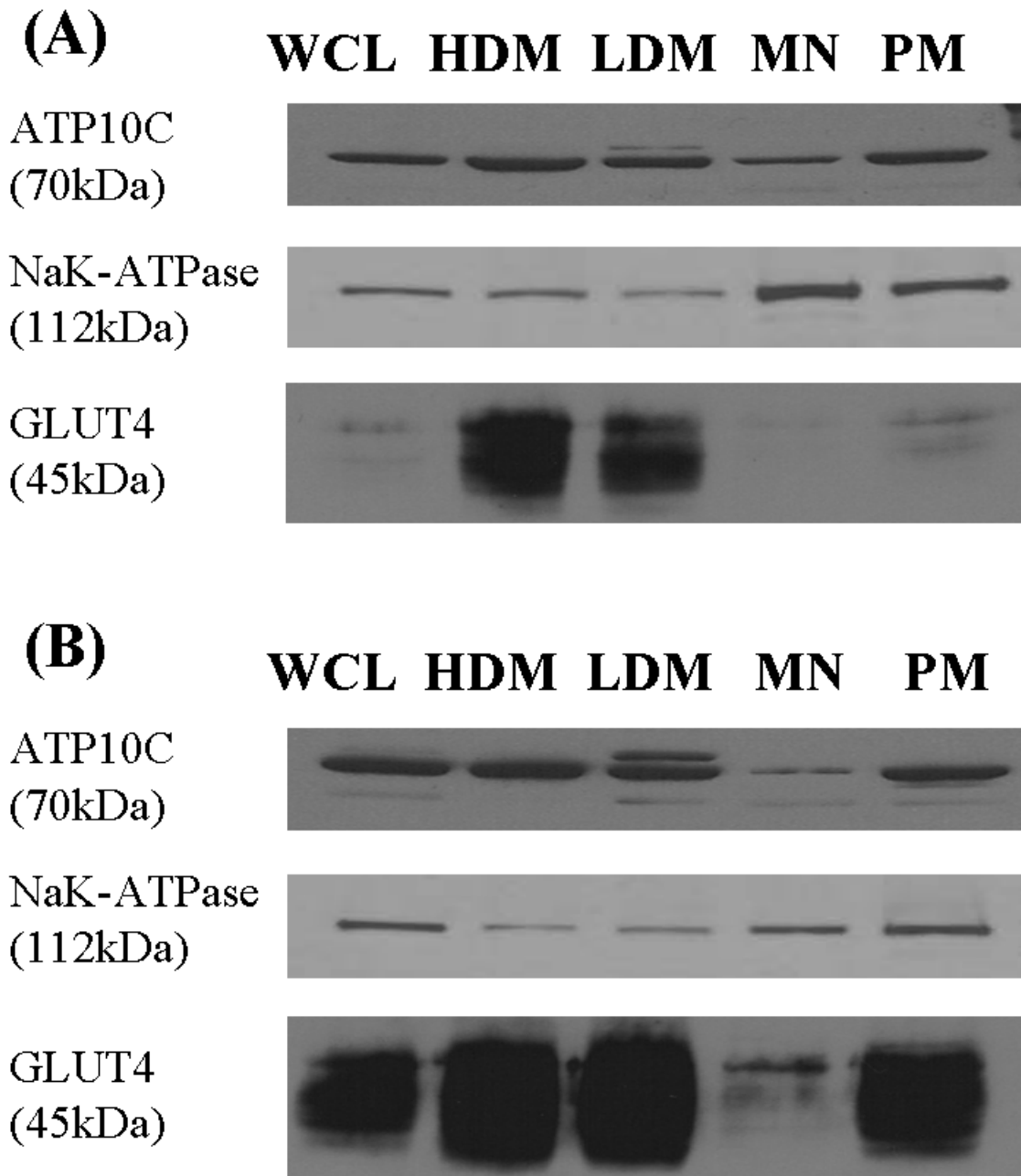


**Figure 29: Subcellular fractionation of 3T3-L1 adipocytes treated with insulin.** Western blotting was used to determine ATP10C, Na<sup>+</sup>K<sup>+</sup>-ATPase, and GLUT4 protein expression in 3T3-L1 adipocytes treated without (A) or with (B) 1 μM insulin for 30 min. Proteins were fractionated into whole cell lysate (WCL), high density microsomal (HDM), low density microsomal (LDM), mitochondrial nuclear (MN), and plasma membrane (PM) fractions.

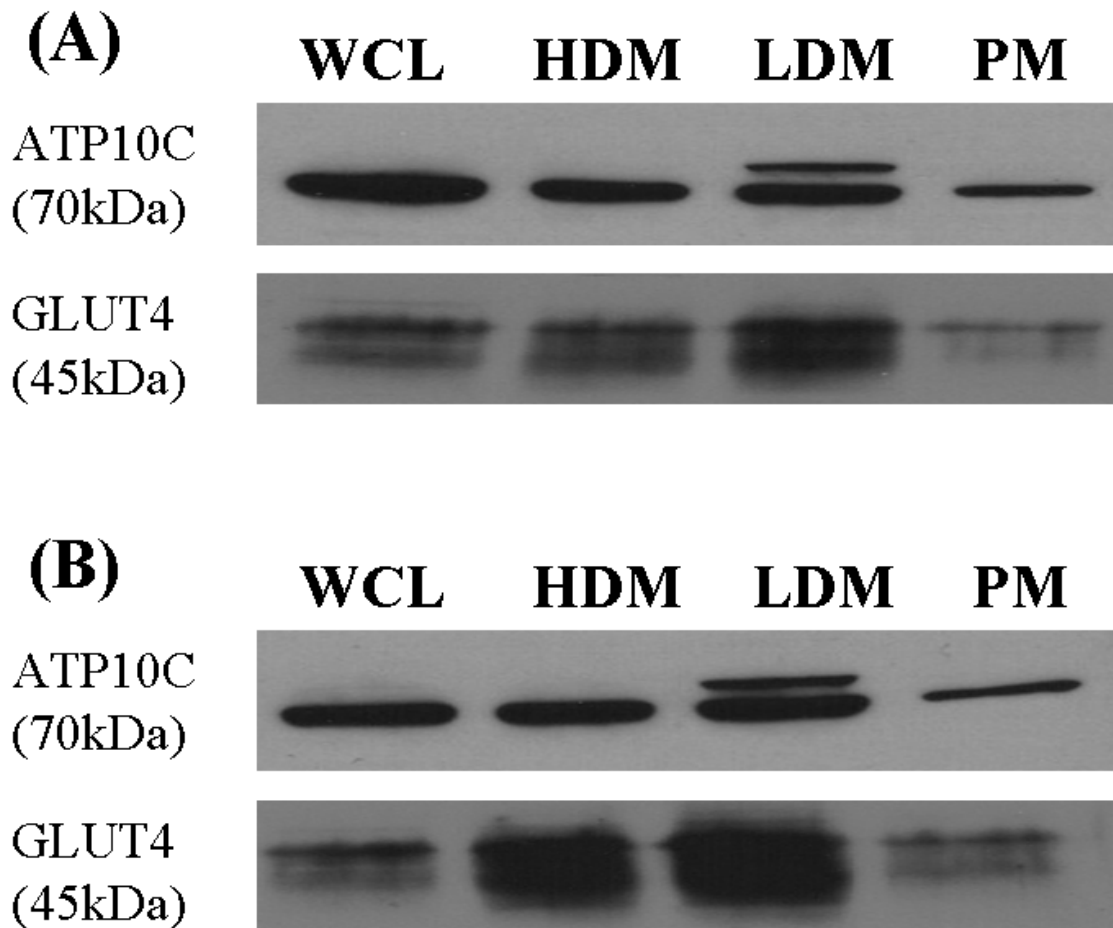


**Figure 30: A second subcellular fractionation of 3T3-L1 adipocytes treated with insulin.**

Western blotting was used to determine ATP10C and GLUT4 protein expression in 3T3-L1 adipocytes treated without (A) or with (B) 1  $\mu$ M insulin for 30 min. Proteins were fractionated into whole cell lysate (WCL), high density microsomal (HDM), low density microsomal (LDM), and plasma membrane (PM) fractions.

membrane, and GLUT4, which increases in the plasma membrane, both serve as internal controls.

## Discussion

*Atp10c* is a type IV P-type ATPase located on mouse chromosome 7.

Heterozygous mice inheriting a maternal deletion of the *Atp10c* gene become obese and exhibit hyperinsulinemia, hyperlipidemia, and hyperglycemia traditionally associated with T2DM [8, 66, 141]. In the study of metabolic diseases, the ability to distinguish between primary and secondary effects is a major problem. Given that *Atp10c* heterozygotes are obese and exhibit these metabolic abnormalities, it becomes difficult to understand if changes in glucose and lipid metabolism directly arise from alterations in ATP10C activity or if they are due to secondary complications. Therefore, the present study was initiated to define the functional importance of *Atp10c* in a cell. A cell system expressing *Atp10c* must first be established in order to use this system to identify factors modulating *Atp10c* expression and elucidate a biological role for *Atp10c*/ATP10C in the process of adipogenesis and the insulin signaling pathway.

The commercially available Swiss murine 3T3-L1 cell line [10] was used as an *in vitro* model while primary preadipocytes isolated from mouse adipose tissue and differentiated in culture were used as an *ex vivo* model. In order to use these systems in this project, the presence of *Atp10c* needed to first be demonstrated. The expression of *Atp10c* mRNA was shown in both the undifferentiated and differentiated adipocytes *in vitro* (Figure 8) and *ex vivo* (Figure 9). Quantitative analysis showed that *Atp10c* mRNA is 2-fold down-regulated in 3T3-L1 adipocytes during differentiation (Figure 8). This

decrease in expression was also seen in primary preadipocytes and adipocytes isolated from mouse adipose tissue (Figure 9A). However, *Atp10c* expression was slightly up-regulated in primary adipocytes differentiated in culture (Figure 9B). The addition of 100 nM insulin to primary adipocytes also slightly increased *Atp10c* expression (Figure 18). Thus, the up-regulation in primary adipocytes differentiated in culture is most likely due to the higher concentration of insulin present in the differentiation media that is only used for primary cultures. It has been previously shown that insulin may increase or decrease expression of a number of mRNAs coding for obesity and diabetes genes [157, 158]. In this study, it may stimulate up-regulation of *Atp10c* in primary adipocytes by increasing the turnover rate or the stability of *Atp10c* mRNA.

The down-regulation of *Atp10c* is opposite to that observed for *resistin* and *PPAR $\gamma$*  (Figures 8, 14), which are key molecules involved in the regulation of adipogenesis. This decrease during differentiation is also seen with preadipocyte factor-1, or *pref-1*, a member of the epidermal growth factor (EGF)-like family of proteins [159]. Similar to *Atp10c*, *Pref-1* is highly expressed in undifferentiated cells and down-regulated during differentiation, serving as an excellent marker for preadipocytes. The DNA sequence element involved in this differentiation-dependent down-regulation has already been identified and the protein binding characterized [160]. Due to the fact that *Atp10c* shows a differentiation-dependent expression pattern similar to *pref-1*, further research on *Atp10c* may elucidate a complementary role as a negative regulator of adipogenesis.

Upon confirmation of the decrease in *Atp10c* mRNA expression during differentiation in these cell systems, the next step was to characterize the protein

expression of ATP10C. Based on the molecular weight, a protein band at 169 kDa was expected in Western blotting; a band at this size was faint or unseen with the first sample loading buffer used. After testing multiple sample loading buffers with or without a reducing agent (Figure 10), protein bands in the high molecular weight range of 140 kDa and the low molecular weight range of 70 kDa were apparent with certain sample loading buffers. Due to the fact that neither of these bands was the expected molecular weight of ATP10C, a peptide neutralization experiment was performed (Figure 11). This demonstrated that the actual band for ATP10C using the antibody generated against the 15 amino acid peptide located between transmembrane helices four and five on the cytoplasmic loop is 70 kDa.

Although *Atp10c* mRNA decreased during differentiation, ATP10C protein was shown to increase (Figure 12). This was an unexpected result because traditionally the transcribed mRNA is translated into an amino acid polypeptide chain that codes for a protein; as mRNA levels increase, protein levels would also be expected to increase. There are multiple potential correlations between the molecular weight discrepancy and the opposite pattern of *Atp10c* mRNA and ATP10C protein expression.

DNA contains genes that code for a unique protein. Protein synthesis begins when the sequence of DNA is transcribed into mRNA in the nucleus of a cell. The mRNA is processed and then moves out into the cytoplasm, where it is translated into a polypeptide chain that codes for a specific protein with the use of ribosomes located on the endoplasmic reticulum (ER).

Since ATP10C is located in the ER once it is synthesized before transportation to another part of the cell, one reason for a lower molecular weight band may be due to



endoplasmic reticulum-associated protein degradation (ERAD). Conditions that interfere with the normal functioning of the ER are collectively known as ER stress [161]. One response to ER stress is the degradation of misfolded or unassembled proteins by ERAD [162]. This degradation may result in the production of a smaller protein, potentially explaining the 70 kDa ATP10C band when it was expected to be 169 kDa. ER stress has been shown to not only be related to numerous monogenic diseases [163], but also to the more complex diseases of obesity [164] and T2DM [161, 165]. Özcan *et al* and others have identified ER stress as a molecular link between obesity, decreased action of insulin, and the development of T2DM [164, 166]. Using cell culture and mouse models, it has been shown that obesity causes ER stress, which may correlate to the increased production of the 70 kDa ATP10C protein during differentiation. As the 3T3-L1 cells become adipogenic, there may be an increase in the degree of ER stress, which leads to ERAD and an increased production of the 70 kDa degraded ATP10C protein.

If the ATP10C protein is not misfolded or unassembled in the ER to be targeted for ERAD, a molecular chaperone should transport ATP10C from the ER to the plasma membrane. However, a defect in the molecular chaperone would keep ATP10C in the ER, allowing it to be targeted for ERAD as described above. Leptin is a hormone secreted in adipocytes that has been shown to modulate the secretion of the proinflammatory cytokine interferon- $\gamma$  (IFN- $\gamma$ ). Research in the Pacifico laboratory found that there is an increased production of IFN- $\gamma$  in obese children [167]. Combining this discovery with research concluding that IFN- $\gamma$  induces severe ER stress through the inhibition of molecular chaperones [165], ATP10C may still remain in the ER after protein folding due to a defect in the molecular chaperone. The increased ER stress

caused by adipogenesis would again degrade the ATP10C protein remaining in the ER, producing the smaller 70 kDa form.

Lastly, a post-translational modification of ATP10C may cleave the protein, resulting in multiple fragments. The antibody used in these experiments may only be recognizing the N terminal portion of the cleaved protein. The difference in the expected versus resulting protein size may be related to the antibody, which was generated against a small region of the peptide. In order to prove or disprove that the protein is actually 70 kDa, it will be necessary to generate a new ATP10C antibody against a different region of the peptide.

The process of adipocyte differentiation is associated with a large number of *cis*- and *trans*-acting factors [106, 168, 169]. The regulation of different genes at distinct times after the exposure of cells to differentiation conditions suggests the existence of a regulatory hierarchy or cascade of events [110, 170]. PPAR $\gamma$  is considered to be the master regulator of adipogenesis [110] and controls the expression of adipocyte genes. After investigating the effect of the anti-diabetic drugs MCC555 and TGZ [109, 130] on *Atp10c* expression, it was shown that these PPAR $\gamma$  agonists promoted adipogenesis and further decreased *Atp10c* expression (Figure 13). Adipocytes treated with the PPAR $\gamma$  antagonist GW9662 [156] alone showed *Atp10c* expression similar to that in control cells treated with the vehicle DMSO. However, the combination of the PPAR $\gamma$  agonist and antagonist demonstrated that GW9662 was capable of rescuing some of the decrease in *Atp10c* expression due to MCC555 or TGZ alone.

Because both MCC555 and TGZ are anti-diabetic drugs and PPAR $\gamma$  agonists that decreased *Atp10c* expression, the next experiment to gain further insight into the

transcriptional control of *Atp10c* during adipogenesis used only MCC555 (Figure 14). Confirming that *Atp10c* is down-regulated in adipogenesis, high levels of *Atp10c* were expressed at day 3 that gradually decreased throughout differentiation as opposed to the low levels of *PPAR $\gamma$*  expression that gradually increased throughout differentiation. Cells treated with MCC555 and/or GW9662 showed a similar pattern of decreased *Atp10c* expression and increased *PPAR $\gamma$*  expression. This opposite regulation of *Atp10c* and *PPAR $\gamma$*  suggests a potential role for *Atp10c* as a *PPAR $\gamma$*  modulator.

MCC555 and TGZ are members of the thiazolidinedione (TZD) class of drugs used to treat and manage T2DM through the improvement of insulin sensitivity [115]. These *PPAR $\gamma$*  agonists act to increase transcription of *PPAR $\gamma$* , which then binds to a peroxisome proliferator hormone responsive element (PPRE) usually located in the promoter region in order to increase or decrease gene expression. MCC555 and TGZ both decreased *Atp10c* gene expression while increasing adipocyte differentiation, similar to the inhibition of *leptin* gene expression in 3T3-L1 adipocytes following treatment with TZDs [117]. This is interesting because TZDs are known to increase adipogenesis and *leptin* is predominantly expressed in fat cells. These results suggest that the negative regulation of *leptin* by TZDs may indicate that these compounds induce a state of adipocyte differentiation that is subtly different from that induced by the differentiation cocktail.

Due to the fact that *Atp10c* was expressed and levels were modulated during the differentiation of 3T3-L1 preadipocytes to adipocytes, the regulation of *Atp10c* mRNA expression by effector molecules of glucose and fat metabolism in undifferentiated and differentiated cells was next investigated using the hormonal factors insulin,

dexamethasone, and isoproterenol. Although there was no significant change in *Atp10c* expression in 3T3-L1 or primary preadipocytes, *Atp10c* mRNA increased in 3T3-L1 (Figure 17) or primary (Figure 18) adipocytes when treated with insulin or the glucocorticoid dexamethasone. There was a slight decrease in expression following treatment with the  $\beta$ -adrenergic receptor isoproterenol, although this was not statistically significant. These results suggest transcriptional control of *Atp10c* expression by hormonal factors during differentiation. Insulin is already known to positively or negatively regulate a number of mRNAs coding for obesity and diabetes genes [157, 158]. In this study, it may stimulate *Atp10c* production in 3T3-L1 adipocytes by increasing the turnover rate or the stability of *Atp10c* mRNA. Dexamethasone induces insulin resistance and stimulates *Atp10c* production, which is similar to its effect on *resistin* and *ob* gene expression and leptin production [171]. In contrast, the lack of a significant effect by isoproterenol suggests that *Atp10c* expression is not controlled by adrenoreceptors ( $\beta$ -adrenergic factors) in 3T3-L1 adipocytes [172].

Signaling through the insulin pathway is critical for the regulation of intracellular and blood glucose levels and the avoidance of diabetes. Insulin binds to its receptor leading to the autophosphorylation of the  $\beta$ -subunits and the tyrosine phosphorylation of insulin receptor substrates (IRS-1, 2, 3). IRS phosphorylates the SH2 domain of the tyrosine phosphatase Shp2 and the SH3 domain of the adaptor molecule Grb2. Activated Grb2 recruits Sos1 that, in turn, activates the Ras signaling pathway and gene transcription. IRS also activates phosphoinositide 3-kinase (PI3K) through its SH2 domain, thus increasing the intracellular concentration of PIP<sub>2</sub> and PIP. This, in turn, activates phosphatidylinositol phosphate-dependent kinase-1 (PDK-1), that subsequently

activates a serine-threonine protein kinase Akt/PKB resulting in the translocation of the glucose transporter (GLUT4) from cytoplasmic vesicles to the cell membrane. In all types of obesity and diabetes, the major abnormality lies in the glucose uptake system [93, 96, 97, 173].

With the recent advent of siRNA technology, RNAi-based gene silencing in cultured 3T3-L1 adipocytes has proven to be valuable in examining elements crucial for the insulin signaling pathway leading to translocation of glucose transporter 4 (GLUT4) to the plasma membrane and for adipocyte differentiation [135-137]. Gene silencing in cultured mammalian cells is being used as an effective way to quickly screen the requirement of a specific gene for a biological function. In order to investigate the biological role of *Atp10c*/ATP10C in the insulin signaling pathway, gene and protein levels were silenced using siRNA technology. Knockdown of *Atp10c*/ATP10C was first standardized in both 3T3-L1 preadipocytes (Figures 19, 20) and adipocytes (Figures 21, 22) and shown to be knocked down throughout differentiation (Figure 24) that also affected several key factors of adipogenesis (Figure 23). Then, glucose uptake was used to investigate a biological role for ATP10C in the insulin signaling pathway. When ATP10C was silenced, glucose uptake increased (Figure 27). This also supports the MCC555 and TGZ data because TZDs are anti-diabetic drugs that improve insulin sensitivity by increasing the uptake of glucose, and they also decreased the expression of *Atp10c*. Similarly, when *Atp10c*/ATP10C was decreased with siRNA, glucose uptake was significantly increased. Knockdown of PPAR $\gamma$  has been shown to attenuate glucose uptake in 3T3-L1 adipocytes [113], again corroborating the opposing regulation of *Atp10c* and PPAR $\gamma$ . Park *et al* [174] demonstrated analogous findings to the *Atp10c* data

using cilostazol, which stimulated transcriptional activity of *PPAR* $\gamma$  in human umbilical vein endothelial cells and increased glucose uptake.

The *in vitro* glucose uptake results using 3T3-L1 adipocytes are opposite of those in the whole animal model [141], where knockdown of ATP10C in the heterozygous mutant mice led to decreased glucose uptake. This demonstrates the difficulty in understanding if changes in glucose and lipid metabolism in a whole animal model directly arise from alterations in ATP10C activity or if they are due to secondary complications.

To further investigate the cellular localization of ATP10C with and without insulin stimulation, subcellular fractionation of 3T3-L1 preadipocytes and adipocytes was performed (Figure 28). Following stimulation with insulin, it appeared that ATP10C expression increased in the plasma membrane (Figures 29, 30). However, it becomes difficult to interpret these results due to cross-contamination between fractions.

Based on these results and the current literature, *Atp10c*/ATP10C does have a role in the insulin signaling pathway and may have a potential role in adipogenesis.

## CHAPTER 4. CONCLUSIONS AND FUTURE DIRECTIONS

The aim of this study was to investigate the biological role of *Atp10c*/ATP10C, a type IV P-type ATPase located on mouse chromosome 7, in the process of adipogenesis and the insulin signaling pathway. Heterozygous mice inheriting a maternal deletion of the *Atp10c* gene become obese and exhibit metabolic abnormalities (hyperinsulinemia, hyperlipidemia, and hyperglycemia) traditionally associated with T2DM [8, 66, 141]. The ability to distinguish between primary and secondary effects is a major problem with the use of a whole animal model, making it hard to understand if changes in glucose and lipid metabolism directly arise from alterations in ATP10C activity or if they are due to secondary complications. Therefore, the commercially available Swiss murine 3T3-L1 cell line was used as an *in vitro* model to study changes in *Atp10c*/ATP10C expression and primary preadipocytes isolated from mouse adipose tissue and differentiated in culture were used as an *ex vivo* model.

*Atp10c* mRNA was 2-fold down-regulated during adipogenesis, similar to the known inhibitor of adipocyte differentiation, *pref-1* [159, 160, 175-180]. This is interesting because most of the genes related to obesity are up-regulated during adipogenesis [105, 181-183]. Previous research has shown that constitutive expression of *pref-1* inhibits the process of adipogenesis, suggesting that *pref-1* functions as a negative regulator of the differentiation process [159]. Due to the fact that *Atp10c* shows a similar differentiation-dependent down-regulation to *pref-1*, a future experiment with the constitutive expression of *Atp10c* would elucidate its effect on adipogenesis and its role in regulating the process of differentiation.

Interestingly, ATP10C protein was up-regulated throughout differentiation and showed an unexpected protein band at a lower molecular weight of 70 kDa. This discrepancy may be due to endoplasmic reticulum-associated protein degradation (ERAD) if the protein is misfolded or unassembled in the ER or if there is a defect in the molecular chaperone that would cause ATP10C to remain in the ER and be degraded. It may also be due to a post-translational modification that cleaves the protein so that the antibody that was generated against a 15 amino acid peptide sequence between transmembrane loops four and five on the N terminus is only recognizing one part of the cleaved protein. To resolve these data, generation of a second antibody against a peptide sequence located in a different region on the C terminal end may show the same band at 70 kDa, supporting ERAD of ATP10. However, a protein band at a different molecular weight would support post-translational protein cleavage.

PPAR $\gamma$  is considered to be the master regulator of adipogenesis [110], controlling the expression of adipocyte genes. Throughout differentiation, *Atp10c* and *PPAR $\gamma$*  mRNAs were oppositely regulated, suggesting a potential role for *Atp10c* as a *PPAR $\gamma$*  modulator. Treatment of 3T3-L1 cells with the PPAR $\gamma$  agonists MCC555 and TGZ demonstrated increased adipogenesis and decreased expression of *Atp10c*. These PPAR $\gamma$  agonists are also anti-diabetic drugs that act to improve insulin sensitivity in diabetic patients by increasing glucose uptake. Silencing *Atp10c*/ATP10C with siRNA, similar to the decreased expression seen following treatment with the PPAR $\gamma$  agonists, led to increased glucose uptake, again supporting the role of *Atp10c* as a PPAR $\gamma$  modulator. To further investigate this potential function, the silencing of *PPAR $\gamma$*  in 3T3-L1 cells before,



during, and after differentiation followed by the subsequent analysis of its affect on *Atp10c* expression would be beneficial.

Due to the fact that PPARs bind to PPREs in order to activate or suppress gene expression, analysis of the *Atp10c* gene sequence may also provide valuable evidence of the presence a PPRE. If a PPRE is present, experiments should also be undertaken to confirm if the site is functional, similar to the experiments Frohnert *et al* performed to determine the functionality of the murine fatty acid transport protein (*FATP*) gene PPRE [184].

The knockdown of ATP10C in 3T3-L1 adipocytes led to increased glucose uptake, but another experiment to examine its role in glucose uptake would be to silence ATP10C expression throughout differentiation to see what would happen if ATP10C was completely ablated in preadipocytes. Glucose uptake involves the translocation of GLUT4 from the inner membrane to the outer membrane of a cell in order to take up the glucose from the cytosol. Because ATP10C may have a potential role in this process, future work could be to localize the protein in 3T3-L1 cells. The subcellular fractionation experiments showed that ATP10C could be localized and the effect of insulin stimulation monitored; however, there was a question of cross-contamination between fractions, making it difficult to interpret the results. Additionally, a tremendous number of cells are needed for subcellular fractionation that would render this experiment expensive and unfeasible to look at the effect of transient *Atp10c* knockdown with siRNA. Immunofluorescence microscopy is a technique currently used in research [125, 185] that represents as a more money-conscious and effective way to localize proteins in a cell.

Since *Atp10c* has been successfully knocked down using transient siRNA transfection, which did show an effect on the insulin signaling pathway, experiments can be undertaken to knockdown *Atp10c* in the generation of a stable cell line. This cell line could also be used for subcellular fractionation experiments because there is no longer a need for the expensive siRNA used in transient transfections.

All of the work for this project was performed using the mouse embryonic fibroblast-adipose like 3T3-L1 cell line or primary preadipocytes isolated from mouse adipose tissue and differentiated in culture. However, insulin resistance is due to a defect in both adipose tissue, accounting for 5-10% of the glucose uptake, and skeletal muscle, which disposes of the majority of glucose [92, 94, 96, 97, 186, 187]. Dhar *et al* showed that *Atp10c* expression was significantly down-regulated in *Atp10c* heterozygous mice fed a high-fat diet for 4 and 12 weeks; this decrease was seen only in the soleus muscle and not the adipose tissue at the earlier timepoint [141]. Thus, a future direction for this project would be to examine changes in *Atp10c*/ATP10C expression using the mouse muscle cell line C2C12 [188, 189]. A second benefit to looking at this cell line is that obesity does not cause ER stress in the muscle tissue [164], so this may help support or refute ERAD of ATP10C protein due to ER stress caused by increased adiposity.

In summary, *Atp10c* and the master regulator of adipogenesis *PPAR $\gamma$*  are oppositely regulated and knockdown of *Atp10c*/ATP10C increases glucose uptake in 3T3-L1 adipocytes. This supports a biological role for *Atp10c*/ATP10C the insulin signaling pathway and a potential role in adipogenesis, although further experimentation is necessary to elucidate the exact function.

## LIST OF REFERENCES

## LIST OF REFERENCES

1. Strauss, R.S. and H.A. Pollack, *Epidemic increase in childhood overweight, 1986-1998*. *Jama*, 2001. **286**(22): p. 2845-8.
2. Mokdad, A.H., et al., *Prevalence of obesity, diabetes, and obesity-related health risk factors, 2001*. *Jama*, 2003. **289**(1): p. 76-9.
3. Hedley, A.A., et al., *Prevalence of overweight and obesity among US children, adolescents, and adults, 1999-2002*. *Jama*, 2004. **291**(23): p. 2847-50.
4. Paulusma, C.C. and R.P. Oude Elferink, *Diseases of intramembranous lipid transport*. *FEBS Lett*, 2006. **580**(23): p. 5500-9.
5. Paulusma, C.C. and R.P. Oude Elferink, *The type 4 subfamily of P-type ATPases, putative aminophospholipid translocases with a role in human disease*. *Biochim Biophys Acta*, 2005. **1741**(1-2): p. 11-24.
6. Daleke, D.L., *Phospholipid flippases*. *J Biol Chem*, 2007. **282**(2): p. 821-5.
7. Graham, T.R., *Flippases and vesicle-mediated protein transport*. *Trends Cell Biol*, 2004. **14**(12): p. 670-7.
8. Dhar, M., et al., *A novel ATPase on mouse chromosome 7 is a candidate gene for increased body fat*. *Physiol Genomics*, 2000. **4**(1): p. 93-100.
9. Dhar, M.S., et al., *Mice heterozygous for Atp10c, a putative amphipath, represent a novel model of obesity and type 2 diabetes*. *J Nutr*, 2004. **134**(4): p. 799-805.
10. Green, H. and M. Meuth, *An established pre-adipose cell line and its differentiation in culture*. *Cell*, 1974. **3**(2): p. 127-33.
11. Mokdad, A.H., et al., *The continuing epidemic of obesity in the United States*. *Jama*, 2000. **284**(13): p. 1650-1.
12. Mokdad, A.H., et al., *The spread of the obesity epidemic in the United States, 1991-1998*. *Jama*, 1999. **282**(16): p. 1519-22.
13. Ogden, C.L., et al., *Prevalence of overweight and obesity in the United States, 1999-2004*. *Jama*, 2006. **295**(13): p. 1549-55.
14. Flegal, K.M., et al., *Prevalence and trends in obesity among US adults, 1999-2000*. *Jama*, 2002. **288**(14): p. 1723-7.
15. Ogden, C.L., et al., *Prevalence and trends in overweight among US children and adolescents, 1999-2000*. *Jama*, 2002. **288**(14): p. 1728-32.

16. Sodjinou, R., et al., *Obesity and cardio-metabolic risk factors in urban adults of Benin: relationship with socio-economic status, urbanisation, and lifestyle patterns*. BMC Public Health, 2008. **8**(1): p. 84.
17. Ko, G.T. and J.C. Chan, *Burden of obesity--lessons learnt from Hong Kong Chinese*. Obes Rev, 2008. **9 Suppl 1**: p. 35-40.
18. Chang, L.Y., et al., *Type 2 diabetes and obesity in children and adolescents: experience from studies in Taiwanese population*. Curr Diabetes Rev, 2006. **2**(2): p. 185-93.
19. De Pablos-Velasco, P.L., F.J. Martinez-Martin, and F. Rodriguez-Perez, *Prevalence of obesity in a Canarian community. Association with type 2 diabetes mellitus: the Guia Study*. Eur J Clin Nutr, 2002. **56**(6): p. 557-60.
20. McTernan, C.L., et al., *Resistin, central obesity, and type 2 diabetes*. Lancet, 2002. **359**(9300): p. 46-7.
21. Steppan, C.M., et al., *The hormone resistin links obesity to diabetes*. Nature, 2001. **409**(6818): p. 307-12.
22. Kahn, S.E., R.L. Hull, and K.M. Utzschneider, *Mechanisms linking obesity to insulin resistance and type 2 diabetes*. Nature, 2006. **444**(7121): p. 840-6.
23. McGill, H.C., Jr., et al., *Obesity accelerates the progression of coronary atherosclerosis in young men*. Circulation, 2002. **105**(23): p. 2712-8.
24. Barrett-Connor, E.L., *Obesity, atherosclerosis, and coronary artery disease*. Ann Intern Med, 1985. **103**(6 ( Pt 2)): p. 1010-9.
25. Schwimmer, J.B., et al., *Obesity, insulin resistance, and other clinicopathological correlates of pediatric nonalcoholic fatty liver disease*. J Pediatr, 2003. **143**(4): p. 500-5.
26. Haynes, P., S. Liangpunsakul, and N. Chalasani, *Nonalcoholic fatty liver disease in individuals with severe obesity*. Clin Liver Dis, 2004. **8**(3): p. 535-47, viii.
27. Wild, S., et al., *Global prevalence of diabetes: estimates for the year 2000 and projections for 2030*. Diabetes Care, 2004. **27**(5): p. 1047-53.
28. Robinson, S.W., D.M. Dinulescu, and R.D. Cone, *Genetic models of obesity and energy balance in the mouse*. Annu Rev Genet, 2000. **34**: p. 687-745.
29. Marchesini, G., et al., *Nonalcoholic fatty liver disease: a feature of the metabolic syndrome*. Diabetes, 2001. **50**(8): p. 1844-50.

30. Perusse, L. and Y.C. Chagnon, *Summary of human linkage and association studies*. Behav Genet, 1997. **27**(4): p. 359-72.
31. Berger, J. *Researchers identify link between obesity and type 2 diabetes*. 2002 [cited 2008 March 15]; Available from: <http://www.scienceblog.com/community/older/2002/G/20021096.html>.
32. Man, S., R. Munoz, and R.S. Kerbel, *On the development of models in mice of advanced visceral metastatic disease for anti-cancer drug testing*. Cancer Metastasis Rev, 2007. **26**(3-4): p. 737-47.
33. Ramaswamy, S., J.L. McBride, and J.H. Kordower, *Animal models of Huntington's disease*. Ilar J, 2007. **48**(4): p. 356-73.
34. Burke, F., *Cytokines (IFNs, TNF-alpha, IL-2 and IL-12) and animal models of cancer*. Cytokines Cell Mol Ther, 1999. **5**(1): p. 51-61.
35. Speakman, J., et al., *Animal models of obesity*. Obes Rev, 2007. **8 Suppl 1**: p. 55-61.
36. Rees, D.A. and J.C. Alcolado, *Animal models of diabetes mellitus*. Diabet Med, 2005. **22**(4): p. 359-70.
37. Aponte, J.L., et al., *Point mutations in the murine fumarylacetoacetate hydrolase gene: Animal models for the human genetic disorder hereditary tyrosinemia type I*. Proc Natl Acad Sci U S A, 2001. **98**(2): p. 641-5.
38. Gannon, M., *Molecular genetic analysis of diabetes in mice*. Trends Genet, 2001. **17**(10): p. S23-8.
39. Carroll, L., J. Voisey, and A. van Daal, *Mouse models of obesity*. Clin Dermatol, 2004. **22**(4): p. 345-9.
40. Bergen, W.G. and H.J. Mersmann, *Comparative aspects of lipid metabolism: impact on contemporary research and use of animal models*. J Nutr, 2005. **135**(11): p. 2499-502.
41. Ding, F., et al., *Lack of Pwcr1/MBII-85 snoRNA is critical for neonatal lethality in Prader-Willi syndrome mouse models*. Mamm Genome, 2005. **16**(6): p. 424-31.
42. Bluher, M., *Transgenic animal models for the study of adipose tissue biology*. Best Pract Res Clin Endocrinol Metab, 2005. **19**(4): p. 605-23.
43. Ingalls, A.M., M.M. Dickie, and G.D. Snell, *Obese, a new mutation in the house mouse*. J Hered, 1950. **41**(12): p. 317-8.

44. Zhang, Y., et al., *Positional cloning of the mouse obese gene and its human homologue*. Nature, 1994. **372**(6505): p. 425-32.
45. Kastan, F.H., *Comparative Histological Studies of Endocrine Glands of Yellow (A[unknown]a) and Non-agouti (aa) Mice in Relation to the Problem of Hereditary Obesity*. Science, 1952. **115**(2998): p. 647-649.
46. Chen, H., et al., *Evidence that the diabetes gene encodes the leptin receptor: identification of a mutation in the leptin receptor gene in db/db mice*. Cell, 1996. **84**(3): p. 491-5.
47. Coleman, D.L. and E.M. Eicher, *Fat (fat) and tubby (tub): two autosomal recessive mutations causing obesity syndromes in the mouse*. J Hered, 1990. **81**(6): p. 424-7.
48. Kley, P.W., et al., *Identification and characterization of the mouse obesity gene tubby: a member of a novel gene family*. Cell, 1996. **85**(2): p. 281-90.
49. Farooqi, I.S. and S. O'Rahilly, *Monogenic obesity in humans*. Annu Rev Med, 2005. **56**: p. 443-58.
50. Rankinen, T., et al., *The human obesity gene map: the 2005 update*. Obesity (Silver Spring), 2006. **14**(4): p. 529-644.
51. Russell, L.B. and W.L. Russell, *Frequency and nature of specific-locus mutations induced in female mice by radiations and chemicals: a review*. Mutat Res, 1992. **296**(1-2): p. 107-27.
52. Brinster, R.L., et al., *Regulation of metallothionein--thymidine kinase fusion plasmids injected into mouse eggs*. Nature, 1982. **296**(5852): p. 39-42.
53. Takamura, T., et al., *Transgenic mice overexpressing type 2 nitric-oxide synthase in pancreatic beta cells develop insulin-dependent diabetes without insulinitis*. J Biol Chem, 1998. **273**(5): p. 2493-6.
54. Ruohonen, S.T., et al., *Transgenic Mice Overexpressing Neuropeptide Y in Noradrenergic Neurons: A Novel Model of Increased Adiposity and Impaired Glucose Tolerance*. Diabetes, 2008.
55. Ran, Q., et al., *Transgenic mice overexpressing glutathione peroxidase 4 are protected against oxidative stress-induced apoptosis*. J Biol Chem, 2004. **279**(53): p. 55137-46.
56. Heine, P.A., et al., *Increased adipose tissue in male and female estrogen receptor-alpha knockout mice*. Proc Natl Acad Sci U S A, 2000. **97**(23): p. 12729-34.

57. Ravinet Trillou, C., et al., *CBI cannabinoid receptor knockout in mice leads to leanness, resistance to diet-induced obesity and enhanced leptin sensitivity*. Int J Obes Relat Metab Disord, 2004. **28**(4): p. 640-8.
58. Augustine, K.A., et al., *Noninsulin-dependent diabetes mellitus occurs in mice ectopically expressing the human Axl tyrosine kinase receptor*. J Cell Physiol, 1999. **181**(3): p. 433-47.
59. Johnson, D.K., et al., *Molecular analysis of 36 mutations at the mouse pink-eyed dilution (p) locus*. Genetics, 1995. **141**(4): p. 1563-71.
60. Russell, L.B., et al., *Complementation analyses for 45 mutations encompassing the pink-eyed dilution (p) locus of the mouse*. Genetics, 1995. **141**(4): p. 1547-62.
61. Dhar, M.S. and D.K. Johnson, *A microsatellite map of the pink-eyed dilution (p) deletion complex in mouse chromosome 7*. Mamm Genome, 1997. **8**(2): p. 143-5.
62. Dhar, M., L. Hauser, and D. Johnson, *An aminophospholipid translocase associated with body fat and type 2 diabetes phenotypes*. Obes Res, 2002. **10**(7): p. 695-702.
63. Herzing, L.B., et al., *The human aminophospholipid-transporting ATPase gene ATP10C maps adjacent to UBE3A and exhibits similar imprinted expression*. Am J Hum Genet, 2001. **68**(6): p. 1501-5.
64. Meguro, M., et al., *A novel maternally expressed gene, ATP10C, encodes a putative aminophospholipid translocase associated with Angelman syndrome*. Nat Genet, 2001. **28**(1): p. 19-20.
65. Russo, S., et al., *Novel mutations of ubiquitin protein ligase 3A gene in Italian patients with Angelman syndrome*. Hum Mutat, 2000. **15**(4): p. 387.
66. Dhar, M.S., et al., *Physical mapping of the pink-eyed dilution complex in mouse chromosome 7 shows that Atp10c is the only transcript between Gabrb3 and Ube3a*. DNA Seq, 2004. **15**(4): p. 306-9.
67. Jiang, Y.H., et al., *Mutation of the Angelman ubiquitin ligase in mice causes increased cytoplasmic p53 and deficits of contextual learning and long-term potentiation*. Neuron, 1998. **21**(4): p. 799-811.
68. Nicholls, R.D., *Strange bedfellows? Protein degradation and neurological dysfunction*. Neuron, 1998. **21**(4): p. 647-9.
69. Nicholls, R.D. and J.L. Knepper, *Genome organization, function, and imprinting in Prader-Willi and Angelman syndromes*. Annu Rev Genomics Hum Genet, 2001. **2**: p. 153-75.



70. Gabriel, J.M., et al., *A transgene insertion creating a heritable chromosome deletion mouse model of Prader-Willi and angelman syndromes*. Proc Natl Acad Sci U S A, 1999. **96**(16): p. 9258-63.
71. Cattanach, B.M., et al., *A candidate model for Angelman syndrome in the mouse*. Mamm Genome, 1997. **8**(7): p. 472-8.
72. Lossie, A.C., et al., *Distinct phenotypes distinguish the molecular classes of Angelman syndrome*. J Med Genet, 2001. **38**(12): p. 834-45.
73. Halleck, M.S., et al., *Multiple members of a third subfamily of P-type ATPases identified by genomic sequences and ESTs*. Genome Res, 1998. **8**(4): p. 354-61.
74. Halleck, M.S., et al., *Differential expression of putative transbilayer amphipath transporters*. Physiol Genomics, 1999. **1**(3): p. 139-50.
75. Halleck, M.S., R.A. Schlegel, and P.L. Williamson, *Reanalysis of ATP11B, a type IV P-type ATPase*. J Biol Chem, 2002. **277**(12): p. 9736-40.
76. Flamant, S., et al., *Characterization of a putative type IV aminophospholipid transporter P-type ATPase*. Mamm Genome, 2003. **14**(1): p. 21-30.
77. Daleke, D.L. and J.V. Lyles, *Identification and purification of aminophospholipid flippases*. Biochim Biophys Acta, 2000. **1486**(1): p. 108-27.
78. Williamson, P. and R.A. Schlegel, *Transbilayer phospholipid movement and the clearance of apoptotic cells*. Biochim Biophys Acta, 2002. **1585**(2-3): p. 53-63.
79. Axelsen, K.B. and M.G. Palmgren, *Evolution of substrate specificities in the P-type ATPase superfamily*. J Mol Evol, 1998. **46**(1): p. 84-101.
80. van Meer, G., et al., *ABC lipid transporters: extruders, flippases, or floppless activators?* FEBS Lett, 2006. **580**(4): p. 1171-7.
81. Williamson, P. and R.A. Schlegel, *Back and forth: the regulation and function of transbilayer phospholipid movement in eukaryotic cells*. Mol Membr Biol, 1994. **11**(4): p. 199-216.
82. Hua, Z., P. Fatheddin, and T.R. Graham, *An essential subfamily of Drs2p-related P-type ATPases is required for protein trafficking between Golgi complex and endosomal/vacuolar system*. Mol Biol Cell, 2002. **13**(9): p. 3162-77.
83. Natarajan, P., et al., *Drs2p-coupled aminophospholipid translocase activity in yeast Golgi membranes and relationship to in vivo function*. Proc Natl Acad Sci U S A, 2004. **101**(29): p. 10614-9.

84. Liu, K., et al., *Yeast P4-ATPases Drs2p and Dnf1p are essential cargos of the NPFxD/Sla1p endocytic pathway*. Mol Biol Cell, 2007. **18**(2): p. 487-500.
85. Paterson, J.K., et al., *Lipid specific activation of the murine P4-ATPase Atp8a1 (ATPase II)*. Biochemistry, 2006. **45**(16): p. 5367-76.
86. Paulusma, C.C., et al., *Atp8b1 deficiency in mice reduces resistance of the canalicular membrane to hydrophobic bile salts and impairs bile salt transport*. Hepatology, 2006. **44**(1): p. 195-204.
87. Van den Eijnde, S.M., et al., *Phosphatidylserine plasma membrane asymmetry in vivo: a pancellular phenomenon which alters during apoptosis*. Cell Death Differ, 1997. **4**(4): p. 311-6.
88. Zeghari, N., et al., *Adipose peroxisome proliferator-activated receptor gamma mRNA expression in insulin-resistant obese patients: relationship with adipocyte membrane phospholipids*. Lipids, 1999. **34 Suppl**: p. S161.
89. Fickova, M., et al., *Dietary (n-3) and (n-6) polyunsaturated fatty acids rapidly modify fatty acid composition and insulin effects in rat adipocytes*. J Nutr, 1998. **128**(3): p. 512-9.
90. Rao, G., *Insulin resistance syndrome*. Am Fam Physician, 2001. **63**(6): p. 1159-63, 1165-6.
91. Saltiel, A.R. and C.R. Kahn, *Insulin signalling and the regulation of glucose and lipid metabolism*. Nature, 2001. **414**(6865): p. 799-806.
92. Shepherd, P.R. and B.B. Kahn, *Glucose transporters and insulin action--implications for insulin resistance and diabetes mellitus*. N Engl J Med, 1999. **341**(4): p. 248-57.
93. Kido, Y., J. Nakae, and D. Accili, *Clinical review 125: The insulin receptor and its cellular targets*. J Clin Endocrinol Metab, 2001. **86**(3): p. 972-9.
94. Watson, R.T. and J.E. Pessin, *Intracellular organization of insulin signaling and GLUT4 translocation*. Recent Prog Horm Res, 2001. **56**: p. 175-93.
95. Klemm, D.J., et al., *Insulin-induced adipocyte differentiation. Activation of CREB rescues adipogenesis from the arrest caused by inhibition of prenylation*. J Biol Chem, 2001. **276**(30): p. 28430-5.
96. Watson, R.T., M. Kanzaki, and J.E. Pessin, *Regulated membrane trafficking of the insulin-responsive glucose transporter 4 in adipocytes*. Endocr Rev, 2004. **25**(2): p. 177-204.

97. Wallberg-Henriksson, H. and J.R. Zierath, *GLUT4: a key player regulating glucose homeostasis? Insights from transgenic and knockout mice (review)*. Mol Membr Biol, 2001. **18**(3): p. 205-11.
98. Fujimoto, W.Y., *The importance of insulin resistance in the pathogenesis of type 2 diabetes mellitus*. Am J Med, 2000. **108 Suppl 6a**: p. 9S-14S.
99. Stahl, A., *A current review of fatty acid transport proteins (SLC27)*. Pflugers Arch, 2004. **447**(5): p. 722-7.
100. Schaffer, J.E., *Fatty acid transport: the roads taken*. Am J Physiol Endocrinol Metab, 2002. **282**(2): p. E239-46.
101. Eehalt, R., et al., *Translocation of long chain fatty acids across the plasma membrane--lipid rafts and fatty acid transport proteins*. Mol Cell Biochem, 2006. **284**(1-2): p. 135-40.
102. Stahl, A., et al., *Insulin causes fatty acid transport protein translocation and enhanced fatty acid uptake in adipocytes*. Dev Cell, 2002. **2**(4): p. 477-88.
103. Kim, J.K., et al., *Inactivation of fatty acid transport protein 1 prevents fat-induced insulin resistance in skeletal muscle*. J Clin Invest, 2004. **113**(5): p. 756-63.
104. Wu, Q., et al., *FATP1 is an insulin-sensitive fatty acid transporter involved in diet-induced obesity*. Mol Cell Biol, 2006. **26**(9): p. 3455-67.
105. Ntambi, J.M. and K. Young-Cheul, *Adipocyte differentiation and gene expression*. J Nutr, 2000. **130**(12): p. 3122S-3126S.
106. Rosen, E.D., et al., *Transcriptional regulation of adipogenesis*. Genes Dev, 2000. **14**(11): p. 1293-307.
107. Morrison, R.F. and S.R. Farmer, *Insights into the transcriptional control of adipocyte differentiation*. J Cell Biochem, 1999. **Suppl 32-33**: p. 59-67.
108. Berger, J. and D.E. Moller, *The mechanisms of action of PPARs*. Annu Rev Med, 2002. **53**: p. 409-35.
109. Hammarstedt, A., et al., *The effect of PPARgamma ligands on the adipose tissue in insulin resistance*. Prostaglandins Leukot Essent Fatty Acids, 2005. **73**(1): p. 65-75.
110. Farmer, S.R., *Regulation of PPARgamma activity during adipogenesis*. Int J Obes (Lond), 2005. **29 Suppl 1**: p. S13-6.

111. Gerhold, D.L., et al., *Gene expression profile of adipocyte differentiation and its regulation by peroxisome proliferator-activated receptor-gamma agonists*. Endocrinology, 2002. **143**(6): p. 2106-18.
112. Hamm, J.K., B.H. Park, and S.R. Farmer, *A role for C/EBPbeta in regulating peroxisome proliferator-activated receptor gamma activity during adipogenesis in 3T3-L1 preadipocytes*. J Biol Chem, 2001. **276**(21): p. 18464-71.
113. Liao, W., et al., *Suppression of PPAR-gamma attenuates insulin-stimulated glucose uptake by affecting both GLUT1 and GLUT4 in 3T3-L1 adipocytes*. Am J Physiol Endocrinol Metab, 2007. **293**(1): p. E219-27.
114. Mukherjee, R., et al., *A selective peroxisome proliferator-activated receptor-gamma (PPARgamma) modulator blocks adipocyte differentiation but stimulates glucose uptake in 3T3-L1 adipocytes*. Mol Endocrinol, 2000. **14**(9): p. 1425-33.
115. Noble, J., M.O. Baerlocher, and J. Silverberg, *Management of type 2 diabetes mellitus. Role of thiazolidinediones*. Can Fam Physician, 2005. **51**: p. 683-7.
116. Kurebayashi, S., et al., *A novel thiazolidinedione MCC-555 down-regulates tumor necrosis factor-alpha-induced expression of vascular cell adhesion molecule-1 in vascular endothelial cells*. Atherosclerosis, 2005. **182**(1): p. 71-7.
117. Kallen, C.B. and M.A. Lazar, *Antidiabetic thiazolidinediones inhibit leptin (ob) gene expression in 3T3-L1 adipocytes*. Proc Natl Acad Sci U S A, 1996. **93**(12): p. 5793-6.
118. Fujiwara, T., et al., *Characterization of new oral antidiabetic agent CS-045. Studies in KK and ob/ob mice and Zucker fatty rats*. Diabetes, 1988. **37**(11): p. 1549-58.
119. Ciaraldi, T.P., et al., *In vitro studies on the action of CS-045, a new antidiabetic agent*. Metabolism, 1990. **39**(10): p. 1056-62.
120. Iwamoto, Y., et al., *Effect of new oral antidiabetic agent CS-045 on glucose tolerance and insulin secretion in patients with NIDDM*. Diabetes Care, 1991. **14**(11): p. 1083-6.
121. Johnson, M.D., L.K. Campbell, and R.K. Campbell, *Troglitazone: review and assessment of its role in the treatment of patients with impaired glucose tolerance and diabetes mellitus*. Ann Pharmacother, 1998. **32**(3): p. 337-48.
122. HHS. *Rezulin to be withdrawn from the market*. 2000 [cited 2008 March 15]; Available from: <http://www.fda.gov/bbs/topics/NEWS/NEW00721.html>.

123. Hong, Y.H., et al., *Up-regulation of adipogenin, an adipocyte plasma transmembrane protein, during adipogenesis*. Mol Cell Biochem, 2005. **276**(1-2): p. 133-41.
124. Mineo, H., et al., *Thiazolidinediones exhibit different effects on preadipocytes isolated from rat mesenteric fat tissue and cell line 3T3-L1 cells derived from mice*. Cell Biol Int, 2007. **31**(7): p. 703-10.
125. Huang, J., et al., *Annexin II is a thiazolidinedione-responsive gene involved in insulin-induced glucose transporter isoform 4 translocation in 3T3-L1 adipocytes*. Endocrinology, 2004. **145**(4): p. 1579-86.
126. Kumagai, T., et al., *RWJ-241947 (MCC-555), a unique peroxisome proliferator-activated receptor-gamma ligand with antitumor activity against human prostate cancer in vitro and in beige/nude/ X-linked immunodeficient mice and enhancement of apoptosis in myeloma cells induced by arsenic trioxide*. Clin Cancer Res, 2004. **10**(4): p. 1508-20.
127. Upton, R., et al., *Improved metabolic status and insulin sensitivity in obese fatty (fa/fa) Zucker rats and Zucker Diabetic Fatty (ZDF) rats treated with the thiazolidinedione, MCC-555*. Br J Pharmacol, 1998. **125**(8): p. 1708-14.
128. Liu, L.S., et al., *The new antidiabetic drug MCC-555 acutely sensitizes insulin signaling in isolated cardiomyocytes*. Endocrinology, 1998. **139**(11): p. 4531-9.
129. Reginato, M.J., et al., *A potent antidiabetic thiazolidinedione with unique peroxisome proliferator-activated receptor gamma-activating properties*. J Biol Chem, 1998. **273**(49): p. 32679-84.
130. Yamaguchi, K., et al., *A novel peroxisome proliferator-activated receptor gamma ligand, MCC-555, induces apoptosis via posttranscriptional regulation of NAG-1 in colorectal cancer cells*. Mol Cancer Ther, 2006. **5**(5): p. 1352-61.
131. Furnsinn, C. and W. Waldhausl, *Thiazolidinediones: metabolic actions in vitro*. Diabetologia, 2002. **45**(9): p. 1211-23.
132. Fire, A., et al., *Potent and specific genetic interference by double-stranded RNA in Caenorhabditis elegans*. Nature, 1998. **391**(6669): p. 806-11.
133. Macrae, I.J., et al., *Structural basis for double-stranded RNA processing by Dicer*. Science, 2006. **311**(5758): p. 195-8.
134. Dykxhoorn, D.M., C.D. Novina, and P.A. Sharp, *Killing the messenger: short RNAs that silence gene expression*. Nat Rev Mol Cell Biol, 2003. **4**(6): p. 457-67.
135. Kuwabara, P.E. and A. Coulson, *RNAi--prospects for a general technique for determining gene function*. Parasitol Today, 2000. **16**(8): p. 347-9.

136. Zhou, Q.L., et al., *Analysis of insulin signalling by RNAi-based gene silencing*. Biochem Soc Trans, 2004. **32**(Pt 5): p. 817-21.
137. Tang, X., et al., *An RNA interference-based screen identifies MAP4K4/NIK as a negative regulator of PPARgamma, adipogenesis, and insulin-responsive hexose transport*. Proc Natl Acad Sci U S A, 2006. **103**(7): p. 2087-92.
138. Puri, V., et al., *RNAi screens reveal novel metabolic regulators: RIP140, MAP4k4 and the lipid droplet associated fat specific protein (FSP) 27*. Acta Physiol (Oxf), 2008. **192**(1): p. 103-15.
139. Williams, D., et al., *Golgin-160 is required for the Golgi membrane sorting of the insulin-responsive glucose transporter GLUT4 in adipocytes*. Mol Biol Cell, 2006. **17**(12): p. 5346-55.
140. Chang, L., S.H. Chiang, and A.R. Saltiel, *TC10alpha is required for insulin-stimulated glucose uptake in adipocytes*. Endocrinology, 2007. **148**(1): p. 27-33.
141. Dhar, M.S., et al., *A type IV P-type ATPase affects insulin-mediated glucose uptake in adipose tissue and skeletal muscle in mice*. J Nutr Biochem, 2006. **17**(12): p. 811-20.
142. Rodbell, M., *Metabolism Of Isolated Fat Cells. I. Effects Of Hormones On Glucose Metabolism And Lipolysis*. J Biol Chem, 1964. **239**: p. 375-80.
143. Koopman, R., G. Schaart, and M.K. Hesselink, *Optimisation of oil red O staining permits combination with immunofluorescence and automated quantification of lipids*. Histochem Cell Biol, 2001. **116**(1): p. 63-8.
144. McNeil, M. *Adipocyte Staining with Oil Red O*. 2005 [cited 2008 March 15]; Available from: <http://labs.pbrc.edu/endocrinology/documents/ADIPOCYTESTAININGWITHOILREDO.pdf>.
145. Panomics. *DeliverX and DeliverX Plus siRNA Transfection Kits: User Manual*. September 16, 2006 [cited 2008 March 15]; Available from: [http://www.panomics.com/downloads/DeliverX\\_siRNA\\_UserManual\\_RevC\\_091630.pdf](http://www.panomics.com/downloads/DeliverX_siRNA_UserManual_RevC_091630.pdf).
146. Zhao, G., et al., *The same gamma-secretase accounts for the multiple intramembrane cleavages of APP*. J Neurochem, 2007. **100**(5): p. 1234-46.
147. Roach, W. and M. Plomann, *PACSIN3 overexpression increases adipocyte glucose transport through GLUT1*. Biochem Biophys Res Commun, 2007. **355**(3): p. 745-50.



148. Dhar, M.S. and H.K. Plummer, 3rd, *Protein expression of G-protein inwardly rectifying potassium channels (GIRK) in breast cancer cells*. BMC Physiol, 2006. **6**: p. 8.
149. Rosen, E.D. *Glucose Transport Assay*. The Evan Rosen Lab: Protocols [cited 2008 March 15]; Available from: <http://www.bidmc-endocrine.org/labs/rosen/protocols/insulin.asp>.
150. Shahparaki, A., L. Grunder, and A. Sorisky, *Comparison of human abdominal subcutaneous versus omental preadipocyte differentiation in primary culture*. Metabolism, 2002. **51**(9): p. 1211-5.
151. Ailhaud, G., P. Grimaldi, and R. Negrel, *Cellular and molecular aspects of adipose tissue development*. Annu Rev Nutr, 1992. **12**: p. 207-33.
152. *Gel loading buffer*. [cited 2008 March 15]; Available from: <http://www.protocol-online.org/biology-forums/posts/12885.html>.
153. BioLabs, N.E. *Blue Loading Buffer Pack*. [cited 2008 March 15]; Available from: <http://www.neb.com/nebecomm/products/productB7703.asp>.
154. Laemmli, U.K., *Cleavage of structural proteins during the assembly of the head of bacteriophage T4*. Nature, 1970. **227**(5259): p. 680-5.
155. Millipore. [cited 2008 March 15]; Available from: <http://www.millipore.com/>.
156. Kershaw, E.E., et al., *PPARgamma regulates adipose triglyceride lipase in adipocytes in vitro and in vivo*. Am J Physiol Endocrinol Metab, 2007. **293**(6): p. E1736-45.
157. Sato, M., A. Hiragun, and H. Mitsui, *Preadipocytes possess cellular retinoid binding proteins and their differentiation is inhibited by retinoids*. Biochem Biophys Res Commun, 1980. **95**(4): p. 1839-45.
158. Vaulont, S. and A. Kahn, *Transcriptional control of metabolic regulation genes by carbohydrates*. Faseb J, 1994. **8**(1): p. 28-35.
159. Smas, C.M. and H.S. Sul, *Pref-1, a protein containing EGF-like repeats, inhibits adipocyte differentiation*. Cell, 1993. **73**(4): p. 725-34.
160. Smas, C.M., et al., *Transcriptional control of the pref-1 gene in 3T3-L1 adipocyte differentiation. Sequence requirement for differentiation-dependent suppression*. J Biol Chem, 1998. **273**(48): p. 31751-8.
161. Sundar Rajan, S., et al., *Endoplasmic reticulum (ER) stress & diabetes*. Indian J Med Res, 2007. **125**(3): p. 411-24.

162. Meusser, B., et al., *ERAD: the long road to destruction*. Nat Cell Biol, 2005. **7**(8): p. 766-72.
163. Chen, Y., et al., *ER-associated protein degradation is a common mechanism underpinning numerous monogenic diseases including Robinow syndrome*. Hum Mol Genet, 2005. **14**(17): p. 2559-69.
164. Ozcan, U., et al., *Endoplasmic reticulum stress links obesity, insulin action, and type 2 diabetes*. Science, 2004. **306**(5695): p. 457-61.
165. Eizirik, D.L., A.K. Cardozo, and M. Cnop, *The role for endoplasmic reticulum stress in diabetes mellitus*. Endocr Rev, 2008. **29**(1): p. 42-61.
166. Tsiotra, P.C. and C. Tsigos, *Stress, the endoplasmic reticulum, and insulin resistance*. Ann N Y Acad Sci, 2006. **1083**: p. 63-76.
167. Pacifico, L., et al., *Increased T-helper interferon-gamma-secreting cells in obese children*. Eur J Endocrinol, 2006. **154**(5): p. 691-7.
168. Sadowski, H.B., T.T. Wheeler, and D.A. Young, *Gene expression during 3T3-L1 adipocyte differentiation. Characterization of initial responses to the inducing agents and changes during commitment to differentiation*. J Biol Chem, 1992. **267**(7): p. 4722-31.
169. Spiegelman, B.M., M. Frank, and H. Green, *Molecular cloning of mRNA from 3T3 adipocytes. Regulation of mRNA content for glycerophosphate dehydrogenase and other differentiation-dependent proteins during adipocyte development*. J Biol Chem, 1983. **258**(16): p. 10083-9.
170. Yeh, W.C., et al., *Cascade regulation of terminal adipocyte differentiation by three members of the C/EBP family of leucine zipper proteins*. Genes Dev, 1995. **9**(2): p. 168-81.
171. Desvergne, B., L. Michalik, and W. Wahli, *Transcriptional regulation of metabolism*. Physiol Rev, 2006. **86**(2): p. 465-514.
172. Fasshauer, M. and R. Paschke, *Regulation of adipocytokines and insulin resistance*. Diabetologia, 2003. **46**(12): p. 1594-603.
173. Bevan, P., *Insulin signalling*. J Cell Sci, 2001. **114**(Pt 8): p. 1429-30.
174. Park, S.Y., et al., *Cilostazol increases 3T3-L1 preadipocyte differentiation with improved glucose uptake associated with activation of peroxisome proliferator-activated receptor-gamma transcription*. Atherosclerosis, 2008.
175. Boney, C.M., et al., *Regulation of preadipocyte factor-1 gene expression during 3T3-L1 cell differentiation*. Endocrinology, 1996. **137**(7): p. 2923-8.



176. Lee, K., et al., *Inhibition of adipogenesis and development of glucose intolerance by soluble preadipocyte factor-1 (Pref-1)*. J Clin Invest, 2003. **111**(4): p. 453-61.
177. Mei, B., et al., *Only the large soluble form of preadipocyte factor-1 (Pref-1), but not the small soluble and membrane forms, inhibits adipocyte differentiation: role of alternative splicing*. Biochem J, 2002. **364**(Pt 1): p. 137-44.
178. Sul, H.S., et al., *Function of pref-1 as an inhibitor of adipocyte differentiation*. Int J Obes Relat Metab Disord, 2000. **24 Suppl 4**: p. S15-9.
179. Villena, J.A., K.H. Kim, and H.S. Sul, *Pref-1 and ADSF/resistin: two secreted factors inhibiting adipose tissue development*. Horm Metab Res, 2002. **34**(11-12): p. 664-70.
180. Wang, Y., et al., *Pref-1, a preadipocyte secreted factor that inhibits adipogenesis*. J Nutr, 2006. **136**(12): p. 2953-6.
181. Gong, H., et al., *Resistin promotes 3T3-L1 preadipocyte differentiation*. Eur J Endocrinol, 2004. **150**(6): p. 885-92.
182. Zhou, L., et al., *Transcriptional regulation of the resistin gene*. Domest Anim Endocrinol, 2006. **30**(2): p. 98-107.
183. Fu, Y., et al., *Adiponectin promotes adipocyte differentiation, insulin sensitivity, and lipid accumulation*. J Lipid Res, 2005. **46**(7): p. 1369-79.
184. Frohnert, B.I., T.Y. Hui, and D.A. Bernlohr, *Identification of a functional peroxisome proliferator-responsive element in the murine fatty acid transport protein gene*. J Biol Chem, 1999. **274**(7): p. 3970-7.
185. Saito, T., et al., *The interaction of Akt with APPL1 is required for insulin-stimulated Glut4 translocation*. J Biol Chem, 2007. **282**(44): p. 32280-7.
186. Katz, E.B., et al., *The metabolic consequences of altered glucose transporter expression in transgenic mice*. J Mol Med, 1996. **74**(11): p. 639-52.
187. Shulman, G.I., *Cellular mechanisms of insulin resistance*. J Clin Invest, 2000. **106**(2): p. 171-6.
188. Blau, H.M., et al., *Plasticity of the differentiated state*. Science, 1985. **230**(4727): p. 758-66.
189. Yaffe, D. and O. Saxel, *Serial passaging and differentiation of myogenic cells isolated from dystrophic mouse muscle*. Nature, 1977. **270**(5639): p. 725-7.

## APPENDIX

## APPENDIX

### RNA extraction and purification of primary preadipocytes and adipocytes from mouse tissue

1. Clean homogenizer.
  - a. Rinse with clean deionized water, holding beaker underneath to catch drips.
  - b. Spray with 70% EtOH, and wipe with KimWipe.
  - c. Rinse with DEPC water, holding beaker underneath to catch drips.
  - d. Run homogenizer in DEPC water in clean beaker.
  - e. Squirt RNase AWAY on KimWipe, and wipe homogenizer.
2. Weigh tissue into 50 ml tube and add 10 ml of trizol per 1 g of tissue.
3. Homogenize trizol/tissue mix until there are no remaining clumps, approximately 10 seconds and immediately place sample in ice.
4. Repeat steps #1-3 for all samples.
5. Place samples under hood and leave at room temperature for 10 minutes.
6. Under hood, add 5 ml of chloroform per 1 g of tissue to each sample.
7. Vortex samples, place under hood, and leave at room temperature for 5 minutes.
8. Centrifuge at 3K, 4-10°C, 20 minutes.
9. Transfer top layer with pipette to 10 ml tube. If the top layer is “dirty” (contaminated by bottom layer), centrifuge again, and repeat step #8.
10. Under hood, add 5 ml of isopropyl alcohol per 1 g of tissue to each sample.
11. Vortex, place under hood, and leave at room temperature for 20 minutes.
12. Centrifuge at 3K, 4-10°C, 20 minutes.
13. Collect the pellet by dumping the liquid into a separate container without disturbing the pellet.
14. Add 10 ml of 70-75% ethanol alcohol per 1 g of tissue to each sample.
15. Vortex to disperse the pellet.
16. Centrifuge at 3K, 4-10°C, 20-60 minutes.
17. Collect the pellet by dumping the liquid into a separate container without disturbing the pellet.
18. Tilt the tubes until they are approximately upside down, and let the tubes sit under the hood for 10 minutes to dry the pellet.
19. Resuspend pellet in 100 µl of sterile water and transfer to 1.5 ml tube.
20. Make first mix by combining RLT buffer and 2-mercaptoethanol (3 ml of RLT + 30 µl of 2-mercaptoethanol is enough for 6 samples). Vortex mix.
21. Add 350 µl of first mix to each sample. Vortex and centrifuge samples.
22. Add 250 µl of ethanol to each sample. Vortex and centrifuge samples.
23. Transfer sample mix into the pink column.
24. Make sure centrifuge lid is in place, and then centrifuge samples for 15 seconds.
25. Pull column out. Dump liquid out of 1.5 ml tube. Replace column in top of 1.5 ml tube.
26. Add 500 µl of RPE buffer to pink column.
27. Make sure centrifuge lid is in place, and then centrifuge samples for 15 seconds.
28. Repeat steps #25-27.

29. Pull column out. Dump liquid out of 1.5 ml tube. Replace column in top of 1.5 ml tube.
30. Make sure centrifuge lid is in place, and then centrifuge samples for 1 minute.
31. Move pink column to 1.5 ml tube with ridged edges (pre-labeled).
32. Add 50  $\mu$ l of DEPC to center of white material without touching white material.
33. Make sure centrifuge lid is in place, and then centrifuge samples for 1 minute.
34. Centrifuge again if significantly less than 50  $\mu$ l of water is present at bottom of tube.
35. Toss pink column and keep 1.5 ml tube with elutant.
36. Quantitate RNA using Biophotometer.

### **RNA extraction and purification of 3T3-L1 cells and primary preadipocytes and adipocytes plated and differentiated in culture**

1. Add 400  $\mu$ l RLT buffer from Qiagen kit for a 60 mm dish (600  $\mu$ l for a 100 mm dish). If making RNA immediately, add  $\beta$ -mercaptoethanol to RLT buffer (1  $\mu$ l  $\beta$ -mercaptoethanol per 100  $\mu$ l RLT buffer). If collecting RNA samples and storing at -80°C, do not add  $\beta$ -mercaptoethanol until you are ready to make the RNA.
2. Scrape cells and transfer to a round bottom tube from Qiagen kit if making RNA immediately or transfer to a small Eppendorf tube if storing at -80°C.
3. Syringe each sample up and down five times using a 20-gauge needle.
4. Add an equal amount of 70% ethanol (400  $\mu$ l or 600  $\mu$ l).
5. Transfer solution to pink column (700  $\mu$ l at a time) and centrifuge for 20 seconds at 13K.
6. Dump liquid out of the bottom tube and add 700  $\mu$ l RW1 buffer from Qiagen kit to the pink column; centrifuge for 20 seconds at 13K.
7. Dump liquid out of the bottom tube and add 500  $\mu$ l RPE buffer from Qiagen kit to the pink column; centrifuge for 20 seconds at 13K. Repeat this step again.
8. Dump liquid out of the bottom tube and centrifuge for 1 minute at 13K.
9. Move pink column to 1.5 ml tube (pre-labeled) from Qiagen kit. Add 50  $\mu$ l RNase-free water from Qiagen kit to center of white material in column.
10. Centrifuge samples for 1 minute.
11. Toss pink column and keep 1.5 ml tube with elutant.
12. Quantitate RNA using Biophotometer.

### **Isolation and differentiation of primary preadipocytes (PA) and adipocytes (Ad)**

1. Sacrifice mice by CO<sub>2</sub> asphyxiation.
2. Collect adipose tissue from mice.
3. Mince tissue into small pieces and weigh. Add approximately 2 g tissue to each 50 ml Falcon tube.
4. Add 10ml KRB buffer + 20mg of collagenase (2 mg/ml) to each 2 g of tissue.
5. Shake at 37°C, 25'. If there is still a large amount of floating pieces, continue to shake until there are very few pieces.
6. Filter through 100 µM mesh and rinse with 5ml KRB + collagenase.
7. Centrifuge at 800rpm (low speed), 10'.
8. Collect floating **Ad** using coated pipets, add equal volume HBSS, store on ice temporarily.
9. Add 5 ml FACS buffer to **PA**/KRB + collagenase tube; centrifuge at 1500rpm, 10'.
10. Loosen **PA** pellet by gently flicking the tube, rinse with ~0.5ml HBSS to disperse clumps, and treat with 5 ml 1X RBC (red blood cell) lysis buffer (eBioScience).
11. Leave RBC treated **PA** at RT, 4'.
12. Add 5 ml FACS buffer to **PA**/lysis buffer tube.
13. Centrifuge **PA** and **Ad** at 800rpm (low speed), 10'.
14. Remove HBSS from the bottom of **Ad** using coated pipets.
15. Store **Ad** at -80°C for later use.
16. Remove FACS buffer from **PA** pellet and wash 1X with new FACS buffer.
17. Centrifuge **PA** at 800rpm (low speed), 10'.
18. Remove FACS buffer from **PA** pellet.
19. Count and plate primary preadipocytes (at a density of ~7.5 x 10<sup>5</sup> cells/well) if using in culture or store at -80°C for later use.

## Cell Work Medias

### *Growth Media (GM)*

- 1 L DMEM
- 100 ml 10% FBS
- 10 ml 1% P/S

### *Differentiation Media (DM)*

- 10 ml GM
- 110  $\mu$ l of 0.5 mM isobutyl-methyl-xanthine (MIX)  
(Sigma I-5879, dissolve 250 mg in 25 ml of 95% ethanol)
- 10  $\mu$ l of 1  $\mu$ M dexamethasone  
(Sigma D-4902, dissolve 100 mg in 100 ml of 95% ethanol)
- 1  $\mu$ l of 1  $\mu$ g/ml insulin  
(Sigma I-9278, 1.7 mM ready to use)
- 10  $\mu$ l of 10 mM troglitazone (TGZ)  
(Cayman Chemical 71750, dissolve 10 mg in 2.26 ml DMSO)

### *Maintenance Media (MM)*

- 10 ml GM
- 1  $\mu$ l of 1  $\mu$ g/ml insulin
- 10  $\mu$ l of troglitazone (TGZ)

### *High Insulin Media (HI)*

- 10 ml GM
- 10  $\mu$ l of 1  $\mu$ g/ml insulin

### *Thiazolidinediones (TZDs)*

- 1  $\mu$ l of 10 mM MCC555 per 1 ml media
- 1  $\mu$ l of 10 mM TGZ per 1 ml media
- 1  $\mu$ l of 10 mM GW9662 per 1 ml media

### **Oil Red O staining**

*For all additions and washes, use a volume equal to the volume of media used for the dish. For example, use 2 ml volume for all 60 mm dishes.*

1. Prepare ORO solution by dissolving 0.039 g ORO powder in 5.6 ml of 85% propylene glycol. Warm ORO in water bath (60°C) before use.
2. Rinse dish twice with HBSS.
3. Add 1% formalin to well, leave at RT 5'.
4. Remove formalin (DO NOT discard waste in sink).
5. Add 85% propylene glycol, leave at RT 5' two times.
6. Add ORO, agitate slightly using Belly Dancer on low setting (3-4) at RT, 20'.
7. Add 85% propylene glycol, leave at RT 3'.
8. Rinse dish with tap water until there is no more residual ORO rinsed off (2-5 times).
9. Add hematoxylin counterstain, leave at RT 30 sec.
10. Rinse dish with tap water until there is no more/minimal hematoxylin counterstain rinsed off (2-5 times).
11. Photograph dish.

### **Oil Red O staining for Quantification**

#### **Reagents**

##### *ORO stock*

- 0.7 g ORO  
200 ml Isopropanol
- Stir overnight, then filter with 0.2 µm and store at 4°C

##### *ORO Working Solution*

- 6 parts ORO stock  
4 parts dH<sub>2</sub>O
- Mix and let sit at RT, 20', then filter with 0.2 µm

1. Remove most of the medium and wash once with 1X PBS.
2. Add 10% formalin and incubate at RT, 5'.
3. Discard formalin and add the same volume of fresh formalin.
4. Incubate 1 h or longer at RT.
5. Wash wells with 60% isopropanol.
6. Let the wells dry completely for 5'.
7. Add ORO working solution for 20' (do not touch walls of the wells) (on the belly dancer).
8. Remove all ORO and IMMEDIATELY add dH<sub>2</sub>O; wash with H<sub>2</sub>O four times.
9. Photograph dish if desired.
10. Remove all water and let dry at 37° for 10'.
11. Elute ORO by adding 100% isopropanol; incubate about 15' (can be longer).
12. Pipet the isopropanol with ORO up and down several times to be sure that all ORO is in the solution.
13. Measure OD at 540 nm. Read 200 µl in a 96 well plate.
14. Use 100% isopropanol as a blank and isopropanol from an empty well stained as previously described as a control.



## siRNA Transfections

### *Preadipocytes*

*Cells were transfected with 200 nM of Atp10c siRNA.*

1. Combine equal volumes of 20  $\mu\text{M}$  *Atp10c* siRNA and HiPerfect transfection reagent (40  $\mu\text{l}$  total volume is required per dish).
2. Flick tube to mix and leave at RT for 10'.
3. Add 40  $\mu\text{l}$  of the transfection complex to the medium of each cell culture dish by gently pipetting into the medium.
4. Gently swirl dishes to disperse the transfection complex.
5. Incubate under standard cell culture conditions.
6. Transfect cells each time the medium is changed.

### *Adipocytes*

*Cells were transfected with 30 nM of Atp10c siRNA.*

1. Prepare working siRNA transfection complex as follows [145].

Step	Action	Scale-Up Volumes and Sonication Times		
		1X	2X	3X
1	Prepare 5 $\mu\text{M}$ siRNA working stocks using TE buffer.			
2	Dilute 5 $\mu\text{M}$ siRNA working stocks with Buffer-1. a. Add Buffer-1: b. SiRNA:	37 $\mu\text{l}$ 13 $\mu\text{l}$	74 $\mu\text{l}$ 26 $\mu\text{l}$	111 $\mu\text{l}$ 39 $\mu\text{l}$
3	Prepare siRNA Transfection Reagent. a. Sonicate the siRNA Transfection Reagent: b. Mix Buffer-2 with: c. siRNA Transfection Reagent: d. Vortex and sonicate solution again for:	3-5 min 42 $\mu\text{l}$ 8 $\mu\text{l}$ 3-5 min	3-5 min 84 $\mu\text{l}$ 16 $\mu\text{l}$ 3-5 min	3-5 min 126 $\mu\text{l}$ 24 $\mu\text{l}$ 3-5 min
4	Form concentrated siRNA transfection complex: a. Combine appropriate tubes from steps 2 and 3. b. Briefly vortex and then incubate for 20 min at 37°C.			
5	Prepare complex dilution buffer. a. Mix Buffer-1 with: b. Buffer-2:	200 $\mu\text{l}$ 200 $\mu\text{l}$	400 $\mu\text{l}$ 400 $\mu\text{l}$	500 $\mu\text{l}$ 500 $\mu\text{l}$
6	Prepare working siRNA transfection complex: a. Add complex dilution buffer to prepared concentrated siRNA transfection complexes:	300 $\mu\text{l}$	600 $\mu\text{l}$	900 $\mu\text{l}$

2. Wash cells with 1X PBS (1500  $\mu\text{l}$ /well).
3. Add working transfection complex (300  $\mu\text{l}$ /well) and incubate at RT, 3-5'.
4. Add serum-free media (300  $\mu\text{l}$ /well) and incubate under normal cell culture conditions for 2-4 h.
5. Add complete growth medium (1000  $\mu\text{l}$ /well) and incubate under normal cell culture conditions for 24-72 h.

## Semi-quantitative RT-PCR and agarose gel

### Recipes

#### *50X TAE buffer*

- 242 g tris-BASE
- 57.1 ml glacial acetic acid
- 100 ml 0.5 M EDTA, pH 8.0
- fill to 1 L with nanopure water
- filter solution

#### *1X TAE buffer*

- 20 ml 50X TAE
- fill to 1 L with nanopure water

1. Prepare 1X cDNA samples using RNA samples and BioRad cDNA kit.
  - RNA (1  $\mu$ g)
  - sterile H<sub>2</sub>O (10  $\mu$ l – volume of RNA used)
  - 5X buffer (2  $\mu$ l)
  - enzyme (0.5  $\mu$ l)
  - run cDNA samples in PCR machine using Biorad RT program
2. Prepare RT-PCR primers (P<sub>1</sub> + P<sub>2</sub>).
  - 10  $\mu$ l forward primer (P<sub>1</sub>)
  - 10  $\mu$ l reverse primer (P<sub>2</sub>)
  - 80  $\mu$ l sterile H<sub>2</sub>O
3. Prepare RT-PCR samples using cDNA samples.
  - 1  $\mu$ l cDNA
  - 2.5  $\mu$ l P<sub>1</sub> + P<sub>2</sub>
  - 9  $\mu$ l H<sub>2</sub>O
  - 12.5  $\mu$ l GoGreen Taq Master Mix
4. Run in PCR machine at 54°C annealing, 30 cycles.
5. Prepare 1% agarose gel.
  - For a small gel, dissolve 1.25 g agarose in 125 ml fresh 1X TAE buffer.
  - For a large gel, dissolve 3.5 g agarose in 350 ml fresh 1X TAE buffer.
  - Microwave 1-2 min until all of the agarose dissolves.
  - Allow to cool at RT, but do not allow to solidify.
  - Add 2  $\mu$ l ethidium bromide per 1 g agarose.
  - Pour into taped gel holder and add well combs.
6. Load RT-PCR samples in 1% agarose gel and run at 75 V for 1 h 15 min for small gels or 1 h 45 min for large gels.

**RT-PCR primer list**

<i>β-actin</i>	ORN 559 (F): 5'-ATGGGTCAGAAGGACTCCTA-3'	520 bp
	ORN 560 (R): 5'-CAACATAGCACAGCTTCTCT-3'	
<i>Atp10c</i>	ORN 554 (F): 5'-CCTGTGCTCTTCATTCTGGC-3'	886 bp
	ORN 555 (R): 5'-CACTGCAGCTGTGAATCTGT-3'	
<i>ap2</i>	ORN 697 (F): 5'-GACCTGGAAACTCGTCTCCA-3'	320 bp
	ORN 698 (R): 5'-CATGACACATTCCACCACCA-3'	
<i>C/EBPα</i>	LACS 130 (F): 5'-CAGTTTGGCAAGAATCAGAGCA-3'	391 bp
	LACS 131 (R): 5'-GGGTGAGTTCATGGAGAATGG-3'	
<i>GLUT4</i>	LACS 134 (F): 5'-TGGCCCTAAGTATTCAAGTTCTG-3'	168 bp
	LACS 135 (R): 5'-TTCCTTCTATTTGCCGTCCTC-3'	
<i>PPARγ</i>	LACS 128 (F): 5'-GGTGAAACTCTGGGAGATTC-3'	268 bp
	LACS 129 (R): 5'-CAACCATTGGGTCAGCTCTT-3'	
<i>resistin</i>	LACS 3 (F): 5'-ACTGAGTTGTGTCCTGCTAAG-3'	386 bp
	LACS 4 (R): 5'-CCACGCTCACTTCCCCGACATC-3'	

## Protein extract preparations: total membrane proteins

### Reagents

#### *PARP buffer*

- 50 mM tris, pH 6.8
- 8 M urea
- 2% SDS

#### *PARP buffer + protease inhibitors + DTT*

- 100  $\mu$ l PARP buffer
- 1  $\mu$ l of 100X pi
- 1  $\mu$ l of 100 mM DTT

#### *Homogenization buffer*

- 2 ml of 1 M HEPES, pH 7.5 (to give 20 mM)
- 1 ml of 1 M KCl (to give 10 mM)
- dilute to 100 ml with nanopure H<sub>2</sub>O

1. Prepare samples:
  - a. For tissues, resuspend 500 mg tissue in 5 ml homogenization buffer plus 50  $\mu$ l pi per sample. Homogenize with Polytron for 10 sec and pass through 20-gauge needle 30X.
  - b. For cells, resuspend pellet in 2 ml homogenisation buffer plus 20  $\mu$ l pi per sample. Homogenize through 20-gauge needle 30X.
2. Centrifuge at 800 rpm for 10' at 4°C.
3. If supernatant is clear, re-pass through needle and centrifuge at 800 rpm.
4. Transfer supernatant to a new tube and centrifuge at 25000 x g (13000 rpm) for 30' at 4°C.
5. Remove and save supernatant (cytosolic proteins).
6. Resuspend pellet in 100-300  $\mu$ l PARP buffer + 1 mM DTT + 1 mM pi.

## **Protein extract preparations: whole cell lysates with SDS lysis buffer**

### ***Reagents***

#### *SDS lysis buffer*

- 2.5 ml of 1 M HEPES (to give 50 mM)
- 7.5 ml of 1 M NaCl (to give 150 mM)
- 20 ml of 10% SDS (to give 4% SDS)
- dilute to 50 ml with nanopure H<sub>2</sub>O

1. Wash cells twice with PBS at RT.
2. Add 1 ml of SDS lysis buffer with DTT (10 mM) and pi (1:1000).
3. Isolate cells with cell scraper and collect in eppendorf tube.
4. Heat to 100°C for 5 min.
5. Store at -80°C.

## **Protein extract preparations: whole cell lysates with RIPA buffer**

### ***Reagents***

#### *RIPA buffer + inhibitors*

- 1 ml RIPA buffer
- 5 µl of 200X Na<sub>3</sub>VO<sub>4</sub>
- 5 µl of 200X NaF
- 5 µl of 200X PMSF
- 1 µl of leupeptin
- 1 µl of aprotinin

1. Wash cells twice with PBS on ice.
2. Add RIPA buffer + inhibitors (100 µl per 60 mm dish).
3. Isolate cells with cell scraper and collect in eppendorf tube.
4. Store at -80°C.

## Protein extract preparations: subcellular protein fractionations

### Recipes

#### DMEM/BSA

- add 100 mg BSA to 100 ml DMEM

#### HES buffer

- 250 mM sucrose (42.8 g), 20 mM HEPES (2.38 g), 1 mM EDTA (0.15 g)
- dilute to 100 ml with water
- pH to 7.4 and store at RT

#### HES/pi buffer

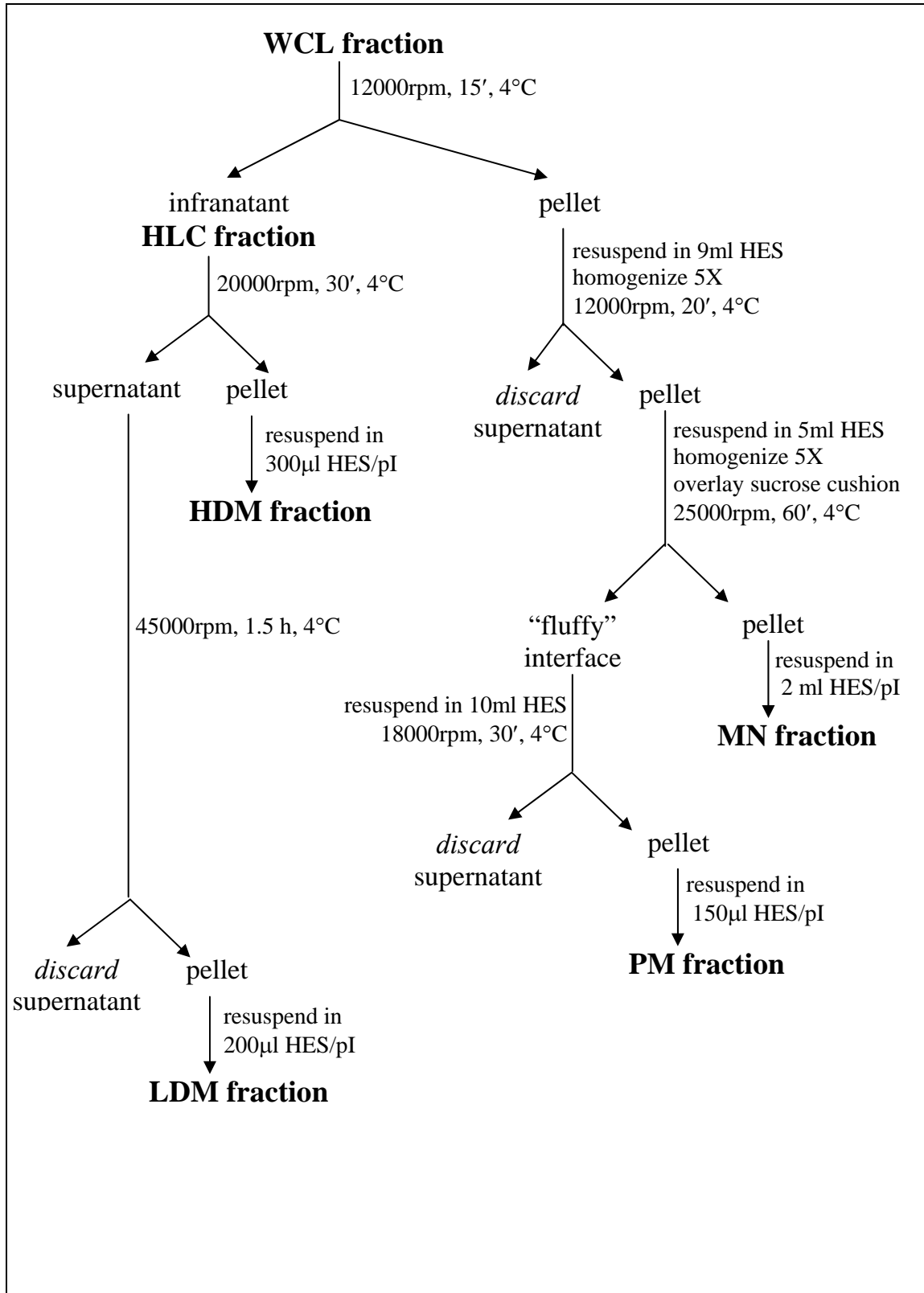
- add 1  $\mu$ l pi for every 1 ml HES buffer

#### 1.12M Sucrose buffer

- add 29.78 g sucrose to 60 ml HES and stir vigorously
- dilute to 100 ml with HES and store at room temperature overnight
- place on ice prior to use

1. serum starve 3T3-L1 cells O/N at 37°C
  - wash cells 1X  $\subseteq$  DMEM
  - add 10 ml DMEM/BSA (1 mg/ml) to each dish
2. remove cells from incubator and bring to benchtop
3. add DMEM with or without insulin (1  $\mu$ M = 18  $\mu$ l insulin in 30 ml DMEM) and incubate flasks at 37°, 30'
4. wash 1X  $\subseteq$  1 ml HES, RT
5. add 3 ml HES/pi to each T75 flask (3 flasks for each sample)
6. scrape 3T3-L1 cells at RT using soft cell scraper
7. collect cells in 50 ml Falcon tubes
8. homogenize 10sec  $\subseteq$  Polytron followed by syringing  $\uparrow$  and  $\downarrow$   $\subseteq$  20-gauge needle 30X  
~~~~~ALL STEPS ON ICE FROM HERE ON OUT~~~~~
9. transfer homogenate to black cap (11ml) centrifuge tubes on ice
10. save 300  $\mu$ l of each as whole cell lysates (**WCL**) in a 1 ml Eppy tube
11. centrifuge 12000 rpm, 15', 4°C in 75Ti rotor
12. carefully remove fat layer and transfer infranant to black cap (11 ml) centrifuge tubes for further fractionation (~9 ml) – this is the **HLC fraction**
13. wipe side walls with Kim wipes to remove excess fat
14. resuspend pellet in 9 ml cold HES
15. homogenize  $\subseteq$  20-gauge needle and syringe 5X
16. centrifuge 12000 rpm, 20', 4°C in 75Ti rotor
17. remove supernatant and discard
18. resuspend pellet in 5 ml HES
19. homogenize  $\subseteq$  20-gauge needle and syringe 5X

20. overlay homogenate on 6 ml of a 1.12M sucrose cushion made up in HES; top up tube  $\subseteq$  HES
21. centrifuge 25000 rpm, 60', 4°C in SW28 swinging rotor
22. collect cloudy, "fluffy" interface between top buffer and sucrose cushion (~1 ml)
23. resuspend this interface in 10ml HES in black cap tubes (11 ml)
24. centrifuge 18000 rpm, 30', 4°C in 75Ti rotor
25. during centrifugation, remove remaining sucrose in SW28 tube and rinse pellet with HES
  - resuspend this pellet in 2 ml HES/pi, transfer to a 2 ml Eppy tube, and label as mitochondrial/nuclear fraction (**MN**)
26. after centrifugation, remove supernatant
  - resuspend pellet in 150  $\mu$ l HES/pi, transfer to a 1 ml Eppy tube, and label as plasma membrane (**PM**)
27. centrifuge the **HLC fraction** from earlier 20000 rpm, 30', 4°C in 75Ti rotor
  - transfer supernatant into another black cap centrifuge tube (11 ml) (for LDM fractionation)
  - resuspend pellet in 300  $\mu$ l HES/pi (**HDM**)
28. Centrifuge supernatant at 45000 rpm, 1.5h, 4°C
  - discard supernatant (cytosolic fraction)
  - resuspend pellet in 200  $\mu$ l HES/pi (**LDM**)
29. BCA assay to quantitate proteins
  - 9 standards in duplicate, all samples in duplicate
  - 200  $\mu$ l mix per well of 50 parts A : 1 part B (1 ml A + 20  $\mu$ l B)
  - assay: 10  $\mu$ l standard OR 1  $\mu$ l sample + 9  $\mu$ l PBS with 200  $\mu$ l mix
  - 37°C, 30'
  - 10 samples + 9 standards = 19 in duplicate = 38 total x 200  $\mu$ l = 7600  $\mu$ ,  
8 ml A + 160  $\mu$ l B





## Pouring gels for Western blot

### Recipes

#### Solution A

- 40% w/v bis-acrylamide solution

#### Solution B

- 25 ml 3M tris-HCl, pH 8.8
- 23 ml H<sub>2</sub>O
- 2 ml 10% SDS

#### Solution C

- 25 ml 1M tris-HCl, pH 7.0
- 23 ml H<sub>2</sub>O
- 2 ml 10% SDS

#### 10% APS

- 0.5 g ammonium persulfate
- 5 ml H<sub>2</sub>O

1. Set up gel pouring apparatus.
2. Prepare resolving gel (normally 10%) by combining the ingredients according to the table. This is enough to pour 2 gels. Add TEMED and APS *immediately* before pouring into the gel apparatus.

|                       | 6%   | 8%   | <b>10%</b>  | 12%  | 14%  | 16%  |
|-----------------------|------|------|-------------|------|------|------|
| Solution A (ml)       | 2.25 | 3.00 | <b>3.75</b> | 4.50 | 5.25 | 6.00 |
| Solution B (ml)       | 3.75 | 3.75 | <b>3.75</b> | 3.75 | 3.75 | 3.75 |
| H <sub>2</sub> O (ml) | 9.00 | 8.25 | <b>7.50</b> | 6.75 | 6.00 | 5.25 |
| TEMED (μl)            | 10   | 5    | <b>5</b>    | 5    | 5    | 5    |
| 10% APS (μl)          | 75   | 75   | <b>75</b>   | 75   | 75   | 75   |

3. Pour resolving gel into the gel apparatus and top off with a thin layer of isopropyl alcohol.
4. Allow the resolving gel to set/solidify.
5. Prepare 4% stacking gel by combining 0.60 ml Solution A, 1.50 ml Solution C, 3.96 ml H<sub>2</sub>O, 10 μl TEMED, and 40 μl 10% APS. Add TEMED and APS *immediately* before pouring into the gel apparatus.
6. Pour off the isopropyl alcohol and add stacking gel. Immediately put in the well combs.
7. Allow the stacking gel to set/solidify.
8. Use the same day or store at 4°C wrapped in moist towels and stored in a Tupperware container for up to 3 days.

## Western blot analysis

### Recipes

#### *1X Tris-glycine buffer*

- 100 ml 10X tris-glycine
- 900 ml nanopure water

#### *20X transfer buffer*

- 116 g tris-BASE
- 58 g glycine
- 74 ml 10% SDS
- fill to 1 L with nanopure water

#### *1X transfer buffer*

- 50 ml 20X transfer buffer
- 200 ml methanol
- 750 ml nanopure water

#### *20X TBS*

- 200 ml 1M tris-HCl (pH 8)
- 87.66 g NaCl
- fill to 1 L with nanopure water

#### *1X TBS*

- 50 ml 20X TBS
- 750 µl Tween-20
- fill to 1 L with nanopure water

#### *1% Blocking Solution*

- 1 g nonfat milk
- 1 g BSA
- 100 ml 1X TBST

1. Prepare protein samples.
2. Boil samples for 5', place on ice briefly, and spin down before loading onto gel.
3. Run protein gel at 125 V for 1.5 h at RT in 1X tris-glycine buffer.
4. Run transfer at 100 V for 1 h surrounded with ice in 1X transfer buffer.
5. Shake membrane in blocking solution for 1 h at RT.
6. Shake membrane in 1° antibody overnight at 4°C.
7. Wash membrane: one quick wash followed by three 10 min washes with 1X TBST.
8. Shake membrane with 2° antibody for 1 h at RT.
9. Wash membrane: one quick wash followed by three 10 min washes with 1X TBST.
10. Develop membrane with ECL Western Blotting Substrate kit, using approximately 1 ml substrate per blot (equal volumes detection reagent 1 and 2).
  - Allow membrane to sit 1'.
  - Blot excess substrate on paper towel.
  - Cover membrane with saran wrap.
11. Develop membrane with X-ray.
12. Store membrane at 4°C.
13. To reprobe membranes:
  - Shake membrane in Western stripping solution for 15' at RT.
  - Shake membrane in 1X TBST for 15' at RT.
  - Follow protocol above starting at step 6 (1° antibody).

**Western blot antibodies**

| <b>1° Antibody</b>                     |                                     |             | <b>2° Antibody</b> |            | <b>MW</b> |
|----------------------------------------|-------------------------------------|-------------|--------------------|------------|-----------|
| ATP10C                                 | Sigma<br>(purified)                 | 10 µl/10 ml | anti-rabbit        | 5 µl/10 ml | 70 kDa    |
| GLUT1                                  | Alpha<br>Diagnostic<br>(GT11-A)     | 10 µl/10 ml | anti-rabbit        | 5 µl/10 ml | 40-80 kDa |
| GLUT4                                  | AbCam<br>(ab654)                    | 4 µl/10 ml  | anti-rabbit        | 5 µl/10 ml | 70 kDa    |
| Na <sup>+</sup> -K <sup>+</sup> ATPase | Novus<br>Biologicals<br>(NB300-146) | 2 µl/10 ml  | anti-mouse         | 5 µl/10 ml | 112 kDa   |
| β-TUBULIN                              | Sigma<br>(T2200)                    | 6 µl/10 ml  | anti-rabbit        | 5 µl/10 ml | 55 kDa    |

## Glucose uptake

### Recipes

#### *Krebs-Ringer HEPES (KRH) buffer*

- 121 mM NaCl (7.07 g), 4.9 mM KCl (0.365 g), 1.2 mM MgSO<sub>4</sub> (0.144 g), 0.33 mM CaCl<sub>2</sub> (0.048 g), 12 mM HEPES (2.86 g)
- dilute to 1 L with water
- pH to 7.4
- add 25 mM D-glucose (2.25 g) to 500 ml of the buffer for KRH (+) glucose
- sterile filter both KRH (-) glucose and KRH (+) glucose and store at 4°C

#### *Digitonin release buffer*

- 0.25 M mannitol (22.78 g), 17 mM MOPS (1.78 g), 2.5 mM EDTA (2.5 ml of 0.5 M EDTA), 0.25 M digitonin (8 mg/ml, 0.4 g)
- dilute to 500 ml with water and pH to 7.4
- heat to 98°C to dissolve, leave on benchtop overnight to bring back to room temperature

#### *cold 2-deoxyglucose (2-DOG)*

- add 0.13 g 2-deoxyglucose in 40 ml KRH (-) glucose
- store at -20°C

#### *cytochalasin B*

- stock (Sigma C-6762) is 1 mM in 100% ethanol
- add 5 µl cytochalasin B/1 ml cocktail

#### *cocktail*

| # wells | KRH (-) glucose | Cold 2-DOG | <sup>3</sup> H 2-DOG |
|---------|-----------------|------------|----------------------|
| 10      | 9.94 ml         | 50 µl      | 10 µl                |
| 20      | 19.88 ml        | 100 µl     | 20 µl                |
| 25      | 24.86 ml        | 125 µl     | 25 µl                |
| 30      | 29.82 ml        | 150 µl     | 30 µl                |
| 35      | 34.80 ml        | 175 µl     | 35 µl                |
| 40      | 39.76 ml        | 200 µl     | 40 µl                |
| 45      | 44.74 ml        | 225 µl     | 45 µl                |
| 50      | 49.70 ml        | 250 µl     | 50 µl                |

1. In the morning, wash cells with DMEM 2X
2. Serum starve cells 3-5hrs in DMEM only
3. Set-up 6-well plate as follows:

|    |     |     |     |
|----|-----|-----|-----|
|    | -C  | -C  | +C  |
| -I | (1) | (2) | (3) |
| +I | (4) | (5) | (6) |

4. Add fresh DMEM with or without insulin (100 nM insulin = 0.6  $\mu$ l and 1  $\mu$ M insulin = 6  $\mu$ l in 10 ml DMEM) and incubate 37°, 30'
5. Wash plates twice with 1 ml of KRH (-) glucose at RT
6. Add 1 ml of "cocktail" with or without cytochalasin B per well
  - "cocktail" without cytochalasin B (-C), 24 wells, 25 ml
    - 24.85 ml KRH (-) glucose
    - + 125  $\mu$ l cold 2-DOG
    - + 25  $\mu$ l  $^3$ H 2-DOG
  - "cocktail" with cytochalasin B (+C), 12 wells, 15 ml
    - 14.9 ml KRH (-) glucose
    - + 75  $\mu$ l cold 2-DOG
    - + 15  $\mu$ l  $^3$ H 2-DOG
    - + 75  $\mu$ l cytochalasin B
7. Incubate at 37° for 5' exactly
8. Terminate incorporation by aspirating off cocktail
9. Wash plate TWICE with 1ml of ice cold KRH (+) glucose
10. Add 2.2 ml of digitonin release buffer at RT to each plate; incubate 5'
11. Scrape cells and transfer to labeled (1-6) 5 ml eppendorf tube
12. Vortex to break clumps
13. Add 2 ml of the lysates to a scintillation vial with 10 ml scintillation fluid
14. Save remaining 200  $\mu$ l lysate and store at -80°
15. To another scintillation vial, add 66 $\mu$ l of "cocktail" (without cytochalasin B), 1934  $\mu$ l of digitonin release buffer, and 10 ml scintillation fluid (this tells you the specific activity)
16. Count for 5 min in a scintillation counter

## VITA

Amanda Lynn Peretich was born in Leesburg, VA, on April 7, 1983. She graduated from James Madison University with a Bachelor of Science degree in Chemistry with a certification in ACS Biochemistry in May 2005. Under the Continuing Education program at James Madison University, she completed a second major in Biology in December 2005. Amanda then attended the University of Tennessee-Knoxville, where she received a Master of Science degree in Comparative and Experimental Medicine in May 2008. She is currently an adjunct instructor in Chemistry at South College in Knoxville and is looking forward to what the future will bring.